TERMINAL MICROBIAL METABOLISMS IN THE DEEP SUBSURFACE UNDER CONDITIONS RELEVANT TO CO_2 SEQUESTRATION AND ENHANCING METHANOGENESIS FROM COAL

By

Andrew Glossner

© Copyright 2013
by
Andrew W. Glossner
All Rights Reserved

A thesis submitted to the Faculty and the Board of Trustees of the Colorado School of Mines in partial fulfillment of the requirements for the degree of Doctor of Philosophy (Geochemistry).

Golden, Colorado

Date May 14, 2013

Signed: ______________________

Andrew W. Glossner

Signed: ______________________

Dr. Kevin W. Mandernack
Thesis Advisor

Golden, Colorado

Date ______________

Signed: ______________________

Dr. David Wu
Professor and Head

Department of Chemistry and Geochemistry

ABSTRACT

Microbial life in the deep subsurface may extend several kilometers below the surface, and by some estimates surpasses the mass of all life on the surface of the Earth. Microbes living in the subsurface play important roles in the global carbon cycle, through the breakdown of organic matter and methane formation. The goal in this thesis is to describe the microbial dynamics of two deep subsurface environments, and relate how porewater geochemistry and human-induced changes to those environments affect microbial carbon cycling and community structure. The environments of interest in this thesis are 1) deeply buried coal seams, and 2) sandstone reservoirs. The goals in this thesis include the characterization of microbial community structure and metabolic function in methanogenic coal microcosm experiments in response to imposed geochemical gradients, and the characterization of a microbial community in response to supercritical CO_2 injection.

Acetate was found to be a key intermediate in methanogenic coal microcosms. Experiments with variable concentrations of sulfate showed the same methanogenic potential as molybdate inhibited experiments, showing that sulfate concentration is not a determining factor in methanogenesis from coal. Experiments amended with acetate showed a decreasing proportion of acetate consumed by methanogens as acetate concentrations increased, suggesting that in situ acetate concentrations determine the relative importance of methanogenesis and sulfate reduction in coal seams. The growth of sulfate reducers and methanogens was monitored using phospholipid fatty acids (PLFA) and quantitative polymerase chain reaction (qPCR) for the functional genes for methanogens (mcrA) and sulfate reducers (dsrA). Bioindicators for SRM, including

10Me16:0, and cy17:0 correlated positively with acetate amendment, which also corresponded with an increase in dsrA and mcrA copy numbers in experiments without molybdate, showing that sulfate reducers and methanogens could metabolize acetate simultaneously in coal bed aquifers with low acetate concentrations.

Experiments with variable pCO_2 and urea amendment showed that methanogenesis from coal was relatively insensitive to pCO_2 at pressures up to 2.5 atm, but urea concentrations above 2.5 g/L caused a cessation of methanogenic activity, most likely due to a pH effect. Methanogenic potential in coal microcosms was also shown to be a function of the metabolic activity of fermenters making acetate prior to the start of each experiment. The consortium of organisms used for experiments with coal was also utilized for experiments with supercritical CO_2 ($scCO_2$) at 40 ˚C and 10 MPa. Pre-incubation of sandstone cores caused a 30-60% reduction in permeability of Berea sandstone cores, which was not recovered following $scCO_2$ injection. The injection of a microbial enrichment into sterile sandstone cores also reduced the measured permeability up to 83%. $scCO_2$ did not have a significant impact on the bacterial or archaeal microbial community, as measured by PLFA, phosphoether lipid, and most probable number (MPN) analyses of injection system effluent as well as extracts of the solid cores post-experiment, suggesting that either contact time with $scCO_2$, or heterogeneous flow are major factors in microbial susceptibility to $scCO_2$.

TABLE OF CONTENTS

LIST OF FIGURES

LIST OF TABLES

ACKNOWLEDGMENT

I would first like to thank my advisor, Dr. Kevin Mandernack, for his support and guidance throughout my PhD work. I would also like to acknowledge the gracious input and help I received from my committee, including Dr. Junko Munakata Marr, Dr. Dag Nummedal, Dr. Craig Simmons, Dr. Kent Voorhees, Dr. John Curtis, and Dr. Christopher Mills. In particular, Dr. Junko Munakata Marr, was like a second advisor, and always giving of her time and knowledge throughout my work with her on the RPSEA project. Dr. Chris Mills was also especially gracious in allowing me to use his lab during my final months, as well as providing invaluable guidance with phospholipid analysis. I would also like to acknowledge Dr. Lee Landkamer, not only for his scientific input throughout our work together, but for allowing me to live in his house during my final tenure as a student. Special acknowledgement should also go to Tom Boyd, Dean of the Graduate School, for helping with funding multiple times during my final year at Mines, as well as Dr. Marte Gutierrez for funding my final semester and giving me the opportunity to work in his lab.

I would next like to thank my wife, Hallgerd Eydal, for her constant support and encouragement over the last 3 years of my PhD work. I would also like to thank Stephanie Carr for being a great friend and lab mate over the past 6 years. In my time in Colorado I have also had the privilege of sharing in adventures in the mountains with many friends, including Andy Vermilyea, Justin Engle, Hillary Easter, Nate Rebeck, Michael Morse, Nick Labue, Andy Mention, Ben Petri, Dan Perl, and too many others to name. Our time together in the wild places makes all the hours in the lab worth it.

CHAPTER 1

Introduction

1.1 Life in the subsurface

The ubiquity and incredible magnitude of microorganisms in the terrestrial subsurface has been well documented in the last two decades, and may exceed the total biomass of all life on the surface (Gold, 1992; Whitman et al., 1998). In the deep subsurface microbes are responsible for mediating or catalyzing numerous redox reactions and can play a major role in the subsurface carbon cycle. Most studies examining microbial life in the deep subsurface focus on water-saturated zones (Lovley and Chapelle, 1995), but limited subsurface microbial activity occurs without water saturation in environments in extremely arid regions (Brockman et al., 1992; Kieft et al., 1993). Hydrologically, the deep subsurface can be defined as being distinct from shallow groundwater aquifers and not subject to short-term fluctuations in water chemistry or flow rate as a result of surface precipitation events (Lovley and Chapelle, 1995). As such, deep subsurface environments are generally characterized by a lack of oxygen, labile carbon, and slow, diffusion- or nutrient limited-microbial metabolisms. The work described in this dissertation seeks to enhance our understanding of microbial communities in the oligotrophic subsurface, particularly in coal deposits, their responses to environmental stress, and the interactions between different metabolic groups.

The extent to which microbes are responsible for the transformation of carbon depends broadly on the geochemistry of the rocks and formation water, temperature, and availability of electron donors and acceptors. In the deep subsurface, temperature is controlled by the geothermal gradient and thus depth may become the limiting factor. While some have speculated that life may exist at temperatures up to 150 ˚C (Stetter et al., 1990), an upper limit has been established thus far at 121 ºC (Kashefi and Lovley, 2003). More recently, however, growth of the methanogen *Methanopyrus kandleri* at 122 ˚C and 20 MPa was documented (Takai et al., 2008). The second broadly limiting factor is energy availability. In deep granitic or basaltic aquifers the primary source of energy is thought to be H_2 resulting from water-rock interactions with iron-rich minerals (Stevens and McKinley, 1995; Ward et al., 2004). Lithoautotrophy is considered the primary microbial metabolic pathway in organic carbon- and electron donor-limited ecosystems like these. In contrast, systems rich in organic carbon such as oil reservoirs, shale and coal aquifers may exhibit a variety of metabolisms based on the breakdown of ancient organic matter. These may include heterotrophic pathways such as fermentation, Fe(III), nitrate or sulfate reduction, as well as acetogenesis and methanogenesis. Metabolizing complex and recalcitrant organic matter in such systems is thought to be dependent upon complex consortia of syntrophic organisms who may ultimately be electron acceptor limited (Fredrickson et al., 1991a; Fredrickson and Balkwill, 2005). However, relatively little is known about the roles of specific organisms in systems with sedimentary organic matter and how the microbial community responds to changes in the organic matter itself.

1.2 Subsurface microbial diversity and abundance

Before discussing the range of biomass estimates obtained from studies of the terrestrial subsurface it is important to recognize the differences between sampling methodologies employed in studies of the microbial community. Early studies of subsurface microbial communities were primarily culture-based (Balkwill et al., 1989;

Balkwill, 1989; Fredrickson et al., 1991b), and as such probably dramatically underestimated both diversity and abundance because most organisms are non-cultivable (Amann et al., 1995). Culture independent methods such as lipid analysis and molecular techniques like 16S rRNA gene sequencing have been employed more widely in the last 20 years, but are not without limitations or biases. Diversity and biomass have been shown to differ depending on whether the sample is from groundwater or surrounding rock matrix (Lehman et al., 2007). Additionally, microbial diversity can be highly variable when groundwater composition is heterogeneous, as in contaminated aquifers (Chapelle et al., 2002a). Spatial variability with respect to groundwater flow and aquifer connectivity can also be an important factor contributing to diversity (Stevens and McKinley, 1995). While diversity itself can be interesting, it may not completely describe metabolic activity or ecosystem function.

The number of microbial cells in an environment can also be an important measure of ecosystem health and carbon cycling capacity. Biodensity (cells per unit volume) in deep, oligotrophic subsurface aquifers is generally on the order of 10^3-10^5 cells/mL (Fry et al., 1997; Haveman et al., 1999; Murakami et al., 2002; Moser et al., 2003; Onstott et al., 2003; Lehman et al., 2004; Kieft et al., 2005; Mills et al., 2010). Studies of subsurface microbial biodensity often use some combination of direct cell counts (usually employing DNA-based dyes such as acridine orange or SYBR Green), and estimates based upon the extraction of cellular membrane phospholipid fatty acids (PLFAs), or phosphoether lipids (PELs) from archaea, which have been shown to be roughly equivalent quantification methods for viable microbial biomass (Balkwill et al., 1988; Green and Scow, 2000; Mills et al., 2010; Carr et al., 2013).

While the number and density of microbial cells in the subsurface is now widely acknowledged, the variety and importance of microbial metabolic processes is now beginning to be recognized. Subsurface microorganisms play important roles in global biogeochemical cycles, and include regulating the global methane cycle (Kotelnikova, 2001), altering oceanic crust (Thorseth et al., 1995), as well as playing a major role in the sulfur cycle (Sievert et al., 2007). This dissertation attempts to expand our knowledge of the role of microbes in subsurface carbon cycling, particularly as they relate to geologic energy systems.

1.3 Sulfate reduction and methanogenesis

Sulfate reducing microorganisms (SRM) are ubiquitous in anaerobic surface and subsurface environments and contribute significantly to the global carbon cycle. Generally SRM utilize sulfate as their electron acceptor for the oxidation of organic compounds or inorganic substrates such as hydrogen. They have been found to be important members of microbial communities in lacustrine (Holmer and Storkholm, 2001) and marine sediments (Oremland and Taylor, 1978), engineered environments such as anaerobic bioreactors (J.W.H et al., 1994), petroleum reservoirs (Rueter et al., 1994; Grabowski et al., 2005), as well as flooded rice paddies (Liesack et al., 2000). SRM are categorized into two different groups based on their carbon metabolism; organisms that oxidize carbon to acetate, and those that oxidize compounds completely to CO_2 (Muyzer and Stams, 2008). Sulfate reducers have been shown in pure culture and environmental studies to utilize a variety of carbon substrates including simple substrates such as acetate, lactate, and propionate (Widdel and Pfennig, 1977; Widdel and Pfennig, 1981), saturated alkane hydrocarbons (Aeckersberg et al., 1991; Coates et al., 1997; Caldwell et al., 1998), aromatic compounds (Beller et al., 1996; Coates et al., 1997; Harms et al., 1999; Widdel and Rabus, 2001), and even complex substrates such as petroleum (Rueter et al., 1994). Some SRM can also utilize alternative electron acceptors in the absence of sulfate, including nitrate, nitrite, thiosulfate, sulfite, elemental sulfur, Fe (III), U(VI), Te(VII), Se(VI), Cr(VI), As(VI), and even organic compounds such as fumarate, dimethylsulfoxide, and sulfonates (Muyzer and Stams, 2008).

In many anaerobic environments sulfate reducers and methanogens perform the final steps in the breakdown of complex organic matter. The competition between SRM and methanogens for common substrates (mainly H_2 and acetate) is essentially governed by environmental factors including substrate and sulfate concentrations. From an energetic standpoint, autotrophic sulfate reduction (Equation 1.4) is more energetically favorable under standard conditions than hydrogenotrophic methanogenesis (Equation 1.1). The same is true for acetate oxidation via sulfate reduction (Equation 1.3) versus acetoclastic methanogenesis (Equation 1.2) (Madigan and Martinko, 2006). Furthermore, sulfate reducers are known to outcompete methanogens for these substrates under both freshwater (Lovley and Klug, 1983; Lovley and Klug, 1986) and marine sulfate concentrations (Oremland and Taylor, 1978; Mitterer, 2010) due to their higher substrate affinity and lower threshold concentrations for these substrates (Schönheit et al., 1982; Kristjansson et al., 1982; Muyzer and Stams, 2008). In marine sediments the commonly accepted model for the distribution of these two processes holds that methanogenesis will not take over as the dominant terminal electron accepting process until all of the sulfate has been depleted (Martens and Berner, 1974; Oremland and Taylor, 1978; Jørgensen and Kaster, 2006). However, in marine sediments, methane is thought to be oxidized under anaerobic conditions by the combined action of SRM and archaea (Hinrichs et al., 2000; Orphan et al., 2001; Wegener et al., 2008). Recent evidence, however, suggests that a single archaeal organism may be responsible for both sulfate reduction and methane oxidation (Milucka et al., 2012). Because the concentration of sulfate in marine sediments is typically much higher (10-50 mM SO_4^{2-}) than in freshwater sediments (10-500 µM SO_4^{2-}), sulfate reducers often account for the majority of carbon mineralized under high sedimentation rates in marine sediments (Canfield et al., 2005). Under freshwater sulfate concentrations, however, SRM have adapted to the typically lower sulfate concentrations by having much lower half-saturation constants for sulfate (Ingvorsen et al., 1984) but will still rapidly deplete the available sulfate in freshwater sediments (Canfield et al., 2005).

Methanogenic reactions

$$CO_2 + 4H_2 \rightarrow CH_4 + 4H_2O \quad \Delta G^{0\prime}\text{: -131 kJ/mol} \tag{1.1}$$

$$CH_3COO^- + H_2O \rightarrow CH_4 + HCO_3^- \quad \Delta G^{0\prime}\text{: -31 kJ/mol} \tag{1.2}$$

Sulfate reduction reactions

$$CH_3COO^- + SO_4^{2-} + 3H^+ \rightarrow 2CO_2 + H_2S + 2H_2O \quad \Delta G^{0\prime}\text{: -57.5 kJ/mol} \tag{1.3}$$

$$4H_2 + H^+ + SO_4^{2-} \rightarrow HS^- + 4H_2O \quad \Delta G^{0\prime}\text{: -152 kJ/mol} \tag{1.4}$$

There are numerous examples of sulfate reduction and methanogenesis co-occurring in marine and freshwater environments (Oremland and Polcin, 1982; Oremland et al., 1982; Crill and Martens, 1986; Raskin et al., 1996; Hoehler et al., 1998). Typically, these environments are characterized by low sulfate concentrations and relatively high labile organic matter resulting in ample substrates for methanogenesis. Alternatively, SRM and methanogens may co-exist without competing for the same substrates (Oremland and Polcin, 1982). Mountfort et al. (2003) found that in ponds of the McMurdo Ice Shelf, Antarctica, the majority of acetate was consumed by SRM while the majority of H_2 was consumed by methanogens, and that the relative importance of each process was dictated by the freeze-thaw cycle of the ponds, illustrating how both processes may occur under low-temperature conditions. The same study also found that under low sulfate conditions the ratio of the rate of methanogenesis to sulfate reduction was a function of both the sulfate concentration and the temperature, indicating that thermodynamic limitations influence the relative importance of sulfate reduction at low sulfate concentrations (Mountfort et al., 2003). This apparent thermodynamic constraint on sulfate reduction at low sulfate concentrations has also been used to explain the co-occurrence of methanogenesis with sulfate reduction at Cape Lookout Bight in North Carolina (Hoehler et al., 2001).

The rates of methanogenesis and sulfate reduction can be highly variable and site-dependent, but in general the rate of methanogenesis will be greater than the rate of sulfate reduction in freshwater sediments due to the low sulfate concentration (Canfield et al., 2005). Table 1.1 shows a compilation of rates of methane production and sulfate reduction from a variety of freshwater sites with low sulfate concentrations. The competition between the two processes is also influenced by the rate of organic matter decomposition supplying acetate as the substrate. Where the rate of organic matter decomposition is slow, the SRM become limited by acetate and are able to more completely consume acetate through a greater depth in the sediment, thus dominating carbon mineralization (Lovley and Klug, 1986; Thomsen et al., 2004). When the rate of organic matter decomposition is faster, the SRM may deplete sulfate concentrations down to 30 µM or lower in the upper centimeters of the sediment, allowing methanogenesis to account for the majority of carbon mineralization in such sediments below that depth (Lovley and Klug, 1986).

Table 1.1: Methane production and sulfate reduction rates from freshwater sites (Adapted from Canfield et al., 2005).

Freshwater sites	CH_4 production (µmol $cm^{-2}yr^{-1}$)	%CH_4 from acetate	SRR (µmol cm^{-2} yr^{-1})	MP/SRR	Reference
White oak estuary	2130	72	ND		(Avery et al., 2003)
Buck Hollow	270	51	ND		(Avery et al., 2003)
Orange Pond, Antarctica	8.8	3	ND		(Mountfort et al., 1999)
Lake Constance	ND	100	ND		(Schulz and Conrad, 1996)
Kings Lake Bog	54-142	0.5	ND		(Lansdown et al., 1992)
Lawrence Lake	2008	14	803	2.5	(Lovley and Klug, 1986; Holmer and Storkholm, 2001)
Wintergreen A	17500	80	2700	6.5	(Lovley and Klug, 1986; Holmer and Storkholm, 2001)
Wintergreen B	11300	67	8400	1.3	(Lovley and Klug, 1986; Holmer and Storkholm, 2001)
Lake Mendota	ND	76	ND		(Lovley and Klug, 1986; Holmer and Storkholm, 2001)
Rømø Site 3	68	10	23.4	2.9	(Hansen et al., 2001)
Rømø Site 8	72	10	15	4.8	(Hansen et al., 2001)
Rømø Site 10	11	30	0.12	91	(Hansen et al., 2001)
Lake Washington	14.6	61-85	4.3	3.4	(Kuivila et al., 1990)
Rice paddy soil	ND	69-83	ND		(Rothfuss and Conrad, 1992)
Lake Michigan	0	ND	570	0	(Thomsen et al., 2004)
Créteil (France)	ND	ND	350		(Laverman et al., 2012)
Tresmes (France)	ND	ND	203		(Laverman et al., 2012)

ND: Not determined in this study
MP: Methane production rate
SRR: Sulfate reduction rate

One chapter of this dissertation examines the relative importance of sulfate reduction and methanogenesis in coal microcosms, using a series of experiments with varying sulfate and acetate concentrations. Coal bed methane reservoirs represent a unique "freshwater" environment in which the competition between SRM and methanogens may be governed not by sulfate concentrations but rather by the rate of organic matter decomposition, as will be shown in Chapter 2. The work described in Chapter 2 aims to expand our understanding of the biogeochemistry of coal bed methane reservoirs by showing that SRM and methanogens may coexist in this unique environment.

1.4 Microbial methanogenesis from coal

Methane that is formed from and trapped in deeply buried coal seams is called coal bed methane (CBM). Though the formation of thermogenic gases in coal beds has been directly linked to factors such as thermal maturity and maceral composition (Rice, 1983; Rice et al., 1989; Scott, 2002), no *direct correlation* between these factors and secondary biogenic gas accumulation has been found. In contrast, it seems that the most important physical factor controlling secondary biogenic gas formation is basin hydrogeology. If tectonic processes bring the edges of synclinal basins to within reach of meteoric water recharge, a consortium of bacteria and the necessary nutrients may be introduced that results in the breakdown of coal to form methane. Figure 1.1 shows how the edges of an uplifted and eroded synclinal basin may become exposed for meteoric water recharge (Zhou et al., 2005). The microbes introduced through this process can include fermentative anaerobic species who may then begin breaking down the complex geopolymers originating from plant tissues into long chain fatty acids, and ultimately monomers and oligomers (Faiz and Hendry, 2006). The fatty acids can then be further respired by anaerobic heterotrophs or acetogens to form H_2, CO_2, formate, and acetate (Faiz and Hendry, 2006). These intermediates can then be either reduced (through hydrogenotrophic methanogenesis; Equation 1.1) or disproportionated via acetoclastic methanogenesis (Equation 1.2) to yield methane (Boone et al., 1990).

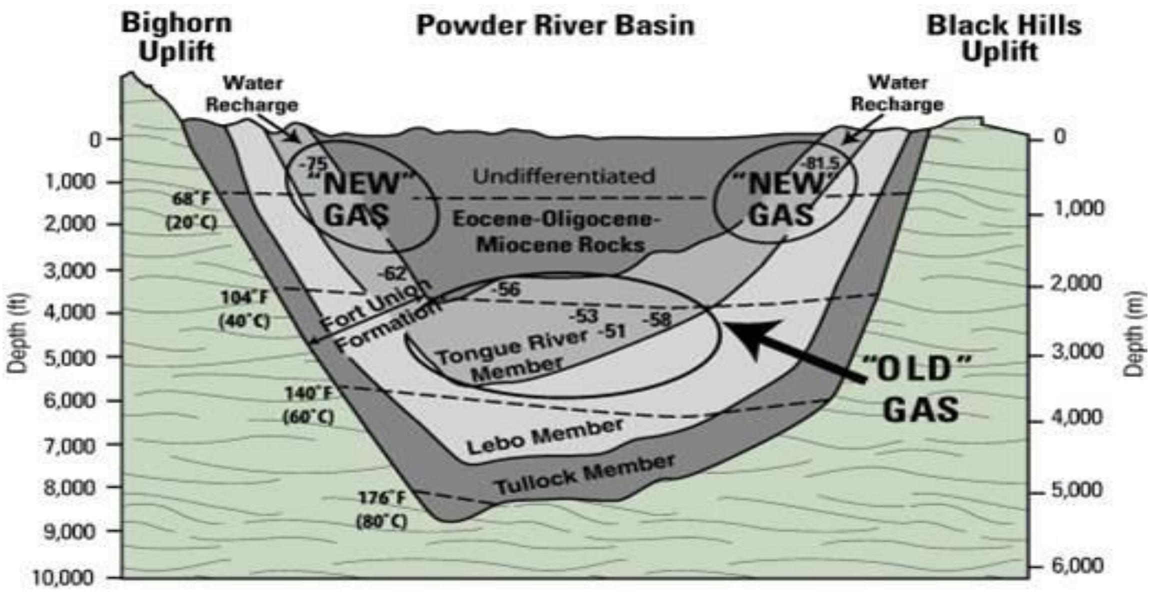

Figure 1.1: West to East cross section of the Powder River Basin in Wyoming and Montana, USA, showing how groundwater recharge in an uplifted basin may infiltrate coal-bearing strata (Flores et al., 2008).

Several recent studies have begun to elucidate the microbial metabolic pathways necessary for methanogenesis from coal. Figure 1.2 shows the model for this process as proposed by Flores et al. (2008). The question of which methanogenic pathway (Equation 1.1 or 1.2) is dominant in coal bearing systems is still debated. In the Powder River Basin, for example, the stable carbon isotopic signatures of the CH_4 and DIC are consistent with hydrogenotrophic methanogenesis being the dominant process in the central part of the basin, with acetoclastic methanogenesis dominating near the basin margins (Flores et al., 2008). In the Illinois Basin hydrogenotrophic methanogenesis has been shown to be the dominant process in microbial enrichment experiments amended with H_2 and acetate (Strąpoć et al., 2008) as well as based upon $\delta^{13}C_{CH4}$ and δD_{CH4}

measurements (Strąpoć et al., 2007). Other studies have identified acetate as the dominant precursor for methanogenesis from abandoned coal mines where H_2 is utilized by homoacetogens to form acetate (Equation 1.7), which is then utilized by methanogens (Beckmann et al., 2011). It is clear that methanogenic pathways vary from basin-to-basin and between enrichment studies, but the reason for this variation is not fully understood.

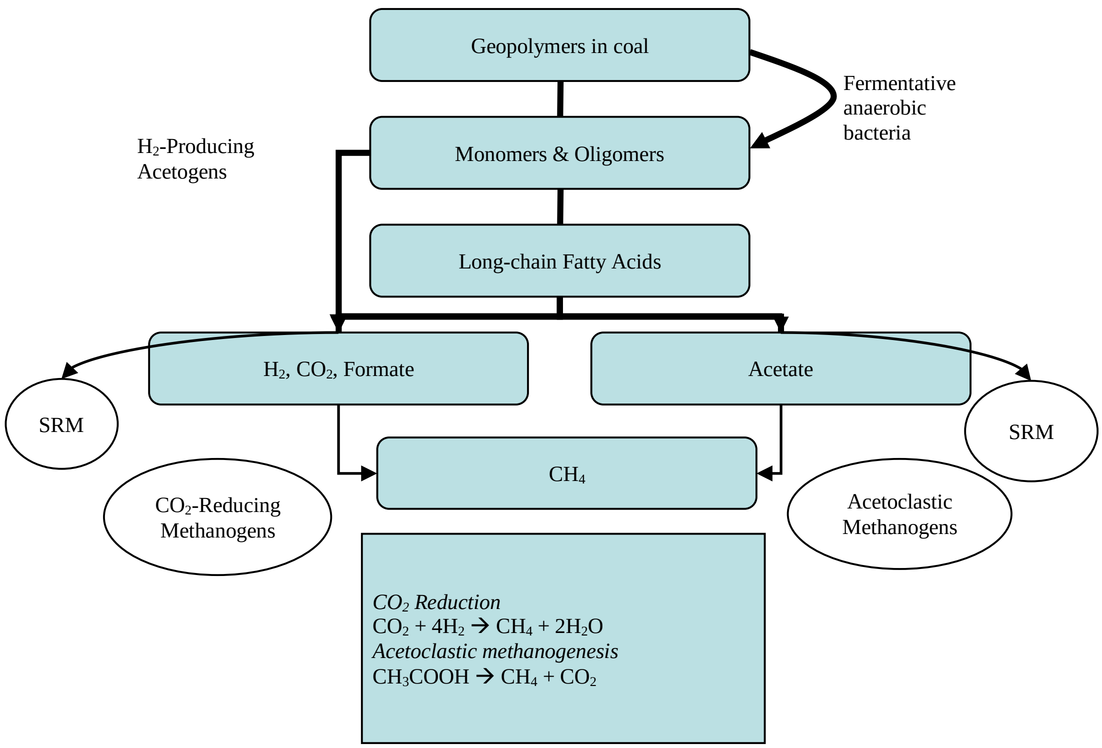

Figure 1.2: Model for microbial methanogenesis from coal. Modified from Flores et al. (2008).

$$CO_{2(aq)} + 4H_{2(aq)} \rightarrow CH_{4(g)} + 2H_2O \qquad (1.5)$$

$$CH_3COOH_{(aq)} \rightarrow CH_{4(g)} + CO_{2(g)} \qquad (1.6)$$

$$2CO_{2(aq)} + 4H_{2(aq)} \rightarrow CH_3COOH_{(aq)} + 2H_2O \qquad (1.7)$$

Another factor necessary for secondary biogenic gas formation is a minimum of sulfate in the formation waters. It is generally accepted that when both sulfate and labile organic matter are present in an environment, sulfate reducers will outcompete methanogens for available resources (Winfrey and Zeikus, 1977; Abram and Nedwell, 1978; Lovley and Klug, 1983). However, evidence for sulfate-reducing and methanogenic microorganisms living in the same subsurface coalbeds has been found in separate studies in Wyoming (Schmidt, 2007) and Montana (Olson et al., 1981). Schmidt (2007) found evidence for sulfate-reducing bacteria in produced waters from coalbed methane wells in the Powder River Basin, WY using phospholipid fatty acid (PLFA) techniques, concurrent with phosphoether lipids (PELs) most likely attributable to methanogenic archaea. However, it was noted in this study that wherever PLFAs for sulfate-reducers were found there was little evidence for PELs from methanogenic Archaea. Roberts (1988) examined the relationship between macerals and sulfur content in Permian coals from South Africa. The author observed a positive correlation between sulfur content and the maceral vitrinite, and a negative correlation between sulfur and the maceral inertinite, suggesting that there may be a relationship between the thermal maturity of coals and their sulfur content (Roberts, 1988). In general, however, the sulfur content of coal is determined by the E_h of the environment at the time of deposition, and therefore varies from basin-to-basin. One would expect the sulfate concentrations in coalbed aquifers to decrease with depth as it is consumed by sulfate-reducing bacteria, as is seen in portions of the Powder River Basin (Rice et al., 2002). It seems unlikely, though possible, that the sulfur content of coal would dictate the sulfate concentrations in coalbed aquifers simply because of the general lack of available electron acceptors that can mediate anaerobic sulfide oxidation in an environment such as this. Nitrate is a common electron acceptor for this reaction (Canfield et al., 2005), but one would expect its concentration to be undetectable in a deep aquifer. It is therefore expected that, in the absence of sufficient sulfate, sulfate reducing bacteria will not dominate organic carbon mineralization in deeply buried coal seams.

While the exact mechanisms of methanogenic coal degradation are not known at this point, there are multiple competing hypotheses for what is the rate-limiting step in the process. Fakoussa and Hofrichter (1999) argue that the rate-limiting step is the breakdown and solubilization of the macromolecules comprising the coal structure. This hypothesis is supported by the observation that long chain organic acid intermediates appeared after experiment initialization and prior to significant methanogenesis in microcosm experiments (Jones et al., 2010). The competing hypothesis suggests that methanogenesis can be the rate-limiting step in the process when trace elements necessary for methanogen growth are limiting (Ünal et al., 2012). This hypothesis is supported by the observation that trace elements (Fe, Co, Ni, Mo, Zn, and Cu) necessary for the growth and enzymatic function of methanogens (Takashima et al., 1990) are generally found at low concentrations in produced water from basins such as the Powder River Basin (McBeth et al., 2003; Jackson and Reddy, 2007). It is also supported by the finding of Ünal et al (2012) who showed that increasing trace element concentrations in microcosm experiments with minimal coal enhanced the methanogenic potential of the microbial community when these element concentrations were approximately two orders of magnitude higher than their respective concentrations in situ.

This dissertation expands our understanding of microbial methanogenesis from coal in two important areas. As previously stated, Chapter 2 will examine the importance of sulfate concentration and the activity of SRM in determining methanogenic potential from coal. Chapter 3 will examine the effects of carbon dioxide and urea on methanogenesis from coal, as well as the importance of fermentative organisms making acetate in determining methanogenic potential.

1.5 Geologic sequestration of carbon dioxide

Carbon dioxide sequestration is a geoengineering process designed to mitigate the effects of the rapidly increasing CO_2 concentration in the Earth's atmosphere. CO_2 capture and storage (CCS) first requires the isolation of CO_2 from either flue or fuel gas streams, compression of that gas into a supercritical fluid (at T = 31.1 ^{o}C, P = 73 atm), and injection of that $scCO_2$ into a deep geologic formation where it can be effectively isolated from the atmosphere for the foreseeable future (White et al., 2003; Zakkour and Haines, 2007). Figure 1.3 shows a schematic representation of CCS, whereby CO_2 is removed from the waste gas stream of a power station, compressed into $scCO_2$, and injected underground.

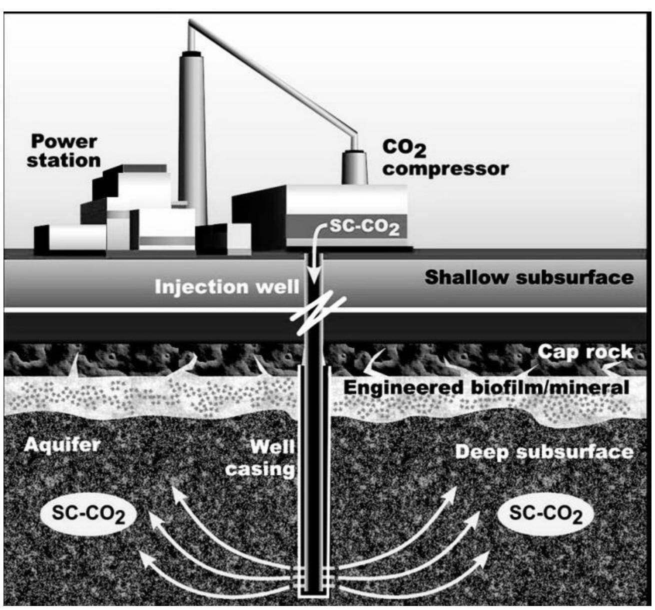

Figure 1.3: Schematic of $scCO_2$ injection into a subsurface target formation, with possible biofilm/mineral trap above injection formation (Mitchell et al., 2010).

The subsurface environments that have been proposed as potential sites for geologic CO_2 sequestration are depleted oil reservoirs, saline aquifers, and deep coal seams (van der Meer, 1993; Hitchon et al., 1999; Bachu, 2000). All are considered target sites for sequestration by the Department of Energy (2007) and the Intergovernmental Panel on Climate Change (2005). Supercritical CO_2 ($scCO_2$) injection has been used in the petroleum industry for years as a means to enhance oil recovery (EOR), but is now being considered as a strategy for reducing CO_2 emissions. Sequestration in deep saline aquifers depends on the same trapping mechanisms as in depleted oil reservoirs. These trapping mechanisms could include 1) 'hydrodynamic trapping' as a supercritical fluid under reservoir seals, 2) 'residual trapping' in reservoir rock pores, 3) 'solution trapping' as dissolved species (e.g. HCO_3^-) in formation waters, and 4) 'mineral trapping' as precipitated calcite, magnesite, siderite, or dawsonite (Kharaka et al., 2009). The mechanisms for trapping in coal seams include adsorption onto cleat surfaces and dissolution into the coal matrix (Larsen, 2004; Perera et al., 2011).

The injection of $scCO_2$ can have direct, physiological impacts on subsurface microbes. High pressure $scCO_2$ has been shown to deactivate cells by extracting intracellular material after solubilization of cellular membranes (Bertoloni et al., 2006; Oule et al., 2006), as well as interfering with protein synthesis (András et al., 2010). Supercritical CO_2 has also been shown to affect the structure and function of key cellular enzymes, though its effects vary greatly depending on enzyme and treatment methodology (Wimmer and Zarevúcka, 2010). In general, higher pressure and temperature will increase the microbiocidal effect of $scCO_2$ by increasing the diffusivity and solubility of $scCO_2$ while increasing the fluidity of cellular membranes, enhancing CO_2 penetration (Isenschmid et al., 1995; Hong and Pyun, 1999; Zhang et al., 2006).

In considering the possible effects on the natural microbial community of a CO_2 sequestration site, it is also important to understand the potential geochemical effects of subsurface CO_2 injection. Although direct contact of $scCO_2$ with cells has been shown to be extremely disruptive to living microorganisms (Zhang et al., 2006), organisms living on the margins of a target aquifer may only experience the secondary geochemical effects of $scCO_2$ injection. Even if geochemical effects can be accurately measured and/or predicted *in situ*, they do not necessarily predict changes in the microbial community. Conversely, measured changes in the microbial community will not necessarily predict changing geochemical conditions.

Using geochemical modeling Onstott (2005) predicts that CO_2-reducing methanogens should experience an increased free energy yield under high pCO_2 conditions. Modeling results also showed that acetoclastic methanogenesis may no longer be viable under such conditions, but could eventually be restored if acetogenesis from CO_2 is coupled to acetoclastic methanogenesis (Onstott, 2005). If both methanogenic pathways are occurring prior to CO_2 injection, then we would expect inhibition of acetolastic methanogens and stimulation of CO_2-reducing methanogens. This shift would also be accompanied by progressively lower $\delta^{13}C_{CH4}$ values due to a larger isotopic fractionation effect associated with the CO_2-reduction pathway (Whiticar, 1999). This hypothesis assumes that the initial pH drop due to higher pCO_2 is buffered in the system by mineral dissolution. However, the situation is complicated by the availability of H_2 for CO_2 reduction. In laboratory incubations the carbon isotopic fractionation factor (α_{CO2-}

$_{CH4}$) has been shown to depend on pH_2, suggesting that microbial CH_4 produced via the CO_2-reduction pathway may isotopically resemble gas formed via the acetoclastic pathway if pH_2 is low (Valentine et al., 2004). Isotopic measurements of gases alone are therefore insufficient to deduce metabolic activity, and must be accompanied by direct microbial biomass and isotopic measurements to understand the complete picture. However, one must also consider that increased CO_2 might effectively "dilute" available H_2, rendering little change in the energy available to microbial metabolic processes. Recent work from the Frio Formation in Texas and a CO_2 sequestration project in Montana showed that the energy available for acetoclastic and hydrogenotrophic methanogenesis changed very little in response to simulated CO_2 injection (Kirk, 2011). In the same study, the energy available to Fe(III) reduction fueled by hydrogen and acetate increased by 30 to 80 kJ/mole as a result of CO_2 injection.

The aforementioned geochemical effects might be anticipated *a priori*, but results from several field-scale studies in recent years provide valuable information for designing lab- scale experiments. Potential changes in formation water chemistry might result from; 1) a change in pH, 2) mineral dissolution, or 3) mineral precipitation. The geochemistry of formation waters will vary depending on the reservoir. However, prior to CO_2-EOR injections most petroleum reservoirs are waterflooded with "fresh" surface water as a means of secondary recovery (Satter et al., 2007). Therefore, the water chemistry is expected to change significantly as CO_2 flooding commences. Prior to CO_2 injection, the water might resemble a diluted brine in such reservoirs, but this may change as a result of reservoir pressurization and mixing with isolated brines post-injection (Gaus, 2010). This situation was observed in the Rangely field in Colorado, a depleted oil/gas reservoir and CO_2 injection site. Total salinity of the formation water increased significantly after CO_2 injection, as did Ca^{2+}, Mg^{2+}, and HCO_3^- in water sampled through 1999. These changes are thought to result from CO_2 and calcite dissolution into the formation water (Equations 5 and 15, respectively), and the mixing of previously isolated brines of higher salinity (Klusman, 2003). As expected there was a decrease in pH, but acidification was buffered by the dissolution of carbonate minerals. To illustrate the complexity of the matter, in recent flow-through experiments, Ca^{2+} has been shown to play an important role in regulating pH in artificial groundwater under high *p*CO2, both through the formation of solution phase complexes and biomineralization (Dupraz et al., 2009). Therefore, constituents released as a result of increased pCO_2 may play an important role in both buffering the system and promoting biomineralization. In a more complex system, one would expect geochemical changes to affect some organisms more than others, favoring acidotolerant, halophilic, or methanogenic organisms over those unable to tolerate the changing conditions.

The dissolution of CO_2 into groundwater will cause the formation of carbonic acid (Equation 1.8), which will lower the pH (Stumm and Morgan, 1996). Therefore, strategies to buffer the pH change may have the dual benefit of maintaining a physiologically tolerant pH for the native microbial community while increasing the solubility trapping capacity of the reservoir. One strategy being investigated is the amendment of groundwater with dissolved urea. Urea has already been investigated as a way to decrease porosity in caprock in oil reservoirs via bacterial hydrolysis (Ferris et al., 1996), as well as trapping radionuclides via co-precipitation with carbonate minerals (Mitchell and Ferris, 2005; Mitchell and Ferris, 2006; Fujita et al., 2008). Urea is a commonly utilized N-fertilizer that is produced on the industrial scale via reaction of ammonia and carbon dioxide. It is often applied to rice fields, global sources of atmospheric methane, to stimulate plant growth. Urea hydrolysis occurs both abiotically and biotically, with the latter process catalyzed by the urease enzyme at a rate that is 1014 times more rapid than the uncatalyzed reaction (Jabri et al., 1995). The first step of urea hydrolysis requires splitting the urea molecule into carbamic acid and ammonia (Equation 1.8). The carbamic acid is then further decomposed to ammonia and carbonic acid (Equation 1.9). Equations 1.10-12 show the pH-dependent reactions of carbonic acid and ammonia. The net result of urea hydrolysis is an increase in pH, NH_3, and $[CO_3^{2-}]_{Total}$, which can lead to calcite precipitation (Equation 1.13) in some systems when sufficient Ca^{2+} is present (Fujita et al., 2008). While it may be potentially beneficial in subsurface CO_2 reservoirs, the effects of urea on anaerobic microbial consortia have not been investigated. Urea hydrolysis was hypothesized to mitigate the pH drop caused by CO_2 injection, but also provide a ready source of ammonia, potentially stimulating a N-depleted ecosystem. The effects of urea amendment on a methanogenic microbial community metabolizing coal were investigated, and discussed in detail in Chapter 3.

$$CO_{2(g)} + H_2O \Leftrightarrow H_2CO_{3(aq)} \Leftrightarrow H^+_{(aq)} + HCO_3^-{}_{(aq)} \quad (1.8)$$

$$CO(NH_2)_2 + H_2O \rightarrow NH_2COOH + NH_3 \quad (1.9)$$

$$NH_2COOH + H_2O \rightarrow NH_3 + H_2CO_3 \quad (1.10)$$

$$H_2CO_3 \leftrightarrow HCO_3^- + H^+ \quad (1.11)$$

$$2NH_3 + 2H_2O \leftrightarrow 2NH_4^+ + 2OH^- \quad (1.12)$$

$$HCO_3^- + H^+ + 2OH^- \leftrightarrow CO_3^{2-} + 2H_2O \tag{1.13}$$

$$Ca^{2+} + CO_3^{2-} \leftrightarrow CaCO_3(s) \tag{1.14}$$

$$CaCO_{3(s)} + H^+_{(aq)} \Leftrightarrow Ca^{2+}_{(aq)} + HCO_3^-{}_{(aq)} \tag{1.15}$$

Microbes may also play an important role in CO_2 sequestration through the formation of biofilms in injection formations. Biofilms are thought to be the predominant form of microbial life natural environments, and are composed of attached cells embedded in extracellular polymeric substances including proteins and polysaccharides (Watnick and Kolter, 2000; Stoodley et al., 2002; Lewandowski and Beyenal, 2007). Biofilms can cause large changes in porosity and permeability of porous media including sandstone (Taylor and Jaffé, 1990), making them potentially useful for preventing leakage of $scCO_2$ from porous caprocks of CO_2 injection formations (Mitchell et al., 2009; Phillips et al., 2013). These same biofilms could potentially reduce the permeability of target injection formations, making them both a problem and a solution in the context of CO_2 sequestration. Mitchell et al. (2008) found that biofilm-attached cultures of *Bacillus mojavensis* showed a 10 fold reduction in colony forming units after $scCO_2$ exposure, while suspended cells of the same culture showed a 10^3 reduction in viable cells, indicating that biofilms may survive $scCO_2$ injection in subsurface formations. There is a high likelihood that subsurface microbes, whether attached in biofilms or present as pelagic cells, will impact the permanence of CO_2 sequestration, making this an important area of research.

1.6 CO_2 injection and microbial methanogenesis

The primary focus of this dissertation is microbial methanogenesis from coal, and one chapter is devoted to examining the potential effects of increasing pCO_2 on this process. Methanogenesis may be the only metabolic pathway responsible for fixing inorganic carbon in environments without any sedimentary organic carbon. Chappelle et al. (2002b) documented a lithoautotrophic methanogenic community of microorganisms in a basalt aquifer whose sole energy source was hydrogen, presumably produced via water-rock interactions (Chapelle et al., 2002b). This mineral source of hydrogen has been shown to occur in laboratory settings (Stevens and McKinley, 1995; Parkes et al., 2011) , and therefore may be the means by which autotrophic methanogenesis occurs in basalt aquifers. Because autotrophic methanogenesis is dependent upon not only H_2 availability, but also CO_2 for a carbon source, it is reasonable to expect that CO_2 injections will have a significant effect on methanogens.

Because deeply buried coal seams are considered a potential target for CO_2 sequestration, experiments were conducted to determine what effect increased pCO_2 may have on a microbial consortium actively degrading coal to form methane. Of the potential microbially-mediated reactions that may be occurring in deeply buried coal seams, acetogenesis and methanogenesis (Equations 1.1 and 1.2) are expected to be the most significantly impacted by CO_2 injection. Fermentation reactions resulting in CO_2 could become thermodynamically less favorable under high pCO_2 conditions, potentially retarding the microbial breakdown of coal. However, it is also possible that supercritical CO_2 ($scCO_2$) may act as a solvent for small organic monomers in the coal matrix (Kolak and Burruss, 2006), allowing for transport away from the injection site toward conditions more favorable for microbial growth. In this case, CO_2 injection would actually increase nutrient availability, potentially resulting in greater methanogenesis from coal. The same is true for any reservoir rock or formation with sedimentary organic matter (e.g. sandstone, dolomite, or shale) that could be liberated by dissolution into $scCO_2$.

1.7 Phospholipids as biomarkers for subsurface microorganisms

Phospholipid fatty acid (PLFA) analysis is a well-established technique in microbial ecology (Bligh and Dyer, 1959), with extensive advancements made by D.C. White and colleagues in the 1970's applying phospholipid techniques to environmental samples (White et al., 1979). Today, studies of microbial communities in diverse settings often employ multiple techniques, including PLFA analysis and molecular techniques such as 16S rRNA or DNA sequencing to capture a more complete picture of microbial diversity, community structure, and metabolic activities. Because PLFAs degrade rapidly after cell death, biomass estimates based on PLFA analysis are thought to be strictly based upon viable organisms (Harvey et al., 1986), though it may be possible that PLFAs remain intact after cell death under subsurface conditions (Fredrickson et al., 1997; Schouten et al., 2010). Under anaerobic conditions in marine sediments, PLFAs were degraded over the course of several days following cell death, while 16S rRNA copies and archaeal ether lipids remained relatively constant over the course of the experiment (Logemann et al., 2011). This gives PLFA analysis a distinct advantage over other molecular methods (e.g. DNA, 16S rRNA, 16S rDNA), which may detect dead cells. In addition, because PLFA analysis relies upon extraction of lipids from all organisms present in a given environment one avoids possible culture bias from trying to grow the same community in the lab (White et al., 1998). Phospholipid analysis also allows one to track changes in the lipid profile of the microbial assemblage as conditions (e.g. salinity, pH, nutrient amendments) change either *in-situ* (Macnaughton et al., 1999) or in laboratory microcosms (Frostegård et al., 1996).

Archaeal membrane lipids differ from bacterial membrane lipids in four ways, two of which are vital to their identification and separation from bacterial lipids (Koga and Morii, 2006). First, the hydrocarbon portion of archaeal lipids is bound to the glycerol backbone exclusively by an ether-type linkage, as opposed to the ester bond by which bacterial PLFAs are bound to their glycerol backbones. This makes archaeal phosphoether lipids (PEL) less susceptible to hydrolysis under mild alkaline conditions (typical PLFA analysis conditions) and thus easily separated from PLFAs once the PLFAs have been derivatized to fatty acid methyl esters (FAMEs). Second, the hydrocarbon portion of the PEL is predominately observed to be a highly branched, saturated isoprenoid, as opposed to the predominately straight chain fatty acids associated with bacteria. These chemical differences allow for separation and identification of the membrane lipids from both phylogenetic groups when they coexist within the same sample**.** Some archaeal groups, in particular the Crenarchaeota, possess glycerol dialkyl glycerol tetraether (GDGT) core lipids which form a monolayer rather than bilayer cellular membrane (Schouten et al., 2013). Both bi- and tetraether lipids can be found in numerous phylogenetic groups of archaea, though methanogenic archaea tend to possess smaller amounts of tetraether lipids as a proportion of their total lipids (Schouten et al., 2013).

Intact archaeal phosphoether lipids (PELs) are also commonly used as a measure of viable archaeal biomass (Sturt et al., 2004; Lipp et al., 2008). Due to their differing chemical structures and properties, PELs are inherently more difficult to extract and analyze than bacterial PLFAs from environmental samples. This difference in reactivity may cause archaeal intact phospholipids (IPLs) to be preferentially preserved over bacterial IPLs in subsurface sediments (Schouten et al., 2010), potentially leading to an overestimation of living archaeal biomass in such systems. The reactivity of intact PELs is most likely attributable to the identity of the polar head group attached to the glycerol backbone, e.g. glycosidic vs. phospho-containing head groups. While the extraction and quantification of PLFAs is relatively simple and reliable, extracting and quantifying PELs is considered more complex. Early studies of archaeal lipids relied upon the combination of a neutral Bligh-Dyer extraction (Bligh and Dyer, 1959; White and Ringelberg, 1998) with either BBR_3 (Chappe et al., 1980) or 57% HI (e.g. Gattinger et al., 2003) used to break the ether bond between the isoprenoid chain and glycerol backbone. This was followed by a reduction of the resulting alkyl halide with $LiAlH_4$ to a hydrocarbon which could be analyzed either by GC-FID or GC/MS. The addition of an acidified aqueous phase (10% trichloroacetic acid) to the extraction protocol was also shown to increase the recovery of archaeal lipids (Nishihara and Koga, 1987). Today these extraction steps are often done sequentially (neutral first, then acidified) when both bacterial and archaeal lipids are desired (Sturt et al., 2004; Lipp et al., 2008). This method of dual solvents was found to be the best for extracting archaeal IPLs from sediments (Lengger et al., 2012a), though a recent comprehensive study of extraction methods by Huguet et al. (2010) found better yields of IPLs with a 72 hour Soxhlet extraction. Zhang et al. (2012) also found better IPL yields with the combination of neutral and acidified solvents in a Bligh-Dyer extraction.

Once archael IPLs have been extracted there are several avenues for analysis. Archaeal IPLs may be analyzed directly using the combination of high performance liquid chromatography (HPLC) and electro-spray ionization mass spectrometry (ESI-MS) (Sturt et al., 2004). This method utilizes an aqueous mobile phase and glycosylated and phosphorylated IPLs are separated based upon the differences in polarity of the polar head groups (Schouten et al., 2013). Direct measurement of IPLs using HPLC-ESI-MS also has the advantage of avoiding any preparatory column chromatography (e.g. silica columns) or drying over Na_2SO_4, both of which have been shown to affect IPL yield (Pitcher et al., 2009; Huguet et al., 2010; Lengger et al., 2012b). IPLs can also be analyzed as core lipids with their polar head groups removed via acid hydrolysis (5% HCl:methanol) by using HPLC coupled with atmospheric pressure chemical ionization mass spectrometry (APCI-MS) (Hopmans et al., 2000). If the total lipid extract is analyzed in this manner, then both viable biomass and extant core lipids will be quantified. Huguet et al. (2010) showed that the contribution of IPLs to total lipids may be calculated by taking the difference in the amounts of core lipids measured directly from the total lipid extract and those measured after acid hydrolysis. The best quantitative method for core lipid analysis was achieved by using an internal glycerol trialkyl glycerol standard along with HPLC-APCI-MS and calculating individual response factors for each lipid analyzed (Huguet et al., 2006).

Microbial membrane lipid analysis is used extensively in this dissertation to describe the microbial communities associated with coal degradation under various environmental conditions. Chapters 2 and 3 combine PLFA data with quantitative polymerase chain reaction (qPCR) measurements of the functional genes for methanogenic archaea (mcrA) and for sulfate reducing bacteria (dsrA) for a more complete understanding of the microbial community structure and function in these experiments. PLFA and PEL analysis is also utilized in Chapter 4 to measure microbial biomass from sandstone cores injected with $scCO_2$. The analysis of intact PELs has advanced considerably in recent years, and methods in our laboratory have evolved to reflect this new knowledge, such as maximizing extraction efficiency by combining neutral and acidified solvent extracts. However, access to an HPLC-MS, in combination with the scale of microcosm experiments and low archaeal biomass throughout, proved to be limiting factors for measurement of archaeal PELs in the work presented here.

1.8 Thesis organization

The previous studies highlighted in this chapter have shown the complex nature of microbial processes in subsurface environments and the relationships between specific groups of organisms. Two of the chapters in this dissertation expand on this body of knowledge with microbial community analysis using polar membrane lipid techniques to examine microbial carbon flow in microcosm experiments as a proxy for subsurface coal bed methane reservoirs. Chapter 2 describes a suite of experiments designed to examine the interactions between sulfate reducing bacteria and methanogens in coal-degrading microcosms under nutrient-starved conditions. Chapter 3 discusses results from microcosm experiments with a coal-degrading, methanogenic consortium of microbes under varying CO_2 partial pressures and with varying urea amendments designed to determine the effects of CO_2 pressure on the process of methanogenesis from coal and its effect on microbial community structure. The potential buffering effects that urea amendments had on CO_2 injections was also examined. Chapter 4 expands on the topic of

CO_2 sequestration by directly determining the effect of supercritical CO_2 on both bacteria and methanogenic archaea enriched from the previously described coal-degradation experiments; this work was done in collaboration with Drs. Marte Gutierrez and Daisuke Katsuki in the Department of Civil and Environmental Engineering.

1.9 References

Abram J. W. and Nedwell D. B. (1978) Inhibition of methanogenesis by sulfate-reducing bacteria competing for transferred hydrogen. *Arch. Microbiol.* **117**, 89–92.

Aeckersberg F., Bak F. and Widdel F. (1991) Anaerobic oxidation of saturated hydrocarbons to CO_2 by a new type of sulfate-reducing bacterium. *Arch. Microbiol.* **156**, 5–14.

Amann R. I., Ludwig W. and Schleifer K. H. (1995) Phylogenetic identification and in situ detection of individual microbial cells without cultivation. *Microbiol. Rev.* **59**, 143–169.

András C. D., Csajági C., Orbán C. K., Albert C., Ábrahám B. and Miklóssy I. (2010) A possible explanation of the germicide effect of carbon dioxide in supercritical state based on molecular-biological evidence. *Med. Hypoth.***74**, 325–329.

Avery G. B. J., Shannon R. D., White J. R., Martens C. S. and Alperin M. J. (2003) Controls on methane production in a tidal freshwater estuary and a peatland: methane production via acetate fermentation and CO_2 reduction. *Biogeochemistry* **62**, 19–37.

Bachu S. (2000) Sequestration of CO_2 in geological media: criteria and approach for site selection in response to climate change. *Energy Convers. Manage.* **41**, 953–970.

Balkwill D. L. (1989) Numbers, diversity, and morphological characteristics of aerobic, chemoheterotrophic bacteria in deep subsurface sediments from a site in South Carolina. *Geomicrobiol. J.* **7**, 33–52.

Balkwill D. L., Fredrickson J. K. and Thomas J. M. (1989) Vertical and horizontal variations in the physiological diversity of the aerobic chemoheterotrophic bacterial microflora in vertical and horizontal variations in the physiological diversity of the aerobic chemoheterotrophic bacterial microflora in deep so. *Appl. Environ. Microbiol.* **55**, 1058–1065.

Balkwill D. L., Leach F. R., Wilson J. T., NcNabb J. F. and White D. C. (1988) Equivalence of microbial biomass measures based on membrane lipid and cell wall components, adenosine triphosphate, and direct counts in subsurface aquifer sediments. *Microbial Ecol.* **54**, 273–291.

Beckmann S., Lueders T., Krüger M., von Netzer F., Engelen B. and Cypionka H. (2011) Acetogens and acetoclastic methanosarcinales govern methane formation in abandoned coal mines. *Appl. Environ. Microbiol.* **77**, 3749–56.

Beller H. R., Spormann A. M., Sharma P. K., Cole J. R. and Reinhard M. (1996) Isolation and characterization of a novel toluene-degrading , sulfate-reducing bacterium. *Appl. Environ. Microbiol.* **62**, 1188–1196.

Bertoloni G., Bertucco A., Cian V. De and Parton T. (2006) A study on the inactivation of micro-organisms and enzymes by high pressure CO_2. *Biotechnol. Bioeng.* **95**, 155–160.

Bligh E. G. and Dyer W. J. (1959) A rapid method of total lipid extraction and purification. *Can. J. Biochem. Biophys.* **37**, 911–917.

Boone D. R., Rogers J. E. and Whitman W. B. (1990) Ecology of methanogenesis. In *The microbial production and consumption of greenhouse gases: methane, nitrogen oxides, and halomethanes.* American Society of Microbiology, Washington, D.C.

Brockman F. J., Kieft T. L., Fredrickson J. K., Bjornstad B. N., Li S. W., Spangenburg W. and Long P. E. (1992) Microbiology of vadose zone paleosols in south-central Washington State. *Microbial Ecol.* **23**, 279–301.

Caldwell M. E., Garrett R. M. and Prince R. C. (1998) Anaerobic biodegradation of long-chain n-alkanes under sulfate-reducing conditions. *Environ. Sci. Technol.* **32**, 2191–2195.

Canfield D. E., Thamdrup B., Kristensen E., Southward A. J., Tyler P. A., Young C. M. and Fuiman L. A. (2005) *Aquatic Geomicrobiology*, Elsevier Academic Press, New York.

Carr S. A., Vogel S. W., Dunbar R. B., Brandes J., Spear J. R., Levy R., Naish T. R., Powell R. D., Wakeham S. G. and Mandernack K. W. (2013) Bacterial abundance and composition in Marine Sediments beneath the Ross Ice Shelf, Antarctica. *Geobiology* **Accepted**.

Chapelle F. H., Bradley P. M., Lovley D. R., O'Neill K. and Landmeyer J. E. (2002a) Rapid evolution of redox processes in a petroleum hydrocarbon-contaminated aquifer. *Ground Water* **40**, 353–360.

Chapelle F. H., O'Neill K., Bradley P. M., Methe B. A., Ciufo S. A., Knobel L. L. and Lovley D. R. (2002b) A hydrogen-based subsurface microbial community dominated by methanogens. *Nature.* **415**, 312–315.

Chappe B., Michaelis W. and Albrecht P. (1980) Molecular fossils of Archaeabacteria as selective degradation products of kerogen. In *Advances in Organic Geochemistry 1979* (eds. A. G. Douglas and J. R. Maxwell). Pergamon Press, Oxford. pp. 265–274.

Coates J. D., Woodward J., Allen J. O. N. and Philp P. (1997) Anaerobic degradation of polycyclic aromatic hydrocarbons and alkanes in petroleum-contaminated marine harbor sediments. *Appl. Environ. Microbiol.* **63**, 3589–3593.

Crill P. M. and Martens C. S. (1986) Methane production from bicarbonate and acetate in an anoxic marine sediment. *Geochim. Cosmochim. Acta* **50**, 2089–2097.

Dupraz S., Parmentier M., Ménez B. and Guyot F. (2009) Experimental and numerical modeling of bacterially induced pH increase and calcite precipitation in saline aquifers. *Chem. Geol.* **265**, 44–53.

Faiz M. and Hendry P. (2006) Significance of microbial activity in Australian coal bed methane reservoirs- a review. *Bull. Can. Petrol. Geol.* **54**, 261–272.

Fakoussa R. M. and Hofrichter M. (1999) Biotechnology and microbiology of coal degradation. *Appl. Microbiol. Biotechnol.* **52**, 25–40.

Ferris F. G., Stehmeier L. G., Kantzas A. and Mourits F. M. (1996) Bacteriogenic mineral plugging. *Can. J. Petrol. Technol*. **35**, 56–61.

Flores R. M., Rice C. A., Stricker G. D., Warden A. and Ellis M. S. (2008) Methanogenic pathways of coal-bed gas in the Powder River Basin, United States: The geologic factor. *Int. J. Coal. Geol.* **76**, 52–75.

Fredrickson J. K. and Balkwill D. L. (2005) Geomicrobiological processes and biodiversity in the deep terrestrial subsurface. *Geomicrobiol. J.* **23**, 345–356.

Fredrickson J. K., Balkwill D. L., Zachara J. M., Li S. W., Brockman F. J. and Simmons M. A. (1991a) Physiological diversity and distributions of heterotrophic bacteria in deep Cretaceous sediments of the Atlantic coastal plain. *Appl. Environ. Microbiol.* **57**, 402–411.

Fredrickson J. K., Brockman F. J., Workman D. J., Li S. W. and Stevens T. O. (1991b) Isolation and characterization of a subsurface bacterium capable of growth on toluene, naphthalene and other aromatic compounds. *Appl. Environ. Microbiol.* **57**, 796–803.

Fredrickson J. K., McKinley J. P., Bjornstad B. N., Long P. E., Ringelberg D. B., White D. C., Krumholz L. R., Suflita J. M., Colwell F. S., Lehman R. M., Phelps T. J. and Onstott T. C. (1997) Pore-size constraints on the activity and survival of subsurface bacteria in a late Cretaceous shale-sandstone sequence, northwestern New Mexico. *Geomicrobiol. J.* **14**, 183–202.

Frostegård Å., Tunlid A. and Bååth E. (1996) Changes in microbial community structure during long-term incubation in two soils experimentally contaminated with metals. *Soil. Biol. Biochem.* **28**, 55–63.

Fry N. K., Fredrickson J. K., Fishbain S., Wagner M. and Stahl D. A. (1997) Population structure of microbial communities associated with two deep, anaerobic, alkaline aquifers. *Appl. Environ. Microbiol.* **63**, 1498–1504.

Fujita Y., Taylor J. L., Gresham T. L. T., Delwiche M. E., Colwell F. S., McLing T. L., Petzke L. M. and Smith R. W. (2008) Stimulation of microbial urea hydrolysis in groundwater to enhance calcite precipitation. *Environ. Sci. Technol.* **42**, 3025–3032.

Gattinger A., Günther A., Schloter M. and Munch J. C. (2003) Characterisation of Archaea in soils by polar lipid analysis. **1**, 21–28.

Gaus I. (2010) Role and impact of CO_2–rock interactions during CO_2 storage in sedimentary rocks. *Int. J. Greenhouse Gas Cont.* **4**, 73–89.

Gold T. (1992) The deep, hot biosphere. *Proc. Nat. Acad. Sci.* **89**, 6045–6049.

Grabowski A., Blanchet D. and Jeanthon C. (2005) Characterization of long-chain fatty-acid-degrading syntrophic associations from a biodegraded oil reservoir. *Res. Microbiol.* **156**, 814–821.

Green C. T. and Scow K. M. (2000) Analysis of phospholipid fatty acids (PLFA) to characterize microbial communities in aquifers. *Hydrogeol. J.* **8**, 126–141.

Hansen L. K., Jakobsen R. and Postma D. (2001) Methanogenesis in a shallow sandy aquifer, Romo, Denmark. *Geochim. Cosmochim. Acta* **65**, 2925–2935.

Harms G., Zengler K., Rabus R., Minz D., Rosselló-mora R. and Aeckersberg F. (1999) Anaerobic oxidation of o-xylene , m-xylene , and homologous alkylbenzenes by new types of sulfate-reducing bacteria alkylbenzenes by new types of sulfate-reducing bacteria. *Appl. Environ. Microbiol.* **65**, 999–1004.

Harvey H. R., Fallon R. D. and Patton J. S. (1986) The effect of organic matter and oxygen on the degradation of bacterial membrane lipids in marine sediments. *Geochim. Cosmochim. Acta* **50**, 795–804.

Haveman S. A., Pederson K. and Ruotsalainen P. (1999) Distribution and metabolic diversity of microorganisms in deep igneous rock aquifers of Finland. *Geomicrobiol. J.* **16**, 277–294.

Hinrichs K. U., Summons R. E., Orphan V., Sylva S. P. and Hayes J. M. (2000) Molecular and isotopic analysis of anaerobic methane-oxidizing communities in marine sediments. *Org. Geochem.* **31**, 1685–1701.

Hitchon B., Gunter W. D., Gentzis T. and Bailey R. T. (1999) Sedimentary basins and greenhouse gases: a serendipitous association. *Energy Convers. Manage.* **40**, 825–843.

Hoehler T. M., Alperin M. J., Albert D. B. and Martens C. S. (2001) Apparent minimum free energy requirements for methanogenic Archaea and sulfate-reducing bacteria in an anoxic marine sediment. *FEMS. Microbiol. Ecol.* **38**, 33–41.

Hoehler T. M., Alperin M. J., Albert D. B. and Martens C. S. (1998) Thermodynamic control on hydrogen concentrations in anoxic sediments. *Geochim. Cosmochim. Acta* **62**, 1745–1756.

Holmer M. and Storkholm P. (2001) Sulphate reduction and sulphur cycling in lake sediments: a review. *Freshwater Biol.* **46**, 431–451.

Hong S.-I. and Pyun Y.-R. (1999) Inactivation kinetics of Lactobacillus plantarum by high pressure carbon dioxide. *J. Food Sci.* **64**, 728–733.

Hopmans E. C., Schouten S., Pancost R. D., Van der Meer M. T. J. and Sinninghe Damsté J. S. (2000) Analysis of intact tetraether lipids in archaeal cell material and sediments by high performance liquid chromatography/atmospheric pressure chemical ionization mass spectrometry. *Rapid. Commun. Mass. Spectrom.* **14**, 585–589.

Huguet C., Hopmans E. C., Febo-Ayala W., Thompson D. H., Sinninghe Damsté J. S. and Schouten S. (2006) An improved method to determine the absolute abundance of glycerol dibiphytanyl glycerol tetraether lipids. *Org. Geochem.* **37**, 1036–1041.

Huguet C., Martens-Habbena W., Urakawa H., Stahl D. A. and Ingalls A. E. (2010) Comparison of extraction methods for quantitative analysis of core and intact polar glycerol dialkyl glycerol tetraethers (GDGTs) in environmental samples. *Limnol. Oceanogr. Meth*. **8**, 127–145.

Ingvorsen K., Zehnder a J. and Jørgensen B. B. (1984) Kinetics of sulfate and acetate uptake by Desulfobacter postgatei. *Appl. Environ. Microbiol.* **47**, 403–408.

Isenschmid A., Marison I. W. and von Stockar U. (1995) The influence of pressure and temperature of compressed CO2 on the survival of yeast cells. *J. Biotechnol.* **39**, 229–37.

J.W.H S., Elferink O., Visser A., Hulshoff Pol L. W. and Stams A. J. M. (1994) Sulfate reduction in methanogenic bioreactors. *FEMS. Microbiol. Rev.* **15**, 119–136.

Jabri E., Carr M. B., Hausinger R. P. and Karplus P. A. (1995) The crystal structure of urease from Klebsiella aerogenes. *Science.* **268**, 998–1004.

Jackson R. E. and Reddy K. J. (2007) Trace element chemistry of coal bed natural gas produced water in the Powder River Basin, Wyoming. *Environ. Sci. Technol.* **41**, 5953–5959.

Jones E. J. P., Voytek M. A., Corum M. D. and Orem W. H. (2010) Stimulation of methane generation from nonproductive coal by addition of nutrients or a microbial consortium. *Appl. Environ. Microbiol.* **76**, 7013–7022.

Jørgensen B. B. and Kaster S. (2006) Sulfur cycling and methane oxidation. In *Marine Geochemistry* (eds. H. D. Shulz and M. Zabel). Springer, Berlin.

Kashefi K. and Lovley D. R. (2003) Extending the upper temperature limit for life. *Science.* **301**, 934.

Kharaka Y. K., Thordsen J. J., Hovorka S. D., Nance H. S., Cole D. R., Phelps T. J. and Knauss K. G. (2009) Potential environmental issues of CO_2 storage in deep saline aquifers: Geochemical results from the Frio-I Brine Pilot test, Texas, USA. *Appl. Geochem.* **24**, 1106–1112.

Kieft T. L., Amy P. S., Brockman F. J., Fredrickson J. K., Bjornstad B. N. and Rosacker L. L. (1993) Microbial abundance and activities in relation to water potential in the vadose zones of arid and semiarid sites. *Microbial Ecol.* **26**, 59–78.

Kieft T. L., Mccuddy S. M., Onstott T. C., Davidson M., Lin L.-H., Mislowack B., Pratt L., Boice E., Lollar B. S., Lippmann-Pipke, J., Pfiffner S. M., Phelps T. J., Gihring T., Moser D. and Heerden A. V. (2005) Geochemically generated, energy-rich substrates and indigenous microorganisms in deep, ancient groundwater. *Geomicrobiol. J.* **22**, 325–335.

Kirk M. F. (2011) Variation in energy available to populations of subsurface anaerobes in response to geological carbon storage. *Environ. Sci. Technol.* **45**, 6676–6682.

Klusman R. W. (2003) A geochemical perspective and assessment of leakage potential for a mature carbon dioxideenhanced oil recovery project and as a prototype for carbon dioxide sequestration; Rangely field, Colorado. *AAPG Bull.* **87**, 1485–1507.

Koga Y. and Morii H. (2006) Special methods for the analysis of ether lipid structure and metabolism in archaea. *Anal. Biochem.* **348**, 1–14.

Kolak J. J. and Burruss R. C. (2006) Geochemical investigation of the potential for mobilizing non-methane hydrocarbons during carbon dioxide storage in deep coal beds. *Energy Fuels.* **20**, 566–574.

Kotelnikova S. (2001) Microbial production and oxidation of methane in the deep subsurface. *Earth Sci. Rev.* **58**, 367–395.

Kristjansson J. K., Schönheit P. and Thauer R. K. (1982) Different Ks values for hydrogen of methanogenic bacteria and sulfate reducing bacteria: An explanation for the apparent inhibition of methanogenesis by sulfate. *Arch. Microbiol.* **131**, 278–282.

Kuivila K. M., Murray J. W. and Devol A. H. (1990) Methane production in the sulfate-depleted sediments of two marine basins. *Geochim. Cosmochim. Acta* **54**, 403–411.

Lansdown J. ., Quay P. . and King S. . (1992) CH_4 production via CO_2 reduction in a temperate bog: A source of ^{13}C-depIeted CH_4. *Geochim. Cosmochim. Acta* **56**, 3493–3503.

Larsen J. W. (2004) The effects of dissolved CO_2 on coal structure and properties. *Int. J. Coal. Geol.* **57**, 63–70.

Laverman A. M., Pallud C., Abell J. and Cappellen P. Van (2012) Comparative survey of potential nitrate and sulfate reduction rates in aquatic sediments. *Geochim. Cosmochim. Acta* **77**, 474–488.

Lehman R. M., Franklin R. B. and Mills A. L. (2007) Microbial distributions and their potential controlling factors in terrestrial subsurface environments. In *The Spatial Distribution of Microbes in the Environment* (eds. R. B. Franklin and A. L. Mills). Springer, Amsterdam, The Netherlands.

Lehman R. M., O'connell S. P., Banta A., Fredrickson, J. K. Reysenbach A.-L., Kieft T. L. and Colwell F. S. (2004) Microbiological comparison of core and groundwater samples collected from a fractured basalt aquifer with that of dialysis chambers incubated in situ. *Geomicrobiol. J*. **21**, 169–182.

Lengger S. K., Hopmans E. C., Reichart G.-J., Nierop K. G. J., Sinninghe Damsté J. S. and Schouten S. (2012a) Intact polar and core glycerol dibiphytanyl glycerol tetraether lipids in the Arabian Sea oxygen minimum zone. Part II: Selective preservation and degradation in sediments and consequences for the TEX86. *Geochim. Cosmochim. Acta* **98**, 244–258.

Lengger S. K., Hopmans E. C., Sinninghe Damsté J. S. and Schouten S. (2012b) Comparison of extraction and work up techniques for analysis of core and intact polar tetraether lipids from sedimentary environments. *Org. Geochem.* **47**, 34–40.

Lewandowski Z. and Beyenal H. (2007) *Fundamentals of Biofilm Research*., CRC Press Inc., Lewis Publishers, Boca Raton, FL.

Liesack W., Schnell S. and Revsbech N. P. (2000) Microbiology of flooded rice paddies. *FEMS. Microbiol. Rev.* **24**, 625–645.

Lipp J. S., Morono Y., Inagaki F. and Hinrichs K. U. (2008) Significant contribution of Archaea to extant biomass in marine subsurface environments. *Nature.* **454**, 991–994.

Logemann J., Graue J., Köster J., Engelen B., Rullkötter J. and Cypionka H. (2011) A laboratory experiment of intact polar lipid degradation in sandy sediments. *Biogeosciences* **8**, 2547–2560.

Lovley D. R. and Chapelle F. H. (1995) Deep subsurface microbial processes. *Rev. Geophys.* **33**, 365–381.

Lovley D. R. and Klug M. J. (1986) Model for the distribution of sulfate reduction and methanogenesis in freshwater sediments. *Geochim. Cosmochim. Acta* **50**, 11–18.

Lovley D. R. and Klug M. J. (1983) Sulfate reducers can outcompete methanogens at freshwater sulfate concentrations. *Appl. Environ. Microbiol.* **45**, 187–192.

Macnaughton S. J., Stephen J. R., Venosa A. D., Davis G. A., Chang Y. and White D. C. (1999) Microbial population changes during bioremediation of an experimental oil spill. *Appl. Environ. Microbiol.* **65**, 3566–3574.

Madigan M. T. and Martinko J. M. (2006) *Brock Biology of Microorganisms*., Pearson Prentice Hall, Upper Saddle River, NJ.

Martens C. S. and Berner R. A. (1974) Methane production in the interstitial waters of sulfate-depleted marine sediments. *Science.* **185**, 1167–1169.

McBeth I., Reddy K. J. and Skinner Q. D. (2003) Chemistry of trace elements in coalbed methane product water. *Water. Res.* **37**, 884–890.

Van der Meer L. G. H. (1993) The conditions limiting CO_2 storage in aquifers. *Energy Convers. Manage.* **34**, 959–966.

Mills C. T., Amano Y., Slater G. F., Dias R. F., Iwatsuki T. and Mandernack K. W. (2010) Microbial carbon cycling in oligotrophic regional aquifers near the Tono Uranium Mine, Japan as inferred from δ13C and δ14C values of in situ phospholipid fatty acids and carbon sources. *Geochim. Cosmochim. Acta* **74**, 3785–3805.

Milucka J., Ferdelman T. G., Polerecky L., Franzke D., Wegener G., Schmid M., Lieberwirth I., Wagner M., Widdel F. and Kuypers M. M. M. (2012) Zero-valent sulphur is a key intermediate in marine methane oxidation. *Nature.* **491**, 541–6.

Mitchell A. C., Dideriksen K., Spangler L. H., Cunningham A. B. and Gerlach R. (2010) Microbially enhanced carbon capture and storage by mineral-trapping and solubility-trapping. *Environ. Sci. Technol.* **44**, 5270–5276.

Mitchell A. C. and Ferris F. G. (2006) Effect of strontium contaminants upon the size and solubility of calcite crystals precipitated by the bacterial hydrolysis of urea. *Environ. Sci. Technol.* **40**, 1008–1014.

Mitchell A. C. and Ferris F. G. (2005) The coprecipitation of Sr into calcite precipitates induced by bacterial ureolysis in artificial groundwater: Temperature and kinetic dependence. *Geochim. Cosmochim. Acta* **69**, 4199–4210.

Mitchell A. C., Phillips A. J., Hamilton M. A., Gerlach R., Hollis W. K., Kaszuba J. P. and Cunningham A. B. (2008) Resilience of planktonic and biofilm cultures to supercritical CO_2. *J. Supercrit. Fluids*. **47**, 318–325.

Mitchell A. C., Phillips A. J., Hiebert R., Gerlach R., Spangler L. H. and Cunningham A. B. (2009) Biofilm enhanced geologic sequestration of supercritical CO_2. *Int J. Greenhouse Gas Cont.* **3**, 90–99.

Mitterer R. M. (2010) Methanogenesis and sulfate reduction in marine sediments: A new model. *Earth. Planet. Sci. Lett.* **295**, 358–366.

Moser D. P., Onstott T. C., Fredrickson J. K., Brockman F. J., Balkwill D. L., Drake G. R., Pfiffner S. M. and White D. C. (2003) Temporal shifts in the geochemistry and microbial community structure of an ultradeep mine borehole following isolation. *Geomicrobiol. J.* **20**, 517–548.

Mountfort D. O., Kaspar H. F., Asher R. A. and Sutherland D. (2003) Influences of pond geochemistry , temperature , and freeze-thaw on terminal anaerobic processes occurring in sediments of six ponds of the McMurdo Ice shelf near Bratina Island, Antarctica. *Geochim. Cosmochim. Acta* **69**, 583–592.

Mountfort D. O., Kaspar H. F., Downes M. and Asher R. A. (1999) Partitioning effects during terminal carbon and electron flow in sediments of a low-salinity meltwater pond near Bratina Island , McMurdo Ice Shelf , Antarctica. *Appl. Environ. Microbiol.* **65**, 5493–5499.

Murakami Y., Fujita Y., Naganuma T. and Iwatsuki T. (2002) Abundance and viability of the groundwater microbial communities from a borehole in the Tono Uranium deposit area, central Japan. *Microbe. Env.* **17**, 63–74.

Muyzer G. and Stams A. J. M. (2008) The ecology and biotechnology of sulphate-reducing bacteria. *Nat. Rev. Microbiol.* **6**, 441–454.

Nishihara M. and Koga Y. (1987) Extraction and composition of polar lipids from the archaebacterium, Methanobacterium thermoautotrophicum: Effective extraction of tetraether lipids by an acidified solvent. *J. Biochem*. **101**, 997–1005.

Olson G. J., Dockins W. S., McFeters G. A. and Iverson W. P. (1981) Sulfate-reducing and methanogenic bacteria from deep aquifers in Montana. *Geomicrobiol. J.* **2**, 327–340.

Onstott T. C. (2005) Impact of CO_2 injections on deep subsurface microbial ecosystems and potential ramifications for the subsurface biosphere. In *Carbon Dioxide Capture and Storage in Deep Geologic Formations- Results from the CO_2 Capture Project* (ed. S. M. Benson). Elsevier Ltd., New York.

Onstott T. C., Moser D. P., Pfiffner S. M., Fredrickson J. K., Brockman F. J., Phelps T. J., White D. C., Peacock A., Balkwill D., Hoover R., Krumholz L. R., Borscik M., Kieft T. L. and Wilson R. (2003) Indigenous and contaminant microbes in ultradeep mines. *Env. Microbiol.* **5**, 1168–1191.

Oremland R. S., Marsh L. M. and Polcin S. (1982) Methane production and simultaneous sulphate reduction in anoxic, salt marsh sediments. *Nature.* **296**, 143–145.

Oremland R. S. and Polcin S. (1982) Methanogenesis and sulfate reduction: competitive and noncompetitive substrates in estuarine sediments. *Appl. Environ. Microbiol.* **44**, 1270–1276.

Oremland R. S. and Taylor B. F. (1978) Sulfate reduction and methanogenesis in marine sediments. *Geochim. Cosmochim. Acta* **42**, 209–214.

Orphan V. J., Hinrichs K. U., Ussler W., Paull C. K., Taylor L. T., Sylva S. P., Hayes J. M. and DeLong E. F. (2001) Comparative analysis of methane-oxidizing Archaea and sulfate-reducing Bacteria in anoxic marine sediements. *Appl. Environ. Microbiol.* **67**, 1922–1934.

Oule M. K., Tano K., Bernier A. M. and Arul J. (2006) Escherichia coli inactivation mechanism by pressurized CO_2. *Can. J. Microbiol.* **52**, 1208–1217.

Parkes R. J., Linnane C. D., Webster G., Sass H., Weightman A. J., Hornibrook E. R. C. and Horsfield B. (2011) Prokaryotes stimulate mineral H_2 formation for the deep biosphere and subsequent thermogenic activity. *Geology* **39**, 219–222.

Perera M. S. A., Ranjith P. G., Choi S. K. and Airey D. (2011) The effects of sub-critical and super-critical carbon dioxide adsorption-induced coal matrix swelling on the permeability of naturally fractured black coal. *Energy.* **36**, 6442–6450.

Phillips A. J., Lauchnor E., Eldring J. (Joe), Esposito R., Mitchell A. C., Gerlach R., Cunningham A. B. and Spangler L. H. (2013) Potential CO_2 leakage reduction through biofilm-induced calcium carbonate precipitation. *Environ. Sci. Technol.* **47**, 142–149.

Pitcher A., Hopmans E. C., Schouten S. and Sinninghe Damsté J. S. (2009) Separation of core and intact polar archaeal tetraether lipids using silica columns: Insights into living and fossil biomass contributions. *Org. Geochem.* **40**, 12–19.

Raskin L., Rittmann B. E. and Stahl D. A. (1996) Competition and coexistence of sulfate-reducing and methanogenic populations in anaerobic biofilms. *Appl. Environ. Microbiol.* **62**, 3847–3857.

Rice C. A., Bartos T. T., Ellis M. S., Schwochow S. D. and Nuccio V. F. (2002) Chemical and isotopic composition of water in the Fort Union and Wasatch Formations of the Powder River Basin, Wyoming and Montana: Implications for coalbed methane development. In *Coalbed Methane of North America, II* The Rocky Mountain Association of Geologists, Denver. pp. 53–70.

Rice D. D. (1983) Relation of natural gas composition to thermal maturity and source rock type in San Juan basin, northwestern New Mexico and southwestern Colorado. *AAPG Bull.* **67**, 1119–1218.

Rice D. D., Clayton J. L. and Pawlewicz M. J. (1989) Characterization of coal-derived hydrocarbons and source-rock potential of coal beds, San Juan basin, New Mexico and Colorado. *Int. J. Coal. Geol.* **13**, 597–626.

Roberts D. L. (1988) The relationship between macerals and sulfur content of some South African Permian coals. *Int. J. Coal. Geol.* **10**, 399–410.

Rothfuss F. and Conrad R. (1992) Vertical profiles of CH_4 concentrations, dissolved substrates and processes involved in CH_4 production in a flooded Italian rice field. **18**, 137–152.

Rueter P., Rabus R., Wilkes H., Aeckersberg F., Rainey F. A., Jannasch H. W. and Widdel F. (1994) Anaerobic oxidation of hydrocarbons in crude oil by new types of sulphate-reducing bacteria. *Nature.* **372**, 455–458.

Satter A., Iqbal G. M. and Buchwalter J. L. (2007) *Practical Enhanced Reservoir Engineering: Assisted with Simulation Software*., Pennwell Corporation, Tulsa, OK.

Schmidt R. (2007) Characterization of the Bacterial and Archaeal Communitites in Coalbed Methane Aquifers in the Wyodak-Anderson Coal Zone of the Powder River Basin, WY Using Polar Lipid Analysis Techniques. Thesis, Colorado School of Mines, Environmental Science and Engineering.

Schönheit P., Kristjansson J. K. and Thauer R. K. (1982) Kinetic mechanism for the ability of sulfate-reducers to outcompete methanogens for acetate. *Arch. Microbiol.* **132**, 285–288.

Schouten S., Hopmans E. C. and Sinninghe Damsté J. S. (2013) The organic geochemistry of glycerol dialkyl glycerol tetraether lipids: A review. *Org. Geochem.* **54**, 19–61.

Schouten S., Middelburg J. J., Hopmans E. C. and Sinninghe Damsté J. S. (2010) Fossilization and degradation of intact polar lipids in deep subsurface sediments: A theoretical approach. *Geochim. Cosmochim. Acta* **74**, 3806–3814.

Schulz S. and Conrad R. (1996) Influence of temperature on pathways to methane production in the permanently cold profundal sediment of Lake Constance. *FEMS. Microbiol. Ecol.* **20**, 1–14.

Scott A. R. (2002) Hydrogeologic factors affecting gas content distribution in coal beds. *Int. J. Coal. Geol.* **50**, 363–387.

Sievert S. M., Kiene R. P. and Schulz H. (2007) The Sulfur Cycle. In *The Oceanography Society* magazine, 117–123.

Stetter K. O., Fiala G., Huber G., Huber R. and Segerer A. (1990) Hyperthermophilic microorganisms. *FEMS. Microbiol. Rev.* **75**, 117–124.

Stevens T. O. and McKinley J. P. (1995) Lithoautotrophic microbial ecosystems in deep basalt aquifers. *Science.* **270**, 450–454.

Stoodley P., Sauer K., Davies D. G. and Costerton J. W. (2002) Biofilms as complex differentiated communities. *Annu. Rev. Microbiol.* **56**, 187–209.

Strąpoć D., Mastalerz M., Eble C. and Schimmelmann A. (2007) Characterization of the origin of coalbed gases in southeastern Illinois Basin by compound-specific carbon and hydrogen stable isotope ratios. *Org. Geochem.* **38**, 267–287.

Strąpoć D., Picardal F. W., Turich C., Schaperdoth I., Macalady J. L., Lipp J. S., Lin Y.-S., Ertefai T. F., Schubotz F., Hinrichs K.-U., Mastalerz M. and Schimmelmann A. (2008) Methane-producing microbial community in a coal bed of the Illinois basin. *Appl. Environ. Microbiol.* **74**, 2424–2432.

Stumm W. and Morgan J. J. (1996) *Aquatic Chemistry*. 3rd Edition, John Wiley and Sons, Inc., New York City.

Sturt H. F., Summons R. E., Smith K., Elvert M. and Hinrichs K. U. (2004) Intact polar membrane lipids in prokaryotes and sediments deciphered by high-performance liquid chromatography/electrospray ionization multistage mass spectrometry - new biomarkers for biogeochemistry and microbial ecology. *Rapid. Commun. Mass. Spectrom.* **18**, 617–628.

Takai K., Nakamura K., Toki T., Tsunogai U., Miyazaki M., Miyazaki J., Hirayama H., Nakagawa S., Nunoura T. and Horikoshi K. (2008) Cell proliferation at 122 degrees C and isotopically heavy CH_4 production by a hyperthermophilic methanogen under high-pressure cultivation. *Proc. Natl. Acad. Sci. USA.* **105**, 10949–10954.

Takashima M., Speece R. E. and Parkin G. F. (1990) Mineral requirements for methane fermentation. *Crit. Rev. Env. Control.* **19**, 37–41.

Taylor S. W. and Jaffé P. R. (1990) Substrate and biomass transport in a porous medium. Water Resour. Res.**26**, 2181–2194.

Thomsen U., Thamdrup B., Stahl D. A. and Canfield D. E. (2004) Pathways of organic carbon oxidation in a deep lacustrine sediment , Lake Michigan. *Limnol. Oceanogr.* **49**, 2046–2057.

Thorseth I. H., Torsvik T., Furnes H. and Muehlenbachs K. (1995) Microbes play an important role in the alteration of oceanic crust. *Chem. Geol.* **126**, 137–146.

Ünal B., Perry V. R., Sheth M., Gomez-Alvarez V., Chin K.-J. and Nüsslein K. (2012) Trace elements affect methanogenic activity and diversity in enrichments from subsurface coal bed produced water. *Frontier. Microbiol.* **3**, 1–14.

Valentine D. L., Chidthaisong A., Rice A., Reeburgh W. S. and Tyler S. C. (2004) Carbon and hydrogen isotope fractionation by moderately thermophilic methanogens. *Geochim. Cosmochim. Acta.* **68**, 1571–1590.

Ward J. A., Slater G. F., Moser D. P., Lin L. H., Lacrampe-Couloume G., Bonin A. S., Davidson M., Hall J. A., Mislowack B., Bellamy R. E. S., Onstott T. C. and Lollar B. S. (2004) Microbial hydrocarbon gases in the Witwatersrand basin, South Africa: implications for the deep biosphere. *Geochim. Cosmochim. Acta* **68**, 3239–3250.

Watnick P. and Kolter R. (2000) Biofilm, city of microbes. *J. Bacteriol.* **182**, 2675–2679.

Wegener G., Niemann H., Elvert M., Hinrichs K. U. and Boetius A. (2008) Assimilation of methane and inorganic carbon by microbial communities mediating the anaerobic oxidation of methane. *Env. Microbiol.* **10**, 2287–2298.

White C. M., Strazisar B. R., Granite E. J., Hoffman J. S. and Pennline H. W. (2003) Separation and capture of CO_2 from large stationary sources and sequestration in geological formations--coalbeds and deep saline aquifers. *J. Air. Waste. Manage. Assoc.* **53**, 645–715.

White D. C., Davis W. M., Nickels J. S., King J. D. and Bobbie R. J. (1979) Determination of sedimentary microbial biomass by extracting lipid phosphate. *Oecologia.* **40**, 51–62.

White D. C., Flemming C. a, Leung K. T. and Macnaughton S. J. (1998) In situ microbial ecology for quantitative appraisal, monitoring, and risk assessment of pollution remediation in soils, the subsurface, the rhizosphere and in biofilms. *J. Microbiol. Meth.* **32**, 93–105.

White D. C. and Ringelberg D. B. (1998) Signature lipid biomarker analysis. In *Techniques in Microbial Ecology* (eds. R. S. Burlage, R. Atlas, D. Stahl, G. Geesey, and G. Sayler). Oxford University Press, New York.

Whiticar M. J. (1999) Carbon and hydrogen isotope systematics of bacterial formation and oxidation of methane. *Chem. Geol.* **161**, 291–314.

Whitman W. B., Coleman D. C. and Wiebe W. J. (1998) Prokaryotes: the unseen majority. *Proc. Nat. Acad. Sci. USA.* **95**, 6578–6583.

Widdel F. and Pfennig N. (1977) A new anaerobic, sporing, acetate-oxidizing, sulfate-reducing bacterium, Desulfotomaculum (emend.) acetoxidans. *Arch. Microbiol.* **112**, 119–122.

Widdel F. and Pfennig N. (1981) Studies on dissimilatory sulfate-reducing bacteria that decompose fatty acids. *Arch. Microbiol.* **129**, 395–400.

Widdel F. and Rabus R. (2001) Anaerobic biodegradation of saturated and aromatic hydrocarbons. *Curr. Opin. Biotechnol.* **12**, 259–276.

Wimmer Z. and Zarevúcka M. (2010) A review on the effects of supercritical carbon dioxide on enzyme activity. *Int. J. Mol. Sci*. **11**, 233–253.

Winfrey M. R. and Zeikus J. G. (1977) Effects of sulfate on carbon and electron flow during microbial methanogenesis in freshwater sediments. *Appl. Environ. Microbiol.* **33**, 275–281.

Zakkour P. and Haines M. (2007) Permitting issues for CO_2 capture, transport and geological storage: A review of Europe, USA, Canada and Australia. *Int. J. Greenhouse Gas Cont.***1**, 94–100.

Zhang C. L., Wang J., Wei Y., Zhu C., Huang L. and Dong H. (2012) Production of branched tetraether lipids in the ower Pearl River and estuary: effects of extraction methods and impact on bGDGT proxies. *Frontiers Microbiol.* **2**, 274.

Zhang J., Davis T. A., Matthews M. A., Drews M. J., LaBerge M. and An Y. H. (2006) Sterilization using high-pressure carbon dioxide. *J. Supercrit. Fluid.* **38**, 354–372.

Zhou Z., Ballentine C. J., Kipfer R., Schoell M. and Thibodeaux S. (2005) Noble gas tracing of groundwater/coalbed methane interaction in the San Juan Basin, USA. *Geochim. Cosmochim. Acta* **69**, 5413–5428.

CHAPTER 2

Factors controlling the co-occurrence of microbial sulfate reduction and methanogenesis in coal bed reservoirs

Authors: Andrew W. Glossner, Lisa K. Gallagher, Christopher T. Mills, Lee Landkamer, Linda Figueroa, Junko Munakata-Marr, Kevin W. Mandernack

This chapter will be submitted to the journal Applied and Environmental Microbiology. Lisa Gallagher performed the DNA extractions and quantitative polymerase chain reaction (qPCR) measurements, and wrote the methodology pertinent to that work. All other experimental design, measurements, and writing was conducted by Andrew Glossner.

2.1 Abstract

Sulfate reduction and methanogenesis are often the terminal electron accepting processes in anaerobic sediments and subsurface reservoirs. They are generally considered to be mutually exclusive microbial metabolisms as sulfate reducers are able to outcompete methanogens for both hydrogen and acetate. There is ample evidence for the co-occurrence of sulfate reducing microorganisms (SRM) and methanogenic archaea in coal bed methane reservoirs in which methanogenesis is ongoing, suggesting that the model for separation of these processes based on sulfate concentration may not apply to such reservoirs. Here we present results from coal-degrading microcosm experiments with a methanogenic consortium enriched from coal from the Powder River Basin, WY which shows that methanogens and sulfate reducers may both function in coal-bearing reservoirs simultaneously. Experiments with sulfate concentrations from 50 to 1000 µM showed both processes were occurring, with no correlation between methanogenic potential and sulfate concentration. Experiments amended with acetate at defined sulfate

concentrations showed that the proportion of acetate consumed by methanogens increased with initial acetate concentration until the acetate concentration was greater than 500 µM. Phospholipid fatty acid (PLFA) analysis was used to track microbial community changes in these experiments. PLFAs considered bioindicators of SRM, including 10Me16:0 and *cy*17:0 correlated strongly with acetate amendment in experiments with 500 µM sulfate, while *i*15:0 and *i*17:0 correlated strongly in experiments with 200 µM sulfate, suggesting that stimulation of the microbial community with acetate was dependent upon the sulfate concentration. No bacterial PLFAs were correlated with acetate in control experiments with 5 mM molybdate. Data from this study suggest that sulfate reducers and methanogens may compete at very low rates for the same limited pool of acetate in coal bed methane reservoirs.

2.2 Introduction

Coal bed methane (CBM) has become an important energy resource, comprising roughly 10% of natural gas production, with approximately 40% of this gas being microbial in origin (Strąpoć et al., 2011). Some basins, such as the Powder River Basin in Wyoming and Montana, USA, have been shown, in both laboratory and field studies, to harbor active microbial communities capable of converting coal to methane (Harris et al., 2008; Ulrich and Bower, 2008; Jones et al., 2010). There is much commercial interest in developing microbial consortia or other technologies to enhance this process, but doing so requires a fundamental understanding of the interactions of the entire microbial community and metabolisms in these reservoirs.

The process of microbial methanogenesis from coal is complex, but it is thought to be enhanced with introduction of microbes and nutrients through meteoric water recharge (Strąpoć et al., 2011). Many of the largest sources of coal bed methane are biogenic and show this recharge zone as a common feature (Scott et al., 1994; Martini et al., 1996; Tseng, 1997; Martini et al., 1998; Walvoord et al., 1999; Zhou and Ballentine, 2006; Flores et al., 2008; McIntosh et al., 2008; Schlegel et al., 2011a; Schlegel et al., 2011b). Fermentative, anaerobic microorganisms then degrade the large geopolymers of coal to form long chain organic acids, which are then further broken down to monomers and oligomers and ultimately to the substrates necessary for methanogenesis, mainly hydrogen and acetate. For a review of the biogeochemical factors in this process see Strąpoć et al. (2011). In many anaerobic environments sulfate reducing microorganisms (SRM) and methanogenic archaea compete for these latter substrates, making them important microbial mediators of the global carbon cycle.

The competition between SRM and methanogens in anaerobic environments is governed mainly by factors such as sulfate, H_2, and acetate concentrations. However, sulfate reducers are known to outcompete methanogens for these substrates under both freshwater (Lovley and Klug, 1983; Lovley and Klug, 1986) and marine sulfate concentrations (Middelburg et al., 1993; Mitterer, 2010) due to their higher substrate affinity and lower threshold concentrations for these substrates (Schönheit et al., 1982; Muyzer and Stams, 2008). In marine sediments the commonly accepted model for the distribution of these two processes holds that methanogenesis will not emerge as the dominant terminal electron accepting process until all the sulfate has been depleted (Martens and Berner, 1974; Oremland and Taylor, 1978; Jørgensen and Kasten, 2006).

Because the concentration of sulfate in marine sediments is typically much higher (10-50 mM SO_4^{2-}) than in freshwater sediments (10-500 µM SO_4^{2-}) sulfate reducers often account for the majority of carbon mineralized under high sedimentation rates in marine sediments (Canfield et al., 2005). Under freshwater sulfate concentrations, however, SRM have adapted to the typically lower sulfate concentrations by having much lower half-saturation constants for sulfate (Ingvorsen et al., 1984) but will still rapidly deplete the available sulfate in freshwater sediments (Canfield et al., 2005).

Sulfate reduction in coal bed methane reservoirs

While previously discussed freshwater bogs, lake sediments, and surface waters illustrate the fundamental relationships between SRM and methanogens, deep subsurface basins with similarly low sulfate concentrations are different because physicochemical parameters, such as groundwater recharge or mineral dissolution, limit sulfate concentrations and organic matter degradation rates. Subsurface coal bed methane reservoirs can be viewed as essentially closed systems over short time periods because the rates of groundwater recharge and organic matter degradation are slow relative to surface sites (Bates et al., 2011). Thus, determining which process (sulfate reduction or methanogenesis) is dominant becomes a question of timing rather than geochemical zonation as in sediments. Schlegel et al. (2011) argue that in parts of the Illinois Basin sulfate reduction occurred at some point in the past 10 ka, imparting an isotopically lighter signature on the DIC and enriching the remaining sulfate pool in $^{34}SO_4$. The authors argue that methanogenesis occurred subsequent to sulfate reduction and that methanogenesis had not yet overprinted the isotopic signature of the DIC that sulfate reduction had generated. In this model sulfate reduction and methanogenesis are mutually exclusive processes separated by time rather than geochemical zonation. Other studies have found either 16S rRNA (Green et al., 2008; Ulrich and Bower, 2008) or lipid biomarkers (Schmidt, 2007) for SRM in coal bed methane reservoirs or associated with methanogenesis from coal in abandoned mines (Beckmann et al., 2011). It is therefore possible that sulfate reduction and methanogenesis may occur contemporaneously in such reservoirs, albeit at very low rates due to the lack of labile carbon.

In the Powder River Basin in Wyoming and Montana, produced water from the Wyodak-Anderson coal zone tends to have very low sulfate concentrations (median 1.6 µM) (Rice et al., 2008), though localized regions within the basin can have much higher sulfate concentrations (up to 40 mM) (Ulrich and Bower, 2008). Other studies have found evidence for active sulfate reduction in overlying aquifers of the Powder River Basin in Montana, USA (Dockins et al., 1980; Olson et al., 1981). Acetate is another potential limiting nutrient for SRM and methanogens in coal beds, and has also been observed in produced waters from the Powder River Basin, but generally at low levels ($<$ 2 µM) (Ulrich and Bower, 2008). Acetate has been observed to be an important intermediate in the degradation of complex organic matter in environments such as peat bogs (Metje and Frenzel, 2007), oil reservoirs (Bonch-Osmolovskaya et al., 2003), lacustrine sediments (Winfrey and Zeikus, 1979; De Graaf et al., 1996), and various organic-rich shales, clays, and mudstones (Jones et al., 1989; McMahon et al., 1992; Routh et al., 2001) where it is generally maintained at very low concentrations ($<$10 µM) by active methanogenesis. Acetate has also been shown to be an important intermediate in coal degradation both in abandoned coal mines (Beckmann et al., 2011) and in the Forest City Basin CBM reservoir (McIntosh et al., 2008). Given the variability of sulfate concentrations and the limited metabolic activity of the microbial community in CBM wells it is possible that sulfate reduction and methanogenesis co-occur in CBM reservoirs like the Powder River Basin, with both being limited by the availability of acetate.

This study attempts to determine which factor, sulfate concentration or acetate availability, is the controlling factor in regulating the competition between SRM and methanogens in coal beds of the Powder River Basin. A series of microcosm experiments was undertaken with a microbial consortium enriched from coal from the Powder River Basin, WY and maintained on coal. These experiments were conducted under variable concentrations of sulfate and acetate that spanned those measured directly from produced waters in the Powder River Basin (Orem et al., 2007;Rice et al., 2008). The effects that these variations had on the bacterial community structure were analyzed using phospholipid fatty acids (PLFAs). PLFA analysis is a commonly accepted method for determining both living microbial biomass (Balkwill et al., 1988; Boschker et al., 1998; Mills et al., 2010) as well as community structure when specific biomarkers for metabolic groups of organisms can be identified (Dowling et al., 1986; Vainshtein et al., 1992). To track carbon flow in each microcosm experiment, we measured sulfate and acetate concentrations, methane production, and PLFA biomarkers. Additionally, methyl coenzyme-M reductase (mcrA) and dissimilatory sulfite reductase (dsrA), the functional genes for methanogens and sulfate reducers respectively, were measured by quantitative polymerase chain reaction (qPCR) to better understand how environmental conditions affected each group of organisms.

2.3 Methods

Experimental design

Coal was collected in September, 2009 by straining cuttings from the effluent of working drill rigs in the Powder River Basin, Wyoming. Three seams were sampled from the Wyodak- Fort Union formation, including the Big George, Smith, and Felix seams at depths ranging from 240 to 610 meters. Coal cuttings were immediately rinsed with sterile deionized water in the field to remove drilling fluids, placed in sterile whirl-pak bags, sealed in vacuum bags with chemical oxygen scrubbers, and stored at 4˚C until use.

A mixed consortium of microorganisms capable of degrading coal that contained both SRM and methanogens was enriched from these coal cuttings by adding coal cuttings to anaerobic nutrient medium in the same manner described below. This enrichment was continually incubated at 30˚C and maintained by inoculating microcosms with fresh coal every 60 days from the most productive microcosms of the previous set. The mineral solution was modified to exclude sulfate from the medium by replacing $MgSO_4$ with $MgCl_2$, and sulfate was added to the desired concentration as Na_2SO_4. The medium included (g/L) NaCl (0.8), NH_4Cl (1.0), KH_2PO_4 (0.1), KCl (0.1), $MgCl_2 \cdot 6H_2O$ (0.17), $CaCl_2 \cdot 2H_2O$ (0.04), $NaHCO_3$ (1.0), nitrilotriacetic acid (0.02), $MnSO_4 \cdot H_2O$ (0.01), $Fe(NH_4)2SO_4 \cdot 6H_2O$ (0.008), $CoCl_2 \cdot 6H_2O$ (0.002), $ZnSO_4 \cdot 7H_2O$ (0.002), $CuCl_2 \cdot 2H_2O$ (0.0002), $NiCl_2 \cdot 6H_2O$ (0.0002), $Na_2MoO_4 \cdot 2H_2O$ (0.0002), Na_2SeO_4 (0.0002), Na_2WO_4 (0.0002). Medium was prepared by flash-autoclaving DI water to reduce oxygen saturation, then sparging with 4:1 N_2:CO_2 for 15 minutes before adding 10 mL of trace metal solution, 50 mL trace mineral solution, and 1 g/L $NaHCO_3$ just before sealing under N_2:CO_2 and autoclaving. Anaerobic trace vitamin solution (10 mL) which had been filter-sterilized was added after the medium cooled in the anaerobic chamber. Upon sealing with butyl rubber stoppers (Bellco #2048-18150), the headspace of each serum bottle was purged with 4:1 N_2:CO_2 for at least 5 minutes and pressurized to the desired headspace pressure.

All experiments utilized the microbial consortium noted above and were prepared in an anaerobic chamber with 5% H_2, 5% CO_2, and the balance of N_2 atmosphere. Experiments were initiated by weighing 10 g coal in the chamber and adding to sterile 200 mL serum bottles. The anaerobic medium was added at the ratio of 5:1 (vol: wt coal) and all experiments were inoculated with the microbial consortium. Three different sets of experiments were undertaken to examine the competition between SRM and methanogens for substrates derived from coal. The first set of experiments, hereafter referred to as variable sulfate experiments, included variable concentrations of sulfate from 100 µM to 1000 µM to determine if sulfate concentration dictated the competition between the two metabolic groups. The following two sets of experiments were amended with variable concentrations of acetate including 250, 500 and 1000 µM, and each set was initiated with a pre-selected sulfate concentration of either 200 µM or 500 µM, hereafter referred to as 200-$SO_4$and 500-SO_4, respectively. These concentrations were chosen in order to mimic the expected range of measurable sulfate concentrations reported for produced water from the Powder River Basin (Rice et al., 2008). The background levels of acetate in the acetate amendment experiments were 50 µM in 200 µM sulfate and 100 µM in 500 µM sulfate experiments. Every tested sulfate or acetate condition also included the appropriate control experiments utilizing 5 mM sodium molybdate as an inhibitor for sulfate reducers (Yadav and Archer, 1989).

Low molecular weight organic acids (acetate, propionate, formate, succinate, oxalate, and citrate) were monitored by high performance liquid chromatography (HPLC) on an Agilent 1100 Series with a BioRad HPX-87H column (300 x 7.8 mm) and UV/VIS detector set at 210 nm. The concentrations of CH_4 and CO_2 were measured using a GC-17A gas chromatograph (Shimadzu, Kyoto, Japan). CH_4 was separated using a HayesepQ packed column (2m; Supelco) and CO_2 was separated using a molecular sieve (5Å pore size, 2m) held at 100 ˚C with a thermal conductivity detector (200 ˚C) and flame ionization detector (200 ˚C) connected in series for quantification. The calibration of the instrument was checked periodically with authentic CH_4 and CO_2 standards obtained from Scott Specialty Gases (Plumsteadville, PA).

Rate determinations for sulfate reduction and methanogenesis

Determining the rate of microbial sulfate reduction in mixed cell suspensions or sediment slurries is generally accomplished by amending experiments with $^{35}SO_4^{2-}$ and trapping the resulting radiolabelled S^{2-}. This method was not feasible in this work due to the presence of coal as primary substrate in all experiments. In order to test the hypothesis that sulfide could be recovered from coal in a quantitative manner, coal slurries (10g) were amended with 1.0 mM sulfide solutions and allowed to incubate for 24h. The sulfide amended slurries were then extracted for acid volatile sulfide using 6N HCl. The evolved H_2S was trapped with Zn-acetate solutions (EPA, 1996a) and then titrated iodometrically (EPA, 1996b). Relative to controls without coal, less than 50% of the 1 mM sulfide solution added to the coal slurries was recovered using this method, while 100 µM sulfide solutions were consistently overestimated using this method (Table 2.) suggesting that the coal strongly adsorbed the sulfide. Therefore, rates of sulfate reduction in this study were determined by measuring the rate of sulfate consumption. It was assumed that the change in sulfate concentration in experiments not amended with molybdate was due solely to dissimilatory sulfate reduction. The maximum rate of sulfate reduction (R_{SR}) was determined from the change in sulfate concentration during the linear portion of sulfate consumption between days 1 and 17 of the experiment. Rates of methanogenesis were determined from the change in headspace methane concentration during the linear phase of methane accumulation over the same time period.

Microbial Community Analysis by PLFAs

All solvents used for PLFA analysis were HPLC grade, and aqueous solutions were stored over chloroform to remove trace organic contamination. All glassware used in the preparation of PLFAs was baked for at least 6 hours at 460 ˚C prior to use. Once experiments were completed 1.0 mL subsamples were taken for DNA analysis and frozen at -80 ˚C. The remaining contents of each experiment were then frozen at -80 ˚C and the entire sample lyophilized (T = -80 ˚C, P = 0.08 Torr). Samples were then transferred to glass centrifuge tubes and extracted using a modified Bligh-Dyer extraction (White and Ringelberg, 1998) by shaking on a rotary shaker table at 150 rpm for two hours, followed by centrifugation at 1000 rpm for 30 minutes. The supernatant was decanted into separatory funnels and the solvent ratios adjusted to 1:1:0.8 by adding chloroform and 50 mM phosphate buffer and then allowed to separate overnight. The sample was then re-extracted for archaeal phosphoether lipids by adding 75 mL methanol, 37.5 mL chloroform, and 30 mL 10% trichloroacetic acid (wt:vol). The supernatant from this second extraction was phase separated overnight by adding 30 mL water and 37.5 mL chloroform. The volume of both total lipid extracts was reduced under a N_2 stream and then separated into neutral, glyco- and polar lipid classes using silica solid phase extraction columns (Alltech 500mg, 209200). SPE columns were prepared by washing with 5 mL methanol followed by 10 mL chloroform. Following loading of the columns with the total lipid extract, neutral lipids were eluted in 10 mL chloroform, glycolipids in 10 mL acetone, and polar lipids in 10 mL methanol. Fatty acid methyl esters (FAMEs) were prepared by mild alkaline methanolysis by treating the polar lipid phase with 1.0 mL 5% KOH:methanol (wt/vol) and 1.0 mL 1:1 methanol:toluene and incubating for 30 min at 37 ˚C. FAMEs were then extracted three times with 4:1 hexane:chloroform and concentrated. All samples and blanks were injected with an internal standard (C13:0, CAS# 1731-88-0) for quantification. The position of the double bond in monounsaturated PLFAs was determined by making their dimethyl disulfide adducts (Dunkelblum et al., 1985). Two ubiquitous FAMEs were commonly seen in blanks (C16:0 and C18:0) and were generally on the order of 2 nmol total.

GC-MS Procedures

FAMEs were analyzed on an Agilent 7890A gas chromatograph with a DB-1MS column (60m x 0.25 mm I.D.), and quantified using a flame ionization detector (FID) coupled to an Agilent 5975C Inert XL mass spectrometer for FAME identification. The identity of each FAME was preliminarily assigned based on comparison of retention times with those of FAMEs from a standard mixture (Sigma Aldrich #47785-U). The injector temperature was 280˚C, the FID set to 200˚C, and the ion source temperature set to 250˚C. The oven temperature program began at 50˚C, then increased as follows: 150˚C at 20 C˚ min^{-1}, 210˚C at 1.5 C˚ min^{-1}, 280˚C at 10 C˚ min^{-1} and held for a final 8 min at 280˚C. The flow rate in the column was 1.5 mL min^{-1}. FAME identity was confirmed after ionization with electron ionization at 70 eV.

PLFA Nomenclature

Phospholipid fatty acids are described in this work using the following nomenclature: A:BωC, where A is the number of carbon atoms in the molecule, B is the number of points of unsaturation in the molecule, and C is the number of carbons away from the ω end of the lipid at which the double bond is located. The prefix *i* denotes a methyl branch at the *iso* position of the carbon chain, *ai* corresponds to a methyl group at the *anteiso* position, *cy* denotes a *cyclopropyl* ring at an unspecified position within the carbon chain, and 10Me denotes a methyl group at the 10^{th} carbon from the carboxyl end of the lipid.

qPCR of the mcrA gene

Quantitative (real time) polymerase chain reaction (qPCR) analysis was used to enumerate methanogens based on the presence of the mcrA functional gene unique to methanogenic organisms. Bulk deoxyribonucleic acid (DNA) was extracted from samples using the MoBio Powersoil® Kit. Methyl coenzyme reductase, subunit alpha (mcrA) genes were amplified using the primer set mlas/mcrA-rev (Steinberg and Regan 2008; mlas 5'-GGTGGTGTM GGDTTCACMCARTA-3'/ mcrA-rev 5'-CGTTCATBGCGTA GTTVGGRTAGT-3'). Quantification of copy numbers was performed using a LightCycler 480 II instrument (Roche, Branford, CT). Each reaction (20 µl) contained 10 µl Perfecta SYBR Green Supermix (Quanta Biosciences, Gaithersburg, MD), 7 µl nuclease-free water, 1 µl each primer (10 µM each), and 2 µl template DNA. Cycling conditions were as follows: initial denaturation step at 95°C for 3.5 min, followed by 45 cycles of denaturation at 95°C for 30 s, annealing at 55°C for 45 s, and extension at 72°C for 1 min, followed by a final extension step at 72°C for 7 min. Specificity of product formation was confirmed by melt curve analysis (55°C to 95°C with acquisition every 0.5°C). *Methanosarcina mazei* was used as a standard. DNA concentration was calculated based on triplicate measurements on a Bioanalyzer 2100 (Agilent Technologies, Santa Clara, CA). The copy number was calculated based on this concentration, then a standard curve based on 10-fold serial dilutions was constructed to determine gene copy numbers in unknown samples. Samples, standards and controls were run in duplicate. Raw data were exported to LinRegPCR (Ramakers et al., 2003; Ruijter et al., 2009), which estimates fluorescence baseline using an algorithm that constructs the log-linear phase from the plateau stage downward. This software was used to calculate an average efficiency per amplicon, a common window of linearity, fluorescence threshold, and starting concentrations. Average efficiencies ranged from 1.792 to 1.808.

qPCR of the dsrA gene

qPCR analysis was used to enumerate sulfate-reducing bacteria based on the presence of the dsrA functional gene. Bulk DNA was extracted from samples using the MoBio Powersoil® Kit. Dissimilatory sulfate reductase, subunit alpha (dsrA) genes were amplified using the primer set DSR1F/Del1075R (Gittel et al. 2009; DSR1F 5’-AC(GC)CACTGGAAGCACG-3’/ Del1075R 5’-G(CT)TC(ACG)CGGTTCTT(GAT)C-3’). Quantification of copy numbers was performed using a LightCycler 480 II Instrument (Roche). Each reaction (20 µl) contained 10 µl Perfecta SYBR Green

Supermix (Quanta Biosciences), 3 µl nuclease-free water, 1 µl each primer (100 pmol μl^{-1} each), and 5 µl template DNA. Cycling conditions were as follows: initial denaturation step at 95°C for 10 min, followed by 45 cycles of denaturation at 95°C for 30 s, annealing at 58°C for 30 s, and extension at 72°C for 1 min. Specificity of product formation was confirmed by melt curve analysis (58°C to 95°C with acquisition every 0.5°C). *Desulfovibrio vulgaris* was used as a standard. DNA concentration was calculated based on triplicate measurements on a Bioanalyzer 2100 (Agilent Technologies). The copy number was calculated based on this concentration, then a standard curve based on 10-fold serial dilutions was constructed to determine gene copy numbers in unknown samples. Samples, standards and controls were run in duplicate. Raw data were exported to LinRegPCR (Ramakers et al., 2003; Ruijter et al., 2009) to calculate an average efficiency per amplicon, a common window of linearity, fluorescence threshold, and starting concentrations. Average efficiencies ranged from 1.783 to 1.812.

2.4 Results

Methane production

Figure 2.1 shows the methane production for the variable sulfate experiments, with sulfate concentrations ranging from 50 µM to 1000 µM, along with the control experiments with 5 mM sodium molybdate. Increasing sulfate concentrations were hypothesized to decrease methane production as SRM consumed more of the acetate available from the coal. Therefore, inhibiting SRM with 5 mM molybdate was expected to enhance methane production relative to the uninhibited experiments at each sulfate concentration. In both the inhibited and uninhibited experiments, however, the sulfate concentration did not significantly affect methane production. Each experiment produced between 0.8 and 2 µmol CH_4 per gram of coal, with the lowest methane production observed in experiments with 500 µM SO_4. All microcosms inhibited with 5 mM molybdate produced the same amount of methane as their uninhibited counterparts, except for microcosms at 50 µM sulfate, which produced significantly more when inhibited with molybdate (t test, $p < 0.05$; Figure 2.1).

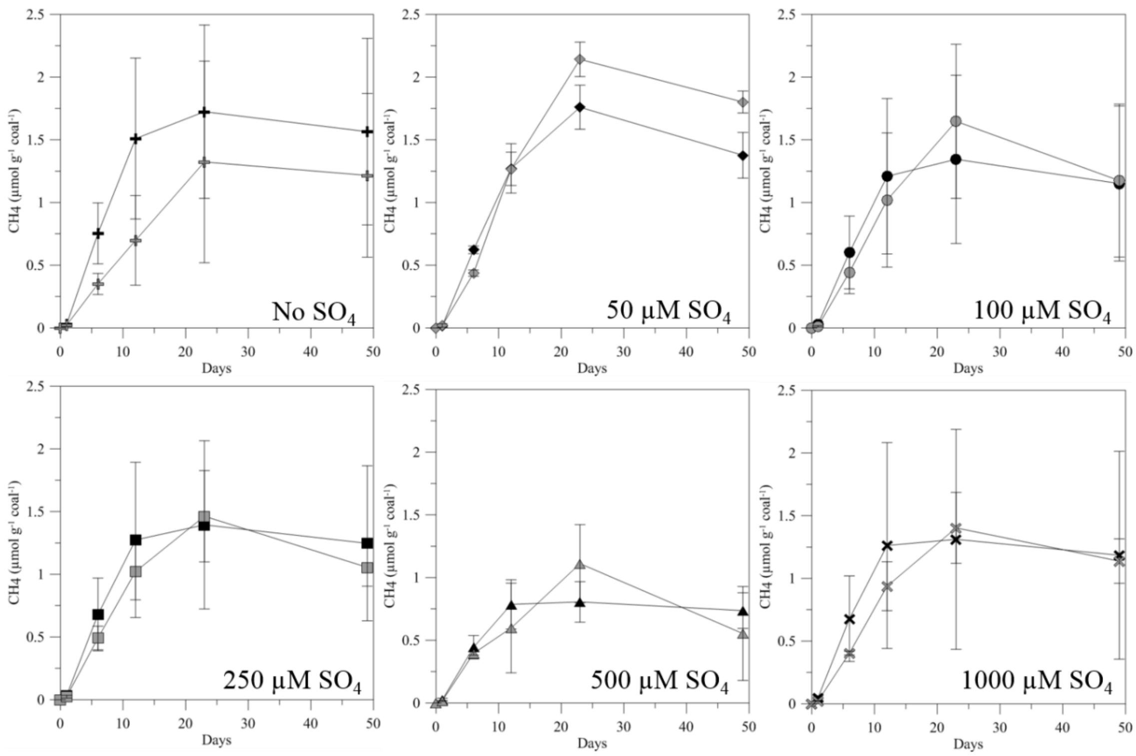

Figure 2.1: CH_4 production in experiments with variable sulfate concentrations. ✚ No sulfate; ♦ 50 µM sulfate; ● 100 µM sulfate; ■ 250 µM sulfate; ▲ 500 µM sulfate; ✖ 1000 µM sulfate. Gray symbols represent 5 mM molybdate controls at each sulfate concentration (error bars represent 1 standard deviation of triplicate incubations).

Because sulfate amendment did not have a discernible effect on methane production, acetate production from the fermentation of coal was hypothesized to ultimately determine the relative dominance of methanogens or SRM in coal-based microcosms. This was tested in microcosms amended with coal, 200 µM SO_4 and 500 μM SO_4 and different acetate concentrations up to 1000 μM. Methane production was greatest in microcosms in which SRM were inhibited with 5 mM molybdate (Figure 2.2). The greatest methane concentration was observed in samples with 1000 μM acetate plus 5 mM molybdate [2.1 ± 0.3 μmoles CH_4 $g^{-1}coal^{-1}$ in 200-SO_4 experiments; 2.8 ± 0.1 μmoles CH_4 $g^{-1}coal^{-1}$ in 500-SO_4 experiments (Figure 2.2)]. The methane production in microcosms with 1000 μM acetate plus 5 mM molybdate was statistically larger than the methane production in uninhibited microcosms at 1000 μM acetate for 200-SO_4 experiments (t-test, 2 tailed, $p < 0.05$). The methane production in microcosms with 500 and 1000 μM acetate was significantly higher than in uninhibited microcosms for 500-SO_4 experiments (t-test, 2 tailed, $p < 0.05$). Methane production correlated strongly with the initial acetate concentration in both acetate amendment experiments with 200-SO_4 500-SO_4 (Pearson's r = 0.739 and 0.649, respectively, $p < 0.05$) suggesting that the methane produced in these experiments resulted from acetoclastic methanogenesis.

Acetate consumption

Acetate was observed in all experiments with variable SO_4, which were not amended with acetate, but at concentrations less than 100 μM it was quickly depleted below detection (10 μM) (data not shown). At the same acetate concentrations, the consumption of acetate was similar for microcosms with or without molybdate in the 200 μM and 500 μM sulfate experiments (Figure 2.3). Acetate was consumed in all microcosms to concentrations below detection after 17 days in experiments with 500 μM sulfate, but remained in experiments with 200 μM sulfate for over 30 days (Figure 2.3). The most rapid decreases in acetate concentration occurred in microcosms without molybdate at both 200 and 500 μM sulfate (Figure 2.3).

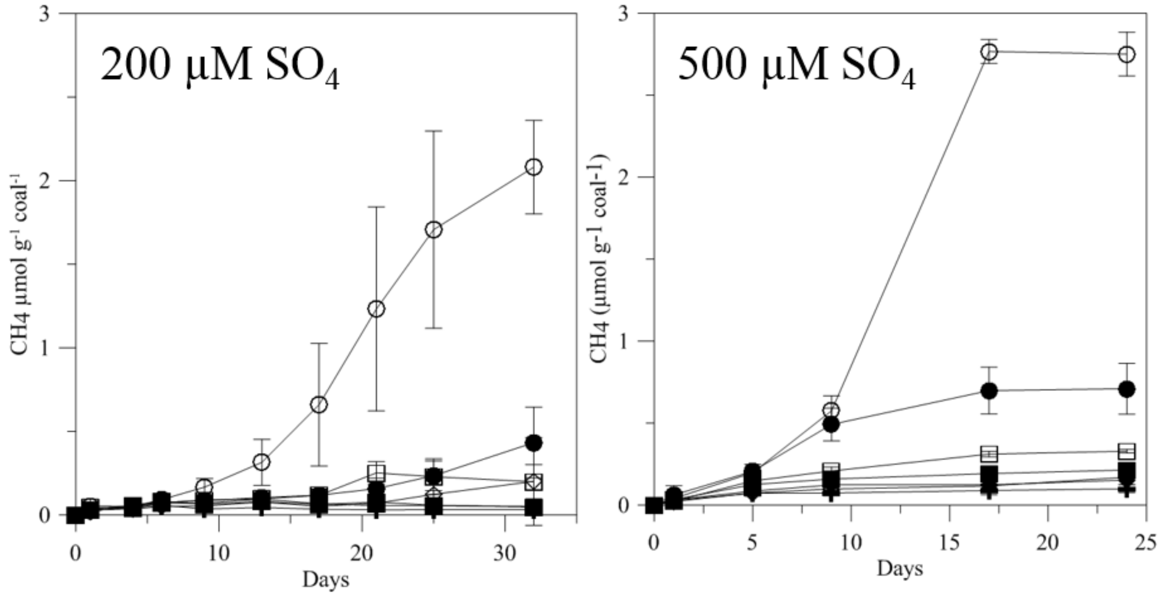

Figure 2.2: CH_4 production in 200 and 500 µM SO_4 experiments. ✚ No acetate; ♦ 250 µM acetate; ■ 500 µM acetate; ● 1000 µM acetate; open symbols correspond to 5 mM molybdate control experiments at the given acetate concentration.

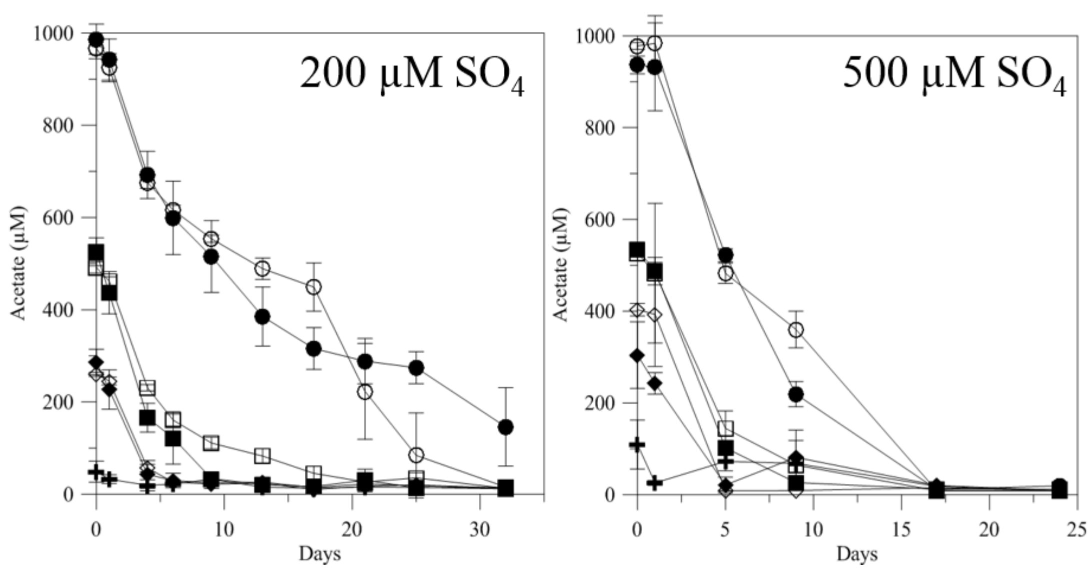

Figure 2.3: Acetate consumption in 200 and 500 µM SO_4 experiments with variable amended acetate concentrations. ✚ No acetate; ♦ 250 µM acetate; ■ 500 µM acetate; ● 1000 µM acetate; open symbols correspond to 5 mM molybdate control experiments at the given acetate concentration.

Sulfate reduction

The addition of 5 mM molybdate inhibited sulfate reduction in the variable sulfate experiments at all of the sulfate concentrations tested (Figure 2.4). In the uninhibited experiments sulfate decreased by approximately 5 µmoles, regardless of the initial sulfate concentration. This decrease occurred over the first 21 days of the experiment, after which sulfate concentrations remained unchanged.

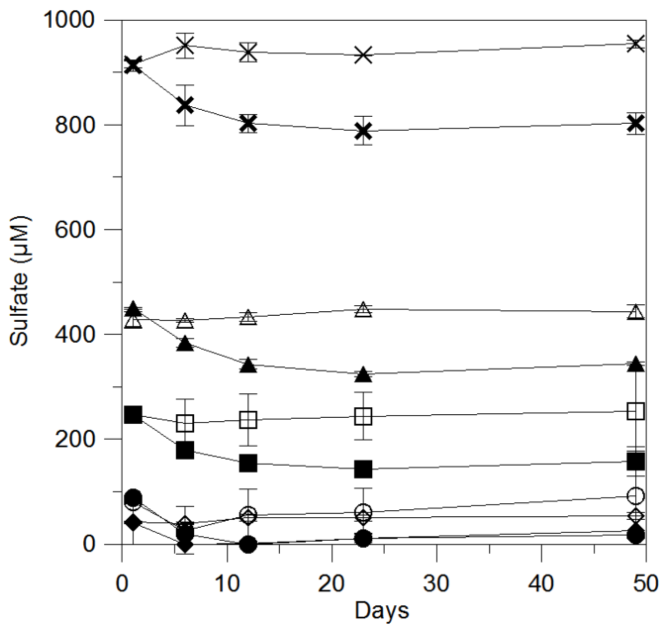

Figure 2.4: Sulfate concentration in Var.SO_4 experiments. ✚No sulfate; ♦ 50 µM sulfate; ● 100 µM sulfate; ■ 250 µM sulfate; ▲ 500 µM sulfate; ✖ 1000 µM sulfate; open symbols correspond to 5 mM molybdate controls.

The amount of sulfate consumed in the acetate amendment experiments with 200 and 500 µM sulfate depended upon the initial acetate concentration (Figure 2.5). All microcosms amended with 5 mM molybdate showed no significant change in sulfate concentration over time (Figure 2.5), consistent with the experiments with variable sulfate (Figure 2.4). In microcosms without molybdate, sulfate consumption directly correlated with the initial amount of acetate added to each sample in experiments with

200 and 500 µM sulfate (Pearson's r = 0.963 and 0.957, respectively, $p < 0.05$), consistent with acetate being a limiting electron donor for sulfate reduction.

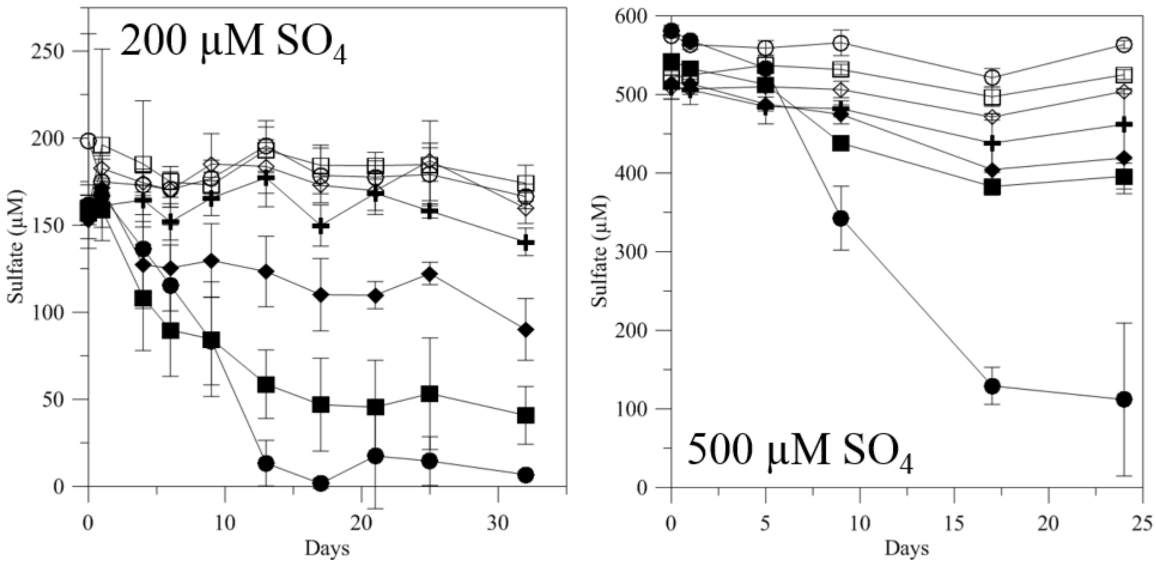

Figure 2.5: Sulfate consumption in 200 and 500 µM SO_4 experiments with variable amended acetate concentrations (Note different scales in vertical axes). ✚ No acetate; ♦ 250 µM acetate; ■ 500 µM acetate; ● 1000 µM acetate; open symbols correspond to 5 mM molybdate control experiments at the given acetate concentration.

Rates of methanogenesis and sulfate reduction

The rates of sulfate reduction and methanogenesis in the acetate amendment experiments with 200 and 500 µM sulfate are presented in Table 2.1. Both processes operated concurrently in all microcosms without molybdate and rates of each were calculated based on the assumption that acetate was the primary electron donor for both. As expected, the sulfate reduction rate (SRR) was dependent on both the sulfate and acetate concentrations, while methane production was directly correlated only to the acetate concentration. The experiments amended with 500 µM sulfate showed significantly higher rates of sulfate reduction than those with 200 µM sulfate, with rates of methane production being similar in both sets of experiments (Table 2.1). The ratio of the sulfate reduction rate to methane production rate (SRR/MPR) remained constant at ~4 in experiments with 500 µM sulfate, while it varied between 0.36 and 21.5 in experiments with 200 µM sulfate. The only microcosms to exhibit a SRR/MPR ratio less than 1 were in the 200-SO_4 experiments with 50 µM acetate. It is possible that 50 µM acetate was below the acetate utilization threshold for the sulfate reducers in this study, though much lower threshold concentrations have been documented (Elferink et al., 1998).

Microbial community analysis

A suite of 15-16 PLFAs was observed in all experiments in this work regardless of experimental condition. The most abundant PLFAs observed in the Var.-SO_4 experiments included 16:0, 16:1ω7*cis*, and 18:0 (Table 2.2). The most abundant PLFAs - observed in the 200-SO_4 and 500-SO_4 experiments included 16:0, 16:1ω7*cis*, 18:1ω7, and 18:0 (Tables 3 and 4, respectively). Every experiment also included lesser amounts of the branched fatty acids *i*15:0 and *ai*15:0, unbranched PLFAs such as 14:0, 15:0, and 17:0 as well as the monoenoic PLFAs 16:1ω5, 16:1ω7*trans*, and 18:1ω9*cis*. The branched PLFA 10Me16:0 was also observed in all samples in the Var.-SO_4 experiment at total amounts between 8 and 42 nmole (Table 2.2). 10Me16:0 was also observed at total amounts on average between 7.6 and 42.9 nmole in the 500-SO_4 experiment (Table 2.4). The PLFA *cy*17:0 was observed in all experiments, with greater amounts observed in 200-SO_4 and 500-SO_4 experiments. Correlation coefficients between individual PLFAs and initial acetate concentration were calculated for 200-SO_4 and 500-SO_4 experiments to determine if acetate stimulated specific microbial community members. The PLFAs observed to correlate strongly with initial acetate concentration in the 200-SO_4 experiments were *i*15:0, 16:1ω7*trans* and *i*17:0 (r = 0.580, 0.773 and 0.845, respectively, $p < 0.05$). The PLFAs observed to have the strongest correlation to initial acetate concentration in the 500-SO_4 experiments were 14:0, 16:1ω7*cis*, 16:1ω5, 16:1ω7*trans*, and *cy*17:0 (r = 0.674, 0.691, 0.669, 0.788, and 0.705, respectively; $p < 0.05$).

The total PLFA quantities extracted from microcosms in the Var.-SO_4 experiments ranged from 427 to 1705 nmole PLFA (average 977 ± 352 nmole PLFA; Table 2.2). Total biomass was estimated based on the conversion factor of 2.4 $x10^4$ cells $pmole^{-1}$ $PLFA^{-1}$ (Balkwill et al., 1988) and ranged from 1.96 $x10^{10}$ to 4.26 $x10^{10}$ cells (average 2.45 $x10^{10}$ ± 8 $x10^9$ cells). No correlation was observed between biomass estimates and the amended sulfate concentration.

The total quantities of PLFA extracted from microcosms in 200 µM sulfate experiments ranged from 1002 ± 250 nmole to 2010 ± 550 nmole, which corresponded to total biomass estimates between 2.5 x 10^{10} ± 6.2 x 10^9 and 5 x 10^{10} ±1.4 x 10^{10} cells (Table 2.3). The biomass estimates calculated for each acetate amendment concentration were not found to be statistically significantly different from their respective molybdate control experiments (t-test, 2 tailed, $p > 0.05$), nor were the biomass estimates for microcosms amended with 250 µM acetate significantly different from the 50 µM acetate (unamended) controls (t-test, 2-tailed, $p > 0.05$). However, biomass estimates for microcosms amended with 500 µM and 1000 µM acetate both with and without molybdate were statistically higher than the 50 µM acetate controls (t test, 2-tailed, $p < 0.05$).

Total PLFA quantities extracted from microcosms in the 500-SO_4 experiments ranged from 1597 ± 640 nmole to 3484 ± 1580 nmole (Table 2.4). The total biomass estimates calculated based on the above conversion factor ranged from 3.99 x10^{10} ± 1.6 x10^{10} to 8.71 x10^{10} ± 4 x10^{10} cells. No statistically significant differences between the biomass estimates for the acetate-amended experiments and the unamended control experiment were observed ($\rho > 0.05$), nor were the differences between the biomass estimates for the various acetate amendments and their respective molybdate controls significant ($\rho > 0.05$).

PLFA profile analysis

A suite of 15-16 PLFAs was observed in all experiments in this work regardless of experimental condition, most likely due to the common inoculum used in each experiment. The most abundant PLFAs observed in the Var.-SO_4 experiments included 16:0, 16:1ω7*cis,* and 18:0. The most abundant PLFAs observed in both the 200-SO_4 and 500-SO_4 experiments included 16:0, 16:1ω7*cis*, 18:1ω7, and 18:0 (Tables 2.3 and 2.4). Every experiment also included lesser amounts of the branched fatty acids *i*15:0 and *ai*15:0, unbranched PLFAs such as 14:0, 15:0, and 17:0 as well as the monoenoic PLFAs 16:1ω5, 16:1ω7trans, and 18:1ω9cis. The branched PLFA 10Me16:0 was also observed in all experiments with variable sulfate concentrations at total amounts between 8 and 42 nmole (Table 2.2). *Cy*17:0 was observed in all experiments, with greater amounts observed in both the 200-SO_4 and 500-SO_4 experiments. The Pearson's correlation coefficient between the initial acetate concentration and the PLFA quantities was calculated for all PLFAs observed in the experiments with 200 and 500 µM sulfate. The PLFAs that correlated strongly with initial acetate concentration in the 200-SO_4 experiments with variable acetate were *i*15:0, 16:1ω7*trans* and *i*17:0 (r = 0.580, 0.773 and 0.845, respectively, $p < 0.05$). The PLFAs observed to have the strongest correlation to initial acetate concentration in the 500-SO_4 experiments were 14:0, 16:1ω7*cis*, 16:1ω5, 16:1ω7*trans*, and *cy*17:0 (r = 0.674, 0.691, 0.669, 0.788, and 0.705, respectively; $p < 0.05$). No PLFAs correlated strongly with acetate concentrations in the 5 mM molybdate microcosms for the 200-SO_4 and 500-SO_4 experiments.

qPCR of mcrA and dsrA

The mcrA and dsrA genes were quantified in order to track changes in the methanogen and sulfate reducer communities, respectively. Experiments with variable sulfate contained approximately 10^6-10^7 mcrA copies mL^{-1} at their start, which increased by approximately an order of magnitude by the end of the experiment to 10^7-10^8 copies mL^{-1} (Figure 2.6). There was no correlation observed between sulfate concentration and mcrA copy number observed for experiments with variable sulfate. Initial dsrA copy numbers were approximately 10^5 copies mL^{-1} and increased to 10^6 to 10^7 copies mL^{-1} in experiments without molybdate, but remained relatively constant at 10^5 copies mL^{-1} in microcosms with molybdate (Figure 2.6). These same genes were quantified for the acetate-amended 500-SO_4 experiments. Initial mcrA copy numbers ranged from 1.2 $x10^6$ to 3.9 $x10^6$ copies mL^{-1}, and remained relatively constant in all microcosms except those with 1000 µM acetate plus molybdate in which mcrA increased to 1.1 $x10^7$ copies mL^{-1} (Figure 2.7). dsrA gene copy numbers increased from 10^6 to 10^7 copies mL^{-1} in microcosms without molybdate, but remained constant at approximately 10^5 copies mL^{-1} in microcosms with molybdate (Figure 2.7). The reason for the difference in dsrA copy numbers for microcosms with and without molybdate at the start of these experiments (10^5 versus 10^6 copies mL^{-1}; Figure 2.7) is not known.

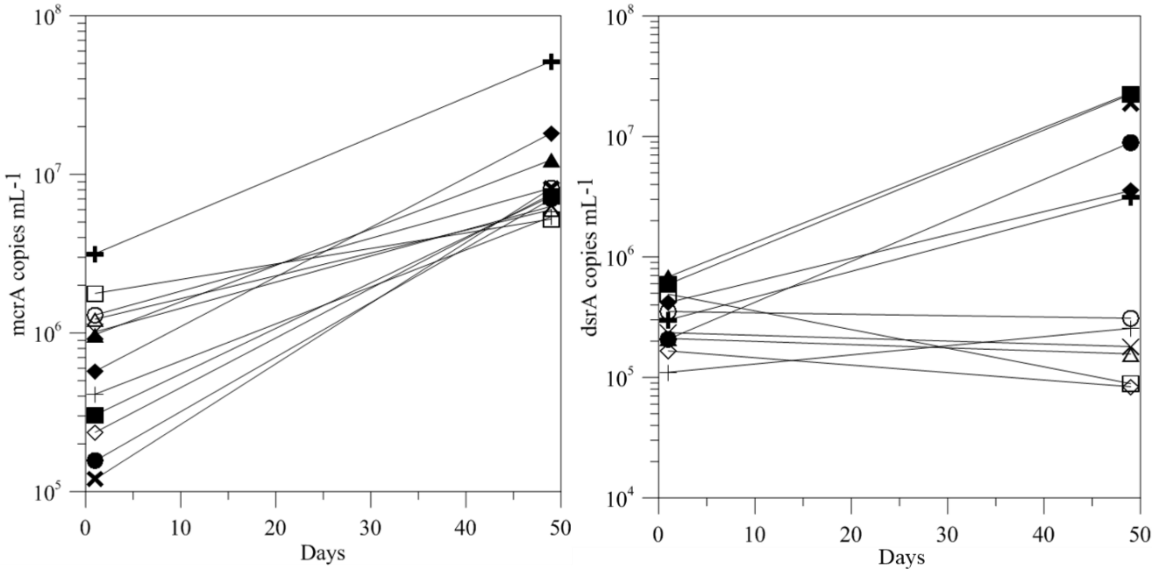

Figure 2.6: qPCR of the mcrA gene (left) and dsrA gene for variable sulfate experiments ✚ No sulfate; ♦ 50 µM sulfate; ● 100 µM sulfate; ■ 250 µM sulfate; ▲ 500 µM sulfate; ✖ 1000 µM sulfate; open symbols correspond to 5 mM molybdate controls.

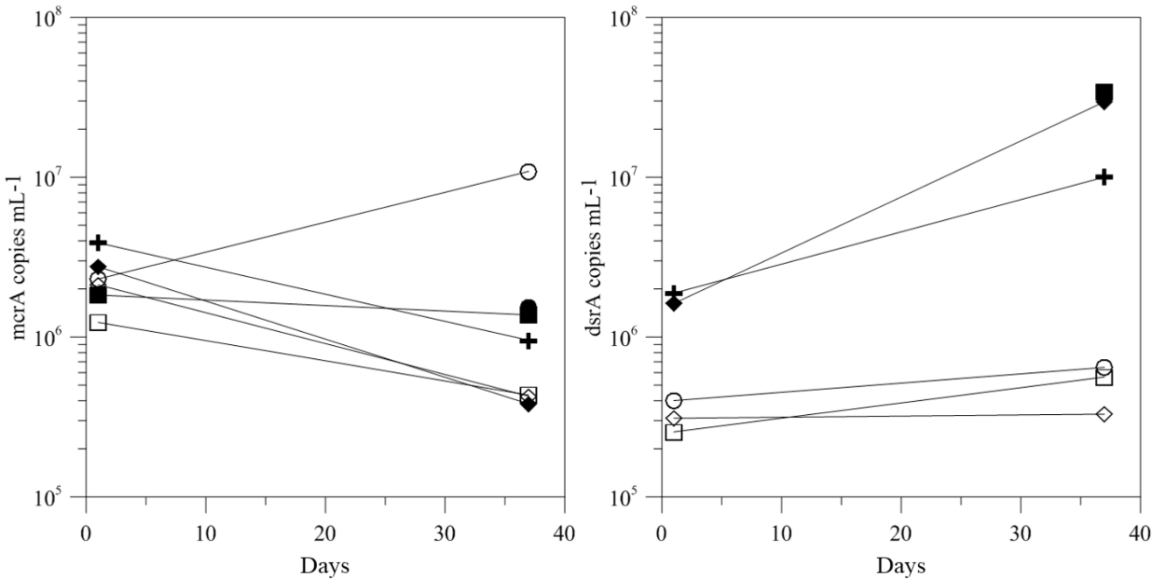

Figure 2.7: qPCR of the mcrA gene (left) and dsrA gene (right) for experiments with 500 µM sulfate and variable acetate concentrations. (✚ No acetate; ♦ 250 µM acetate; ■ 500 µM acetate; ● 1000 µM acetate; open symbols correspond to 5 mM molybdate control experiments).

2.5 Discussion

This study documents the co-occurrence of sulfate reduction and methanogenesis in coal microcosms. Coal seams represent a unique environment from marine sediments, engineered systems, and even freshwater environments, due to the relative lack of both labile carbon as well as sulfate. Nonetheless, sequences associated with sulfate reducing microorganisms are commonly seen in 16S rRNA studies of produced water from coal bed methane wells (Shimizu et al., 2007; Green et al., 2008; Klein et al., 2008; Strąpoć et al., 2008; Ulrich and Bower, 2008). However, the role of sulfate reducing organisms in coal bed aquifers has not been elucidated. The experiments described in this work show that microbial methanogenesis can occur simultaneously with sulfate reduction, with both metabolic groups competing for acetate at the sulfate and acetate concentrations expected in coal bed methane aquifers (Figures 2.1, 2.2, 2.3, 2.4, and 2.5).

Methanogenesis and sulfate reduction in coal microcosms

The experiments conducted with variable sulfate concentrations were designed to determine the sulfate concentration at which SRM were able to outcompete methanogens for the acetate available from coal degradation. It was hypothesized that the rate of sulfate reduction would increase at higher sulfate concentrations, leading to conditions under which methanogenic activity would be essentially negligible. Given that methane production was indistinguishable between the molybdate-inhibited and uninhibited experiments of the Var.-SO_4 experiments (Figure 2.1) suggests that SRM had no influence on methanogenesis, despite their activity in every microcosm without molybdate (Figure 2.1). The exceptions to this observation were microcosms with 50 µM sulfate, in which those with 5 mM molybdate produced more methane than uninhibited samples at the same sulfate concentration (Figure 2.1). The reason for this deviation from the behavior observed in the other microcosms is not clear.

The complete consumption of acetate also corresponded with the cessation of both methanogenic and SRM activity after roughly 21 days in the Var.-SO_4 experiments (Figures 2.1 and 2.2), strongly suggesting that both microbial processes were limited by acetate. The relative recalcitrance of the source organic matter is considered an important indicator of the potential for methane generation in sedimentary reservoirs, as is the metabolic activity of organisms breaking down the recalcitrant molecules in coal to provide the substrates needed for methanogenesis (Rice and Claypool, 1981; Schlegel et al., 2013). It is not well established which factors contribute to the bioavailability of organic matter in coals and shales, though burial history, and thus thermal maturity, may be important factors (Formolo et al., 2008; Jones et al., 2008; Strąpoć et al., 2010). Results from experiments here with a microbial consortium enriched from coal suggest that the activity of fermentative organisms generating acetate from coal determine the activity of both acetoclastic methanogens and SRM.

Tracking both sulfate reduction and methanogenesis, as well as bacterial biomass generated, in acetate-amended microcosms allows for a rough accounting of carbon flow in these experiments. Acetate was assumed to be the primary electron donor for sulfate reduction and methanogenesis in these experiments. This assumption was validated by the observation of the correlation between total sulfate reduced (µmole) and total acetate consumed (µmole) [Pearson's $r = 0.739$, $p < 0.05$ (200 µM sulfate experiments); $r = 0.649$, $p < 0.05$ (500 µM sulfate experiments)]. Methanogenesis accounted for less than

20% of the acetate consumed in the 200 and 500 μM sulfate experiments at all acetate concentrations except at1000 μM acetate with 5 mM molybdate where it accounted for 43% and 68% of the consumed acetate in the 200 and 500 μM sulfate experiments, respectively. The percentage of acetate consumed via sulfate reduction ranged from 28% to 50% in experiments without molybdate. Lovley and Klug (1986) developed a model for freshwater sediments which posited that the relative importance of methanogenesis and sulfate reduction was determined by the rate of organic matter decomposition supplying acetate to both processes rather than the porewater sulfate concentration. Methanogenesis becomes more important in freshwater sediments as the rate of organic matter decomposition increases, thereby increasing the available acetate pool and causing sulfate reducers to consume sulfate in the uppermost sediment until it is below 30 μM. In acetate-amended experiments with 200 and 500 μM sulfate a higher initial acetate concentration could be considered akin to rapidly decaying organic matter. Data from experiments here with initial acetate concentrations < 1000 μM are not consistent with the model of Lovley and Klug (1986), as increasing the initial acetate concentration decreased the relative importance of methanogenesis (Figure 2.8). For both the 200-SO_4 and 500-SO_4 experiments, increasing the acetate concentration stimulated SRM at these intermediate acetate concentrations. However, at 1000 μM acetate, relatively more acetate was consumed by methanogenesis and it also appears to have stimulated bacterial cell growth (Tables 2.3 and 2.4). Methanogenesis accounted for more than 20% of acetate consumption in microcosms with 1000 μM acetate in which SRM were inhibited with molybdate. Taken together these findings suggest that increasing the available acetate concentration moderately in situ may stimulate SRM and inhibit methanogenesis in coal bed reservoirs with available sulfate. However, if acetate concentrations exceed a critical threshold, they may then stimulate methanogenesis.

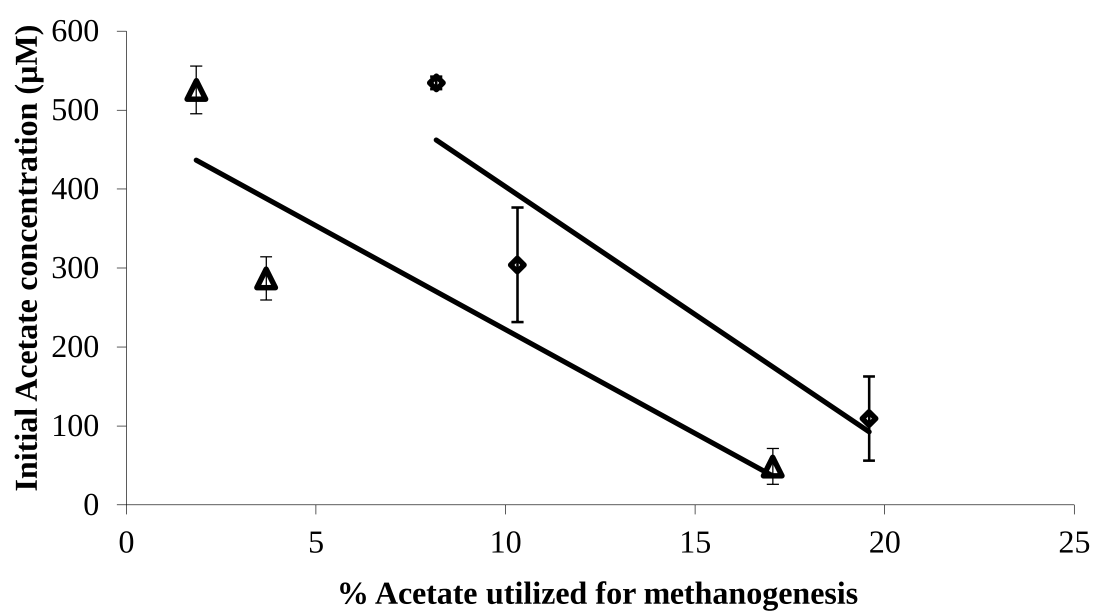

Figure 2.8: Relationship between initial acetate concentration and % of acetate utilized for methanogenesis in experiments with 200 and 500 µM SO_4 for 3 lowest initial acetate concentrations (▲ 200 µM sulfate experiment; ♦ 500 µM sulfate experiment; error bars represent one standard deviation of triplicate incubations).

At intermediate (250 and 500 µM) acetate concentrations the majority of acetate consumed in these experiments (57-87%) appears to have gone to processes other than sulfate reduction or methanogenesis. These processes may include cell growth and maintenance, or growth of heterotrophic organisms. Because the headspace gas in these experiments was 20% CO_2, we were unable to detect small changes in headspace CO_2 as a result of heterotrophic growth. However, the strong correlation between the bacterial PLFAs 14:0, 16:1ω7*cis*, 16:1ω5, 16:1ω7*trans*, and *cyclic*17:0 with the initial acetate concentrations in these experiments suggests that the majority of acetate consumed in these experiments supported cell growth. This suggestion is also supported by a statistically significant increase in bacterial cell abundance in the 200-SO_4 experiments with 500 and 1000 µM acetate in the presence and absence of molybdate (Table 2.3). It is also possible that a significant portion of the acetate consumed in the 500-SO_4 experiments went toward methanogenic archaeal cell growth. PELs were not measured in these experiments, but the lack of significant correlation between T_{final} mcrA copy numbers and initial acetate concentrations suggests that this was not the case.

Microbial community analysis

The PLFA profiles of the three different sets of experiments described herein should be compared carefully as each set of experiments was conducted at different times and with an ever-evolving inoculum source. However, the PLFA profiles observed from all three experiments were quite similar, with the same relative abundances of particular PLFAs. This suggests a relatively stable microbial community composition over time and between experiments. Monounsaturated PLFAs are often considered indicative of gram-negative bacteria, while branched and saturated PLFAs such as anteiso15:0, *i*17:0, and *ai*17:0 are considered indicative of gram-positive bacteria (Lechevalier and Lechevalier, 1988; Pinkart et al., 2002). The monounsaturated PLFAs 16:1ω7*cis*, 16:1ω7*trans*, 16:1ω5, 18:1ω7, and 18:1ω9 were seen in all profiles, suggesting the presence of gram negative bacteria in all experiments. Based on the ratios of saturated to unsaturated PLFA the contribution of gram-negative bacteria to total bacteria population in all experiments ranged from roughly 30% to 50%.

The strong correlation between the PLFAs 16:1ω7*cis* and 16:1ω7*trans* with acetate amendment concentrations suggests that the organisms responsible for making these PLFAs were also primarily responsible for acetate consumption in these experiments. Because methanogens are archaea and do not produce ester-linked PLFAs, PLFA analysis cannot detect their growth. An attempt was made to recover intact archaeal phosphoether lipids from the acetate-amended experiments with 500 µM sulfate but were unable to observe any in the samples with the highest methane production, suggesting that methanogen biomass remained too low to detect with lipid methods at the scale of our experiments. However, mcrA copy numbers increased by approximately 1 order of magnitude in all microcosms with variable sulfate concentrations (Figure 2.6), which is consistent with sulfate concentration having no discernible effect on methane production or methanogen growth when experiments were not amended with acetate. McrA copy numbers only increased in microcosms with 1000 µM acetate plus molybdate in the 500 µM sulfate experiments (Figure 2.7), suggesting that SRM must be inhibited in order to observe an increase in methanogen biomass in response to high acetate amendment.

PLFAs considered biomarkers of SRM were expected to increase as a proportion of the PLFA profile in response to acetate amendment. The branched PLFA 10Me16:0 is considered a biomarker for *Desulfobacter spp*. grown on acetate (Dowling et al., 1986), as well as for certain *Desulfovibrio spp*. (Vainshtein et al., 1992). 10Me16:0 is commonly seen in Actinomycetes as well, but always in the presence of 10Me18:0 (Kroppenstedt et al., 1985) which was not observed in this study. 10Me16:0 was observed in all microcosms in variable sulfate, as well as 200 and 500 µM sulfate experiments (Tables 2.2, 2.3, and 2.4), but did not correlate strongly with acetate or sulfate concentration. The terminally branched PLFAs *i*15:0 and *i*17:0 also correlated strongly with acetate amendment in experiments with 200 µM sulfate ($r = 0.58$ and 0.85, respectively, $p <$

0.05) suggesting the stimulation of gram positive bacteria with acetate amendment as well. However, these PLFAs were only weakly correlated with acetate amendment in experiments with 500 µM sulfate, suggesting that this observation may be dependent on the sulfate concentration. *Cy*17:0 has also been observed in *Desulfobacter spp*. grown on acetate (Dowling et al., 1986) and was observed in all samples in this study at amounts between 7 and 21 nmole in the Var.SO_4 experiments (Table 2.2), between 63 and 95 nmole in 200 µM sulfate experiments (Table 2.3), and between 21 and 232 nmole in 500 µM sulfate experiments (Table 2.4). *Cy*17:0 was found to correlate strongly with initial acetate concentrations (Pearson's $r = 0.71$, $p < 0.05$) in 500 µM sulfate experiments, suggesting that this experiment contained *Desulfobacter* spp. that were able to grow with increasing acetate concentrations. In addition, the monoenoic PLFA 16:1ω7*cis* was observed in all samples across all three experiments as well, and has been observed in the sulfate reducer *Desulfotomaculum acetoxidans* (Dowling et al., 1986). This PLFA is produced in many types of bacteria, however, and therefore cannot be considered a biomarker for SRM. 16:1ω7*cis* also correlated with initial acetate concentrations in the 500-SO_4 experiments, but not in 200-SO_4 experiments. DsrA, the functional gene for sulfate reducers, was also observed to increase significantly in 500 µM sulfate experiments without molybdate (Figure 2.7). Taken together, the correlation of 16:1ω7*cis* and *cy*17:0 with acetate amendment, as well as the increase in dsrA gene copies mL^{-1} in experiments with 500 µM sulfate, suggests that SRM were stimulated by acetate amendment, but that different organisms were stimulated in the 200-SO_4 experiments.

PLFA profiles can also be changed by physiological parameters such as starvation (Kieft et al., 1997; Green and Scow, 2000), often expressed in terms of the ratio of *trans* to *cis* oriented monounsaturated PLFAs. The ratio of 16:1ω7*trans*/16:1ω7*cis* in both sets of experiments amended with acetate decreased as acetate concentrations increased in microcosms without molybdate, indicating that the microbial communities in both sets of experiments were stressed without additional acetate (White et al., 1998). The *trans/cis* ratio of 16:1ω7 in microcosms with molybdate remained almost constant across acetate concentrations in both 200-SO_4 and 500-SO_4 experiments, consistent with the hypothesis that it may have been produced by SRM in these samples.

Implications for coal bed methane reservoirs

The median sulfate concentration in produced waters of the Powder River Basin is 1 μM, but the maximum is ~500 μM (Rice et al., 2008). Our data suggest that even in areas of the basin with the highest sulfate concentrations SRM would be limited by the availability of acetate, for which they would compete with methanogens. Because coal is an inherently recalcitrant material whose resistance to breakdown is well documented, especially under anaerobic conditions (Fakoussa and Hofrichter, 1999) any terminal microbial process will be limited by microbial activity upstream of the terminal process. Acetate has been shown to be an important intermediate in the bioconversion of coal to methane (Green et al., 2008; Jones et al., 2010; Beckmann et al., 2011; this study). Our data suggest that sulfate reduction in coal beds is also limited by the availability of acetate, with both sulfate reduction and methanogenesis potentially occurring simultaneously in coal bed reservoirs with low acetate concentrations (< 1000 μM). Schlegel et al. (2011a) argue that in portions of the Illinois Basin with a high $\delta^{34}S_{SO4}$ and low sulfate concentration (<0.02 mM) microbial sulfate reduction occurred prior to methanogenesis and that methanogenesis has now taken over as the dominant terminal electron accepting process. Other portions of the basin contain waters with high $\delta^{34}S_{SO4}$, low $\delta^{13}C_{CO2}$ (< -40‰), low alpha values for CO_2 and CH_4 ($\alpha_{CO2-CH4}$ < 1.06) and significant methane concentrations, suggesting that sulfate reduction has occurred prior to the onset of methanogenesis but that methanogenesis has not yet had a significant impact on the $\delta^{13}C_{CO2}$ to reflect the dominant methanogenic pathway (Schlegel et al., 2011a). However, it is possible, and our data suggest, that both sulfate reduction and methanogenesis can occur when both sulfate and acetate are maintained at low concentrations (< 1 mM). Acetate in produced waters of the Illinois Basin can range between <0.1 and 200 µM (Schlegel et al., 2013), perhaps preventing both metabolic groups from dominating its consumption. Strąpoć et al. (2008) did not detect SRM in microbial enrichments from Illinois Basin coal, though their enrichment strategy targeted methanogens. In this model the main determining factor for which process is dominant is not the sulfate concentration but the metabolic activity of fermentative organisms supplying acetate to fuel both methanogenesis and sulfate reduction.

2.6 Conclusion

The microcosm experiments conducted in this study showed that microbial methanogenesis and sulfate reduction can occur simultaneously in coal microcosms with low sulfate concentrations (<500 µM) and low acetate concentrations (< 1 mM). Methane production was significantly higher in microcosm experiments amended with at least 500 µM acetate when SRM were inhibited with molybdate. The relative importance of methanogenesis compared to sulfate reduction decreased in microcosms as the acetate concentration increased, up to 500 µM acetate, regardless of sulfate concentration in acetate-amended samples, indicating that SRM were able to outcompete methanogens when acetate was more available. We found that while sulfate concentration influences the rate of sulfate reduction, the primary control on microbial sulfate reduction may be the acetate concentration. This finding may explain why appreciable sulfate concentrations are observed in parts of methane-producing coal and shale basins including the Illinois basin and the Powder River Basin. Our data support the idea that both processes may occur at low rates in sedimentary basins with limited labile carbon and limited microbial acetate production.

Table 2.1: Rates of sulfate reduction and methane production in experiments with 200 and 500 µM SO_4 amended with variable acetate concentrations.

Acetate (µM)	Sulfate (µM)	Sulfate reduction rate (µmol day^{-1})	Methane production rate (µmol day^{-1})	SRR/MPR
100	500	0.21	0.06	3.5
250	500	0.36	0.09	4.0
500	500	0.51	0.13	4.1
1000	500	1.63	0.42	3.9
50	200	0.004	0.01	0.4
250	200	0.14	0.02	8.7
500	200	0.32	0.01	22
1000	200	0.56	0.14	4.1

Table 2.2: PLFAs observed in experiments with variable sulfate concentrations, total PLFAs recovered (nmole), as well as biomass estimates for each sulfate concentration tested along with the molybdate-inhibited controls for each sulfate concentration. Most experimental conditions were extracted in duplicate (2 of 3 incubations) and the reported PLFA quantities are averages of both extractions.

PLFA	*No sulfate*	*50 µM sulfate*	*100 µM sulfate*	*250 µM sulfate*	*500 µM sulfate*	*1mM sulfate*	*No sulfate + moly*	*50 µM + moly*	*100 µM + moly*	*250 µM +moly*	*500 µM + moly*	*1mM + moly*
14:0	72.0	57.6	60.0	55.2	31.6	39.1	51.4	79.8	66.9	90.5	53.7	41.6
i15:0	77.8	66.1	59.4	55.0	26.7	43.4	59.0	79.6	70.2	81.1	57.1	49.5
ai15:0	37.5	32.5	35.3	52.6	27.0	34.8	24.5	33.8	32.7	35.3	23.7	16.5
15:0	24.1	23.7	20.7	20.5	9.8	13.1	29.7	29.1	30.0	26.2	17.1	12.8
16:1ω7cis	291.9	260.0	238.0	175.2	85.9	156.8	175.9	310.9	220.8	287.7	185.8	182.6
16:1ω5cis	29.1	23.5	20.9	18.2	6.7	14.5	10.8	22.8	12.8	21.3	10.9	12.2
16:1 ω9	19.5	13.5	14.8	17.8	7.7	13.8	9.6	15.9	13.4	22.4	10.2	9.3
16:0	435.5	365.9	305.1	299.9	135.4	285.7	255.3	464.2	406.3	683.1	322.9	281.0
10me16:0	30.5	25.2	23.2	21.3	8.2	16.8	22.9	42.2	37.3	35.2	24.0	19.5
i17:0	17.6	15.8	15.2	10.9	6.7	12.1	9.4	17.5	15.9	14.3	9.0	8.9
ai17:0	13.6	13.8	16.7	17.8	6.6	9.8	11.1	17.6	17.7	23.4	11.4	9.1
cy17:0	21.9	10.2	8.5	24.5	7.6	16.2	13.0	16.4	11.7	21.9	6.2	11.3
17:0	11.9	11.0	14.9	7.2	2.4	9.0	8.3	11.1	12.0	8.9	2.7	5.1
18:1ω9cis	43.3	15.1	39.7	39.5	31.3	16.9	37.9	24.1	14.3	46.6	15.4	29.9
18:0	98.6	87.3	54.0	74.3	33.4	102.6	57.2	140.7	111.2	306.6	93.7	77.4
total nmole PLFA	1225	1021	926	890	427	785	776	1306	1073	1705	844	767
Total biomass (cells)	3.06×10^{10}	2.55×10^{10}	2.32×10^{10}	2.22×10^{10}	1.07×10^{10}	1.96×10^{10}	1.94×10^{10}	3.26×10^{10}	2.68×10^{10}	4.26x1010	2.16×10^{10}	1.92×10^{10}
Cells g^{-1} $coal^{-1}$	6.13×10^{8}	5.11×10^{8}	4.63×10^{8}	4.45×10^{8}	2.13×10^{8}	3.92×10^{8}	3.89×10^{8}	6.53×10^{8}	5.37×10^{8}	8.52×10^{8}	4.31×10^{8}	3.83×10^{8}

Table 2.3: PLFA quantities observed in experiments with 200 µM sulfate and variable acetate concentrations. PLFA quantities are averages of extracted quantities from triplicate incubations, standard deviations in parentheses.

PLFA	*50 µM acetate*	*250 µM acetate*	*500 µM acetate*	*1000 µM acetate*	*250 µM acetate + molybdate*	*500 µM acetate + molybdate*	*1000 µM acetate + molybdate*
14:0	22.8(5)	43.8(16)	60.5(10)	47.8(19)	38.0(11)	65.8(9.6)	65.0(1.1)
*i*15:0	25.7(7)	77.5(29)	117(22)	91.6(33)	85.5(18)	129(21)	92.9(5.8)
*ai*15:0	17.6(5)	29.4(12)	32.5(7)	25.5(9.7)	13.9(2.6)	14.7(3)	14.4(2.5)
15:0	3.8(4)	4.5(5)	16.4(13)	11.2(8.9)	11.3(3.2)	18.9(3.9)	16.9(1.7)
16:1ω7*cis*	241(99)	414(177)	676(230)	540(130)	366(35)	488(68)	379.2(19)
16:1ω7*trans*	20.5(11)	21.6(8)	29.2(10)	19.0(5.7)	16.7(2.8)	20.5(5)	17.4(1.4)
16:1ω5	16.1(5)	28.6(10)	49.5(10)	47.1(4.5)	28.3(1.6)	40.0(8.1)	32.0(1.5)
16:0	291(57)	371(160)	529(13)	461.4(79)	346(26)	412(69)	427(58)
*i*17:0	15.1(3)	23.3(8)	34.8(7)	40.6(7.1)	30.7(0.9)	53.1(11)	43.0(1)
17:1ω7*cis*	0.0	1.0(0.4)	1.0(0.1)	0.5(0.5)	0.9(0.2)	0.9(0.8)	0.0
*cy*17:0	66.1(18)	77.6(31)	94.9(19)	79.0(11)	67.5(4.2)	72.4(18)	63.0(8.3)
17:0	7.7(2)	12.2(6)	15.2(2)	10.0(2.4)	6.7(0.6)	7.2(2.2)	6.9(0.6)
18:1ω9*cis*	39.3(12)	47.1(13)	44.9(7)	41.5(11)	37.4(5.8)	37.6(5.1)	39.2(7.1)
18:1ω9*trans*	10.9(1)	11.1(3)	12.4(4)	9.8(1.5)	10.8(2.4)	12.1(3.8)	12.6(2.5)
18:1ω7	157(41)	182(67)	232(68)	184(38)	170.1(13)	191(42)	163.8(21)
18:0	67.9(7)	64.8(37)	66.0(13)	59.2(8.3)	63.1(12)	51.0(23)	85.2(29)
Total nmole PLFA	1002(250)	1410(560)	2010(550)	1668(330)	1293(25)	1615(260)	1459(130)
Total biomass (cells)	$2.5x10^{10}(6.2x10^{9})$	$3.5x10^{10}(1.4x10^{10})$	$5.0x10^{10}(1.4x10^{10})$	$4.2x10^{10}(8.2x10^{9})$	$3.2x10^{10}(6.2x10^{8})$	$4.0x10^{10}(6.6x10^{9})$	$3.6x10^{10}(3.2x10^{9})$
Cells/g coal	$5.0x10^{8}(1.2x10^{8})$	$7.0x10^{8}(2.8x10^{8})$	$1.0x10^{9}(2.7x10^{8})$	$8.3x10^{8}(1.6x10^{8})$	$6.5x10^{8}(1.2x10^{7})$	$8.1x10^{8}(1.3x10^{8})$	$7.3x10^{8}(6.4x10^{7})$

Table 2.4: PLFA quantities (total nanomole) observed in experiments with 500 µM sulfate and variable acetate concentrations. PLFA quantities are averages of extracted quantities from triplicate incubations, except in 100 µM and 250 µM acetate experiments in which one extraction was lost during processing for each condition. Standard deviations in parentheses.

PLFA	*100 µM acetate*	*250 µM acetate*	*500 µM acetate*	*1000 µM acetate*	*250 µM acetate + molybdate*	*500 µM acetate + molybdate*	*1000 µM acetate + molybdate*
14:0	55.7(13)	83.8(38)	119(27)	124(36)	78.5(6)	103(44)	139(95)
i15:0	78.4(60)	143(11)	225(160)	205(90)	234(135)	144(11)	248(167)
ai15:0	206(230)	135(44)	156(140)	126(67)	46.2(29)	64.2(52)	53.3(37)
15:0	59.3(62)	38.1(2)	35.1(38)	37.7(23)	29.4(20)	37.5(24)	35.8(28)
i16:0	24.4(22)	15.9(1)	0	19.0(10)	11.5(4)	24.4(19)	13.3(7)
16:1ω7cis	182.2(88)	333(78)	544(360)	770(350)	504(190)	426(99)	670(470)
16:1ω5cis	25.6(6)	33.7(13)	39.3(25)	73.5(35)	56.5(26)	42.9(7)	97.0(69)
16:1c	18.6(7)	27.6(3)	50.0(20)	93.2(46)	29.4(9)	30.7(8)	41.0(31)
16:0	394(37)	848(624)	1044(380)	1092(447)	618(160)	665(90)	1275(1080)
10me16:0	13.4(5)	22.3(12)	11.0(16)	42.9(28)	7.6(7)	33.0(30)	26.6(17)
i17:0	19.8(9)	14.1(9)	0	33.3(34)	18.9(9)	13.0(12)	14.0(5)
ai17:0	21.9(10)	16.0(4)	0	22.1(14)	10.0(1)	40.6(28)	19.7(10)
cy17:0	63.0(6)	47.0(29)	79.5(26)	232(140)	55.8(23)	43.6(22)	20.9(8)
17:0	20.7(17)	19.4(3)	0	28.5(21)	10.6(2)	20.2(13)	17.3(15)
18:1ω9cis	93.7(22)	116(61)	92.7(28)	91.9(31)	73.8(23)	95.5(15)	124(64)
18:1ω7	218(62)	191(94)	224(110)	329(160)	218(64)	178(34)	269(238)
18:1ω9trans	0.0	0.0	34.5(30)	0.0	33.6(36)	0.0	0.0
18:0	103(22)	271(290)	255(250)	164(74)	139(90)	179(61)	344(310)
Total nmole PLFA	1597(640)	2353(1200)	3106(854)	3484(1580)	2175(357)	2140(430)	3407(2640)
Total biomass (cells)	$3.99 \times 10^{10} (1.6 \times 10^{10})$	$5.88 \times 10^{10} (3 \times 10^{10})$	$7.43 \times 10^{10} (2 \times 10^{10})$	$8.71 \times 10^{10} (4 \times 10^{10})$	$5.40 \times 10^{10} (9 \times 10^{9})$	$5.35 \times 10^{10} (1 \times 10^{10})$	$8.52 \times 10^{10} (7 \times 10^{10})$
Cells/g coal	$7.98 \times 10^{8} (3.2 \times 10^{8})$	$1.18 \times 10^{9} (6 \times 10^{8})$	$1.49 \times 10^{9} (4 \times 10^{8})$	$1.74 \times 10^{9} (8 \times 10^{8})$	$1.08 \times 10^{9} (2 \times 10^{8})$	$1.07 \times 10^{9} (2 \times 10^{8})$	$1.70 \times 10^{9} (1.3 \times 10^{9})$

Table 2.5: Iodometric titration results for sulfide standard solutions with coal. Sulfide could not be recovered quantitatively from coal slurry experiments.

Samples	Vol. $S_2O_3^{2-}$ (mL)	sulfide (g/L)	Conc. (mM)	% recovery
coal blank	8.05	4.73×10^{-3}	0.148	NA
1 mM no coal	4.6	3.64×10^{-2}	1.14	114%
100 µM + coal	8.35	1.39×10^{-2}	0.434	434%
100 µM + coal	7.8	1.72×10^{-2}	0.537	537%
100 µM + coal	8.45	1.33×10^{-2}	0.415	415%
1 mM + coal	9.55	6.70×10^{-3}	0.209	20.9%
1 mM + coal	9.55	6.70×10^{-3}	0.209	20.9%
1 mM + coal	10.1	3.40×10^{-3}	0.106	10.6%

2.7 References

Balkwill D. L., Leach F. R., Wilson J. T., NcNabb J. F. and White D. C. (1988) Equivalence of microbial biomass measures based on membrane lipid and cell wall components, adenosine triphosphate, and direct counts in subsurface aquifer sediments. *Microbial Ecol.* **54**, 273–291.

Bates B. L., McIntosh J. C., Lohse K. A. and Brooks P. D. (2011) Influence of groundwater flowpaths, residence times and nutrients on the extent of microbial methanogenesis in coal beds: Powder River Basin, USA. *Chem. Geol.* **284**, 45–61.

Beckmann S., Lueders T., Krüger M., Von Netzer F., Engelen B. and Cypionka H. (2011) Acetogens and acetoclastic methanosarcinales govern methane formation in abandoned coal mines. *Appl. Environ. Microbiol.* **77**, 3749–56.

Bonch-Osmolovskaya E. A., Miroshnichenko M. L., Lebedinsky A. V, Chernyh N. A., Nazina T. N., Ivoilov V. S., Belyaev S. S., Boulygina E. S., Lysov Y. P., Perov A. N., Mirzabekov A. D., Hippe H., Stackebrandt E., L'Haridon S. and Jeanthon C. (2003) Radioisotopic, culture-based, and oligonucleotide microchip analyses of thermophilic microbial communities in a continental high-temperature petroleum reservoir. *Appl. Environ. Microbiol.* **69**, 6143–6151.

Boschker H. T. S., Nold S. C., Wellsbury P., Bos D., De Graaf W., Pel R., Parkes R. J. and Cappenberg T. E. (1998) Direct linking of microbial populations to specific biogeochemical processes by ^{13}C-labelling of biomarkers. *Nature.* **392**, 801–805.

Canfield D. E., Thamdrup B., Kristensen E., Southward A. J., Tyler P. A., Young C. M. and Fuiman L. A. (2005) *Aquatic Geomicrobiology*., Elsevier Academic Press, New York.

Dockins W. S., Olson G. J., McFeters G. A., Turbak S. C. and Lee R. W. (1980) *Sulfate reduction in groundwater of southeastern Montana*., USGS Water-Resources Investigations Report: 80-9.

Dowling N. J. E., Widdle F. and White D. C. (1986) Phospholipid ester-linked fatty acid biomarkers of acetate-oxidizing sulfate-reducers and other sulfide-forming bacteria. *J. General Microbiol.* **132**, 1815–1825.

Dunkelblum E., Tan S. H. and Silk P. J. (1985) Double-bond location in monounsaturated fatty acids by dimethyl disulfide derivatization and mass spectrometry. *J. Chem. Ecol.* **11**, 265–277.

Elferink S. J. W. H. O., Luppens S. B. I., Marcelis C. L. M. and Stams A. J. M. (1998) Kinetics of acetate oxidation by two sulfate reducers isolated from anaerobic granular sludge. *Appl. Environ. Microbiol.* **64**, 2301–2303.

EPA U. S. (1996a) *U.S. EPA Standard Method 9030B: Acid soluble and insoluble sulfides: distillation*.

EPA U. S. (1996b) *U.S. EPA Standard Method 9034-1: Titrimetric procedure for acid soluble and acid insoluble sulfides*.,

Fakoussa R. M. and Hofrichter M. (1999) Biotechnology and microbiology of coal degradation. *Appl. Microbiol. Biotechnol.* **52**, 25–40.

Flores R. M., Rice C. A., Stricker G. D., Warden A. and Ellis M. S. (2008) Methanogenic pathways of coal-bed gas in the Powder River Basin, United States: The geologic factor. *Int. J. Coal. Geol.* **76**, 52–75.

Formolo M., Martini A. and Petsch S. (2008) Biodegradation of sedimentary organic matter associated with coalbed methane in the Powder River and San Juan Basins, U.S.A. *Int. J. Coal. Geol.* **76**, 86–97.

De Graaf W., Wellsbury P., Parkes R. J. and Cappenberg T. E. (1996) Comparison of acetate turnover in methanogenic and sulfate-reducing sediments by radiolabeling and stable isotope labeling and by use of specific inhibitors: evidence for isotopic exchange. *Appl. Environ. Microbiol.* **62**, 772–777.

Green C. T. and Scow K. M. (2000) Analysis of phospholipid fatty acids (PLFA) to characterize microbial communities in aquifers. *Hydrogeol. J.* **8**, 126–141.

Green M. S., Flanegan K. C. and Gilcrease P. C. (2008) Characterization of a methanogenic consortium enriched from a coalbed methane well in the Powder River Basin, U.S.A. *Int. J. Coal. Geol.* **76**, 34–45.

Harris S. H., Smith R. L. and Barker C. E. (2008) Microbial and chemical factors influencing methane production in laboratory incubations of low-rank subsurface coals. *Int. J. Coal. Geol.* **76**, 46–51.

Ingvorsen K., Zehnder a J. and Jørgensen B. B. (1984) Kinetics of sulfate and acetate uptake by Desulfobacter postgatei. *Appl. Environ. Microbiol.* **47**, 403–408.

Jones E. J. P., Voytek M. A., Corum M. D. and Orem W. H. (2010) Stimulation of methane generation from nonproductive coal by addition of nutrients or a microbial consortium. *Appl. Environ. Microbiol.* **76**, 7013–7022.

Jones E. J. P., Voytek M. A., Warwick P. D., Corum M. D., Cohn A., Bunnell J. E., Clark A. C. and Orem W. H. (2008) Bioassay for estimating the biogenic methane-generating potential of coal samples. *Int. J. Coal. Geol.* **76**, 138–150.

Jones R. E., Beeman R. E. and Suflita J. M. (1989) Anaerobic metabolic processes in the deep terrestrial subsurface. *Geomicrobiol. J.* **7**, 117–130.

Jørgensen B. B. and Kasten S. (2006) Sulfur cycling and methane oxidation. In *Marine Geochemistry* (eds. H. D. Schulz and M. Zabel). Springer Berlin / Heidelberg, Berlin. pp. 271–309.

Kieft T. L., Wilch E., Connor K. O. and Ringelberg D. B. (1997) Survival and phospholipid fatty acid profiles of surface and subsurface bacteria in natural sediment microcosms. *Appl. Env. Microbiol.* **63**, 1531–1542.

Klein D. A., Flores R. M., Venot C., Gabbert K., Schmidt R., Stricker G. D., Pruden A. and Mandernack K. (2008) Molecular sequences derived from Paleocene Fort Union Formation coals vs. associated waters: Implications for CBM regeneration. *Int. J. Coal. Geol.* **76**, 3–13.

Kroppenstedt R. M., Goodfellow M. and Minnikin D. D. (1985) Fatty acid and menaquinone analysis of actinomycetes and related organisms. In *Chemical Methods in Bacterial Systematics* Academic Press, Orlando, FL. p. 410.

Lechevalier H. and Lechevalier M. P. (1988) Chemotaxonomic use of lipids- an overview. In *Microbial Lipids vol. 1* (eds. C. Ratledge and S. G. Wilkinson). Academic Press, San Diego. pp. 869–902.

Lovley D. R. and Klug M. J. (1986) Model for the distribution of sulfate reduction and methanogenesis in freshwater sediments. *Geochim. Cosmochim. Acta* **50**, 11–18.

Lovley D. R. and Klug M. J. (1983) Sulfate reducers can outcompete methanogens at freshwater sulfate concentrations. *Appl. Environ. Microbiol.* **45**, 187–192.

Martens C. S. and Berner R. A. (1974) Methane production in the interstitial waters of sulfate-depleted marine sediments. *Science.* **185**, 1167–1169.

Martini A. M., Budai J. M., Walter L. M. and Schoell M. (1996) Microbial generation of economic accumulations of methane within a shallow organic-rich shale. *Nature.* **383**, 155–158.

Martini A. M., Walter L. M., Budai J. M., Ku T. C. W., Kaiser C. J. and Schoell M. (1998) Genetic and temporal relations between formation waters and biogenic methane: Upper Devonian Antrim Shale, Michigan basin, USA. *Geochim. Cosmochim. Acta* **62**, 1699–1720.

McIntosh J. C., Martini A., Petsch S., Huang R. and Nüsslein K. (2008) Biogeochemistry of the Forest City Basin coalbed methane play. *Int. J. Coal. Geol.* **76**, 111–118.

McMahon P. B., Chapelle F. H., Falls W. F. and Bradley P. M. (1992) Role of microbial processes in linking sandstone diagenesis with organic-rich clays. *J. Sed. Petrol.* **62**, 1–10.

Metje M. and Frenzel P. (2007) Methanogenesis and methanogenic pathways in a peat from subarctic permafrost. *Env. Microbiol.* **9**, 954–964.

Middelburg J. J., Vlug T. and Van der Nat F. J. W. A. (1993) Organic matter mineralization in marine systems. *Global Planet. Change.* **8**, 47–58.

Mills C. T., Amano Y., Slater G. F., Dias R. F., Iwatsuki T. and Mandernack K. W. (2010) Microbial carbon cycling in oligotrophic regional aquifers near the Tono Uranium Mine, Japan as inferred from $\delta^{13}C$ and $\delta^{14}C$ values of in situ phospholipid fatty acids and carbon sources. *Geochim. Cosmochim. Acta* **74**, 3785–3805.

Mitterer R. M. (2010) Methanogenesis and sulfate reduction in marine sediments: A new model. *Earth. Planet. Sci. Lett.* **295**, 358–366.

Muyzer G. and Stams A. J. M. (2008) The ecology and biotechnology of sulphate-reducing bacteria. *Nat. Rev. Microbiol.* **6**, 441–454.

Olson G. J., Dockins W. S., McFeters G. A. and Iverson W. P. (1981) Sulfate-reducing and methanogenic bacteria from deep aquifers in Montana. *Geomicrobiol. J.* **2**, 327–340.

Orem W. H., Tatu C. A., Lerch H. A., Rice C. A., Bartos T. T., Bates A. L., Tewalt S. and Corum M. D. (2007) Organic compounds in produced waters from coalbed natural gas wells in the Powder River Basin, Wyoming, USA. *Appl. Geochem.* **22**, 2240–2256.

Oremland R. S. and Taylor B. F. (1978) Sulfate reduction and methanogenesis in marine sediments. *Geochim. Cosmochim. Acta* **42**, 209–214.

Pinkart H. C., Ringelberg D. B., Piceno Y. M., McNaughton S. J. and White D. C. (2002) Biochemical approaches to biomass measurements and community structure analysis. In *Manual of Environmental Microbiology (Second Edition)* (eds. C. J. Hurst, R. Crawford, G. Knudsen, M. J. McInerney, and L. D. Stezenbach). American Society for Microbiology Press, Washington D.C. pp. 101–113.

Ramakers C., Ruijter J. M., Deprez R. H. L. and Moorman A. F. . (2003) Assumption-free analysis of quantitative real-time polymerase chain reaction (PCR) data. *Neurosci. Lett.* **339**, 62–66.

Rice C. A., Flores R. M., Stricker G. D. and Ellis M. S. (2008) Chemical and stable isotopic evidence for water/rock interaction and biogenic origin of coalbed methane, Fort Union Formation, Powder River Basin, Wyoming and Montana U.S.A. *Int. J. Coal. Geol.* **76**, 76–85.

Rice D. D. and Claypool G. C. (1981) Generation, accumulation, and resource potential of biogenic gas. *AAPG Bull.* **64**, 5–25.

Routh J., Grossman E. L., Ulrich G. and Suflita J. M. (2001) Volatile organic acids and microbial processes in the Yegua formation, east-central Texas. *Appl. Geochem.* **16**, 183–195.

Ruijter J. M., Ramakers C., Hoogaars W. M. H., Karlen Y., Bakker O., Van den Hoff M. J. B. and Moorman a F. M. (2009) Amplification efficiency: linking baseline and bias in the analysis of quantitative PCR data. *Nucleic. Acids. Res.* **37**, e45.

Schlegel M. E., McIntosh J. C., Bates B. L., Kirk M. F. and Martini A. M. (2011a) Comparison of fluid geochemistry and microbiology of multiple organic-rich reservoirs in the Illinois Basin, USA: Evidence for controls on methanogenesis and microbial transport. *Geochim. Cosmochim. Acta* **75**, 1903–1919.

Schlegel M. E., McIntosh J. C., Petsch S. T., Orem W. H., Jones E. J. P. and Martini A. M. (2013) Extent and limits of biodegradation by in situ methanogenic consortia in shale and formation fluids. *Appl. Geochem.* **28**, 172–184.

Schlegel M. E., Zhou Z., McIntosh J. C., Ballentine C. J. and Person M. A. (2011b) Constraining the timing of microbial methane generation in an organic-rich shale using noble gases, Illinois Basin, USA. *Chem. Geol.* **287**, 27–40.

Schmidt R. (2007) Characterization of the Bacterial and Archaeal Communitites in Coalbed Methane Aquifers in the Wyodak-Anderson Coal Zone of the Powder River Basin, WY Using Polar Lipid Analysis Techniques. Thesis, Colorado School of Mines, Environmental Science and Engineering.

Schönheit P., Kristjansson J. K. and Thauer R. K. (1982) Kinetic mechanism for the ability of sulfate-reducers to outcompete methanogens for acetate. *Arch. Microbiol.* **132**, 285–288.

Scott A. R., Kaiser W. R. and Ayers Jr. W. B. (1994) Thermogenic and secondary biogenic gases, San Juan Basin, Colorado and New Mexico- Implications for coalbed gas producibility. *AAPG Bull.* **78**, 1186–1209.

Shimizu S., Akiyama M., Naganuma T., Fujioka M., Nako M. and Ishijima Y. (2007) Molecular characterization of microbial communities in deep coal seam groundwater of northern Japan. *Geobiology.* **5**, 423–433.

Strąpoć D., Mastalerz M., Dawson K., Macalady J. L., Callaghan A. V, Wawrik B., Turich C. and Ashby M. (2011) Biogeochemistry of microbial coal-bed methane. *Annu. Rev. Earth. Planet. Sci.* **39**, 617–656.

Strąpoć D., Mastalerz M., Schimmelmann A., Drobniak A. and Hasenmueller N. R. (2010) Geochemical constraints on the origin and volume of gas in the New Albany Shale (Devonian–Mississippian), eastern Illinois Basin. *AAPG Bull.* **94**, 1713–1740.

Strąpoć D., Picardal F. W., Turich C., Schaperdoth I., Macalady J. L., Lipp J. S., Lin Y.-S., Ertefai T. F., Schubotz F., Hinrichs K.-U., Mastalerz M. and Schimmelmann A. (2008) Methane-producing microbial community in a coal bed of the Illinois basin. *Appl. Environ. Microbiol.* **74**, 2424–2432.

Tseng H. (1997) A tectogenetic origin for the deep subsurface microorganisms of Taylorsville Basin: thermal and fluid flow model constraints. *FEMS. Microbiol. Rev.* **20**, 391–397.

Ulrich G. and Bower S. (2008) Active methanogenesis and acetate utilization in Powder River Basin coals, United States. *Int. J. Coal. Geol.* **76**, 25–33.

Vainshtein M., Hippe H. and Kroppenstedt R. M. (1992) Cellular fatty-acid composition of Desulfovibrio species and its use in classification of sulfate-reducing bacteria. *Syst. Appl. Microbiol.* **15**, 554–566.

Walvoord M. A., Pegram P., Phillips F. M., Person M., Kicft T. L., Fredrickson J. K., Mckinley J. P. and Swenson J. B. (1999) Groundwater flow and geochemistry in the southeastern San Juan Basin: Implications for microbial transport and activity. *Water Resour. Res.* **35**, 1409–1424.

White D. C., Flemming C. a, Leung K. T. and Macnaughton S. J. (1998) In situ microbial ecology for quantitative appraisal, monitoring, and risk assessment of pollution remediation in soils, the subsurface, the rhizosphere and in biofilms. *J. Microbiol. Meth.* **32**, 93–105.

White D. C. and Ringelberg D. B. (1998) Signature lipid biomarker analysis. In *Techniques in Microbial Ecology* (eds. R. S. Burlage, R. Atlas, D. Stahl, G. Geesey, and G. Sayler). Oxford University Press, New York.

Winfrey M. R. and Zeikus J. G. (1979) Anaerobic metabolism of immediate methane precursors in Lake Mendota. *Appl. Environ. Microbiol.* **37**, 244–253.

Yadav V. K. and Archer D. B. (1989) Sodium molybdate inhibits sulphate reduction in the anaerobic treatment of high-sulphate molasses wastewater. *Appl. Microbiol. Biotechnol.* **31**, 103–106.

Zhou Z. and Ballentine C. J. (2006) 4He dating of groundwater associated with hydrocarbon reservoirs. *Chem. Geol.* **226**, 309–327.

CHAPTER 3
The effects of pCO_2 and urea hydrolysis on microbial community structure and methanogenesis from coal

Authors: Andrew W. Glossner, Lisa K. Gallagher, Christopher T. Mills, Lee Landkamer, Linda Figueroa, Junko Munakata-Marr, Kevin W. Mandernack

The experiments in this chapter were designed and conducted by Andrew Glossner, with the exception of the qPCR of the mcrA gene, which was performed by Lisa Gallagher, who also wrote the portion of the methodology section pertinent to that work. This chapter will be submitted to the journal Applied Microbiology and Biotechnology.

3.1 Abstract

Deeply buried coal seams are considered attractive target formations for CO_2 sequestration due to the possibility of enhanced coalbed methane recovery with CO_2 injection. In basins such as the Powder River Basin these coal seams harbor diverse and active microbial communities capable of breaking down the coal to form methane. Little is known about the potential effects of CO_2 sequestration on this microbial community. Microcosm experiments were prepared to measure what the effects of varying CO_2 partial pressures (pCO_2) from 0.2 to 2.5 atmospheres had on methane production, acetate utilization, microbial community structure and total biomass measured using phospholipid fatty acid (PLFA) analysis. Additionally, experiments were amended with urea in order to increase solubility trapping of CO_2 through microbially catalyzed urea hydrolysis. Results show that under the range of experimental conditions tested, increasing pCO_2 has little effect on total methanogenesis from coal. Acetate was the most important precursor observed for methanogenesis and its initial concentration was the

determining factor in total methanogenic potential from coal, regardless of pCO_2. The addition of urea at 1 g/L concentration stimulated methanogenesis, while concentrations above 2.5 g/L caused the microcosm pH to rise above pH 7.5, halting methanogenesis. Additionally the minimum concentration of acetate required for stimulation of bacteria catalyzing urea hydrolysis was observed to be 1 mM acetate.

3.2 Introduction

The mitigation of CO_2 emissions by injecting CO_2 as a supercritical fluid ($scCO_2$) into subsurface geologic formations is known as carbon capture and storage (CCS). Deeply buried coal seams are considered potential target formations for CCS (DOE, 2010). These coal seams can harbor complex microbial communities with the ability to produce economically significant quantities of methane. Interest is also significant in the potential of CO_2-enhanced coalbed methane (CO_2-ECBM), the process whereby CO_2 is injected into deeply buried coal seams for the purpose of CO_2 sequestration as well as enhanced methane recovery (IPCC, 2005). Recent studies have shown that CO_2-ECBM is an economically viable strategy for sequestration of CO_2 in deeply buried coals of Japan (Fujioka et al., 2010) as well as the Powder River Basin in the United States (Ross et al., 2012).

Several highly-productive basins in the continental United States are known to produce gas of biogenic origin, including the Powder River Basin, WY (Rice and Flores, 1991; Flores et al., 2008), the San Juan Basin, CO (Scott et al., 1994), and the Black Warrior Basin, AL (Pashin, 2007). Previous studies have demonstrated the potential for either native microbes or coal samples inoculated with specialized microbial consortia to produce methane under laboratory conditions (Shumkov et al., 1999; Harris et al., 2008;

Jones et al., 2008; Jones et al., 2010). Under anaerobic conditions the process of coal degradation is believed to begin with fermentative cleavage of macromolecules in coal to long chain fatty acids. Recent evidence has confirmed the importance of long chain fatty acids as intermediates in the process (Jones et al., 2010). The long chain fatty acids are then degraded to shorter chain organic intermediates such as lactate, formate, propionate, and acetate, and other products such as hydrogen, methanol, and carbon dioxide by fermentative organisms. The final steps of the conversion of coal to methane require the actions of secondary fermenters, homoacetogenic bacteria, as well as acetoclastic and hydrogenotrophic methanogens (Strąpoć et al., 2011). Because CO_2 is both a product and a substrate in this complex process, it is likely that small changes in pCO_2 would have significant impacts on the process of methanogenesis from coal and the microbial community mediating the process.

Modeling studies have shown that increasing pCO_2 to injection-level pressures (~200 bars at reservoir T and P) would have a negative effect on acetoclastic methanogenesis (Onstott, 2005), a potentially important reaction in coal-bearing methanogenic systems (Beckmann et al., 2011). However, increasing the $CO_{2(aq)}$ and HCO_3^- concentrations increases the free energy yield of the CO_2-reducing methanogenic and acetogenic pathways (Onstott, 2005). Therefore, this could instead lead to enhanced acetoclastic methanogenesis, particularly at locations more distal from the point of CO_2 injection where conditions are likely to be too harsh for microbial survival. The situation is further complicated because of the anticipated effect of decreasing the pH due to CO_2 dissolution. While methanogenesis may remain an active microbial pathway even at a very low pH (~pH 3) (Williams and Crawford, 1985), and acid-tolerant methanogens have been found in acidic peat bogs (Chanton et al., 1995; Bräuer et al., 2004; Kotsyurbenko et al., 2004), a lower pH (<6) is thought to inhibit H_2-consuming and producing processes, including fermentation (Slyter et al., 1966; Lovley and Goodwin, 1988). In addition, decreasing the pH in methanogenic systems is thought to inhibit the acetoclastic pathway as acetate then exists in its protonated form (Fukuzaki et al., 1990). Therefore, even modest changes in pCO_2 could have important implications for methanogenesis in coal-bearing strata where both methanogenic pathways are possible.

Urea can buffer the effects of decreased pH resulting from CO_2 injections as well as serving as a readily available nutrient for a N-limited microbial community (Swensen and Bakken, 1998; Harder Nielsen, 1998). Urea is a commonly utilized N-fertilizer that istypically synthesized via NH_3 and CO_2 in industrial processes. Urea hydrolysis occurs both abiotically and biotically, with the latter process governed by the urease enzyme whose rate is 1014 times more rapid than the uncatalyzed reaction (Jabri et al., 1995). The reactions involved with urea hydrolysis have been summarized elsewhere (Mitchell et al., 2010), but the net result of urea hydrolysis is an increase in pH, NH_3, and $[CO_3^{2-}]_{Total}$, which can lead to calcite precipitation in some systems when sufficient Ca^{2+} is present (Ferris and Stehmeier, 1992; Ferris et al., 1996; Fujita et al., 2000; Fujita et al., 2004). Other studies have suggested the possibility of using urea to stimulate biomineralization in CO_2 storage reservoirs (Ferris et al., 2004; Mitchell et al., 2010). The mechanisms of storage would include both solubility and mineral trapping as a result of the pH increase caused by urea hydrolysis. Mitchell et al. (2010) showed that a pure culture of *Sporosarcina pasteurii* hydrolyzed urea and caused calcite precipitation in microcosm experiments. However, recent work with *S. pasteurii* demonstrated inhibition of this species under anaerobic conditions, suggesting a different organism or assemblage of organisms would be needed to hydrolyze urea and thus enhance CO_2 trapping in anaerobic subsurface reservoirs (Martin et al., 2012).

Because urea is a commonly used agricultural fertilizer, its effects on methane flux from agricultural soils such as rice paddies have been investigated thoroughly. Some studies report stimulation of methane production (Cicerone and Shetter, 1981; Lindau, 1994; Banik et al., 1996; Singh, 1999; Dan et al., 2001) while others report inhibition (Bronson et al., 1997; Bodelier et al., 2000). The effects of urea amendment on a complex consortium of organisms metabolizing coal to methane are not well documented. It was hypothesized that any potential pH buffering associated with urea hydrolysis would help maintain the optimal physiological pH for methanogenesis (~7.5) (Boone et al., 1993) in our system, thereby increasing the methanogenic potential from coal.

In order to understand the effects of increasing pCO_2 and urea amendment on a methanogenic consortium metabolizing coal to methane, three sets of experiments were undertaken. Increasing pCO_2 was hypothesized to reduce the methanogenic potential of this consortium. Because amending "high pCO_2" experiments with urea would buffer the elevated pCO_2, this was also hypothesized to lead to enhanced methanogenesis relative to non-urea amended control experiments at the same pCO_2. One obvious limitation in these experiments is that the pCO_2 levels achievable in laboratory microcosm experiments are much lower than those experienced by microbes under actual reservoir conditions expected at the CO_2 injection site. However, as previously noted, one would expect that a gradient of pCO_2 values will result between the injection site and more distal regions within the reservoir, whereby the microcosm experiments mimic conditions of the latter.

Furthermore, the experiments provided some general observations regarding the effects of changing pCO_2 on the microbial methanogenic community in coal bearing systems.

The goal in all experiments was to track carbon flow in methanogenic microcosm experiments incubated in the laboratory with coal utilized as the only source of organic carbon. These experiments measured changes in headspace gases (CH_4 and CO_2), dissolved short chain organic acids, and the microbial community composition using phospholipid fatty acid (PLFA) analysis and quantitative polymerase chain reaction (qPCR) of the methyl coenzyme-M reductase (mcrA) gene for methanogens. PLFAs are regarded as a reliable indicator of viable bacteria (White et al., 1979; Harvey et al., 1986; Balkwill et al., 1988).The mcrA gene is the key enzyme involved in methanogenesis (Ermler et al., 1997) and is considered diagnostic for methanogenic archaea. Quantification of the mcrA gene has been used to track changes in methanogen numbers when part of mixed consortia of microorganisms in both engineered and environmental systems (Lloyd, 1998; Edwards et al., 1998; Bidle, 1999; Lueders et al., 2001; Luton et al., 2002; Galand, 2002; Chin et al., 2004; Shigematsu et al., 2004; Inagaki et al., 2004; Nunoura et al., 2006; Wilms et al., 2007; Janssen and Kirs, 2008) . This method of quantifying methanogens has the benefits of specificity toward the metabolic group of interest, as well as a lower detection limit for methanogens in environmental samples (Steinberg and Regan, 2009) than lipid-based extraction techniques (Huguet et al., 2010).

3.3 Methods

Experimental design

Three different experiments were conducted to examine the effects of increasing pCO_2 and urea amendment on methanogenesis from coal. Each experiment was conducted in triplicate and all measurements reported are the average values of triplicate microcosms. One experiment (A) included three different partial pressures of CO_2 (pCO_2 = 0.2, 1.1, and 1.3 atm) along with 3 different concentrations of urea (1.0, 2.5, and 5.0 g/L) at pCO_2 = 1.1 and 1.3 atm CO_2. A second experiment (B) was conducted with pCO_2 = 0.2 atm and with 4 different concentrations of urea (0.5, 1.0, 2.5, and 5.0 g/L urea). The final experiment (C) utilized an expanded range of CO_2 pressures (0.2, 1.0, 1.5, and 2.5 atm CO_2) with each pCO_2 microcosm amended with urea at 1.0g/L. This was the optimal concentration of urea for methanogenesis based on results from experiment B.

All experiments were prepared in an anaerobic chamber with 5% H_2, 5% CO_2, and 90% N_2 atmosphere. Coal was collected from the Eocene Fort Union formation of the Powder River Basin, Wyoming by straining drill cuttings from the effluent of working drill rigs. Due to an agreement with the well owners we are unable to reveal the exact locations of the wells sampled. Coal cuttings were immediately rinsed with sterile deionized water in the field to remove drilling fluids then sealed in vacuum bags with chemical oxygen scrubbing packets. Coal cuttings were stored at 4^oC until use. Three sampling trips were conducted to collect coal samples in November, 2008, April, 2009, and again in September, 2009.

Experiments were initiated by weighing 10 g coal in an anaerobic chamber and adding to sterile 200 mL serum bottles. Anaerobic basal nutrient media (Tanner, 2006), prepared to exclude all external organic carbon sources except coal, was added at the ratio of 5:1 (vol: wt coal). All experiments were inoculated with a consortium of organisms enriched from, and maintained on, the same coal cuttings collected from the Powder River Basin, Wyoming. The consortium was maintained at 30^oC and transferred to fresh coal cuttings approximately every 60 days. The trace mineral solution was modified to reduce the amount of sulfate from the media by replacing $MgSO_4$ with $MgCl_2$. The media included (g/L) NaCl (0.8), NH_4Cl (1.0), KH_2PO_4 (0.1), KCl (0.1), $MgCl_2 \cdot 6H_2O$ (0.17), $CaCl_2 \cdot 2H_2O$ (0.04), $NaHCO_3$ (1.0), nitrilotriacetic acid (0.02), $MnSO_4 \cdot H_2O$ (0.01), $Fe(NH_4)2SO_4 \cdot 6H_2O$ (0.008), $CoCl_2 \cdot 6H_2O$ (0.002), $ZnSO_4 \cdot 7H_2O$ (0.002), $CuCl_2 \cdot 2H_2O$ (0.0002), $NiCl_2 \cdot 6H_2O$ (0.0002), $Na_2MoO_4 \cdot 2H_2O$ (0.0002), Na_2SeO_4 (0.0002), Na_2WO_4 (0.0002). Medium was prepared by autoclaving deionized water for 10 minutes to reduce oxygen saturation, then sparged with 80% N_2: 20% CO_2 for 15 minutes before adding 10 mL trace metal solution, 50 mL trace mineral solution (both filter sterilized), and 1 g/L $NaHCO_3$ just before sealing under N_2:CO_2 and autoclaving the complete media for 40 minutes (Tanner, 2006). 10 mL of filter-sterilized trace vitamin solution was added aseptically after cooling the medium in the anaerobic chamber (Tanner, 2006). Coal, media, and inoculum were added to 200 mL serum bottles in an anaerobic chamber, and each bottle sealed with a butyl rubber stopper (Bellco #2048-18150). The headspace of each bottle was then purged with the headspace gas required for the experimental setup (either 80%:20% N_2:CO_2 or CO_2) for at least 5 minutes and pressurized to the required headspace pressure.

Experiment C was designed to examine the effect of CO_2 pressures as high as 2.5 atm, with and without 1 g/L urea. However, after incubating for more than 3 months, less than 1 µmol/g methane had been produced and there was no evidence for urea hydrolysis, based upon measured pH, headspace CO_2 concentration, and the lack of carbamic acid detected by HPLC. In order to test the hypothesis that urea hydrolysis in this system required a threshold acetate concentration greater than 100 µM, a group of 8 microcosms from experiment C were further amended with a 50 mM stock solution of acetate to a 1mM final concentration. These microcosms include 2 replicates of each of the following experiments: 0.2 atm CO_2, 1.3 atm CO_2, 0.2 atm CO_2 + 1 g/L urea, and 1.3 atm CO_2 + 1 g/L urea. These experiments were monitored for an additional 30 days.

The concentrations of low molecular weight organic (acetate, propionate, formate, succinate, oxalic, and citric) were determined by high performance liquid chromatography (HPLC) on an Agilent 1100 Series with a BioRad HPX-87H column (300 x 7.8 mm) and UV/VIS detector set at 210 nm. The concentrations of CH_4 and CO_2 were measured using a GC-17A gas chromatograph (Shimadzu, Kyoto, Japan). Methane was separated using a HayesepQ packed column (2m; Supelco, St. Louis, MO) and CO_2 was separated using a molecular sieve (5Å pore size, 2m) held at 100˚C. Thermal conductivity (200˚C) and flame ionization detectors (200˚C) connected in series were used for quantification of CO_2 and CH_4, respectively. The instrument's calibration was checked regularly with CH_4 and CO_2 standards (Scott Specialty Gases, Plumsteadville, PA).

Phospholipid Fatty Acid (PLFA)Analysis

Phospholipid fatty acid analysis was performed in order to quantify microbial biomass and characterize the bacterial community structure in these experiments. All solvents used were of HPLC grade, and aqueous solutions were stored over chloroform to remove trace organic contamination. All glassware used in the preparation of PLFAs was baked for at least 6 hours at 460˚C prior to use. Once experiments were completed 1.0 mL subsamples were taken from each serum bottle for molecular analysis (qPCR of mcrA gene) and frozen at -80˚C (Phenix™ 1.2 mL Cryovial C-411F). The remaining contents of each vial were then frozen at -20˚C, lyophilized and transferred to glass centrifuge tubes for subsequent PLFA extraction using a modified Bligh-Dyer extraction (White and Ringelberg, 1998). Sample extraction included shaking on a rotary shaker table at 150 rpm for two hours, followed by centrifugation at 1000 rpm for 30 minutes. The supernatant was decanted into separatory funnels, the solvent ratios adjusted to 1:1:0.8 (chloroform: methanol: buffer) by adding chloroform and 50 mM phosphate buffer and then allowed to separate overnight. The sample was then re-extracted for archaeal phosphoether lipids by adding 75 mL methanol, 37.5 mL chloroform, and 30 mL 10% trichloroacetic acid (wt:vol). The supernatant from the phosphoether lipid extraction was phase separated overnight by adding 30 mL water and 37.5 mL chloroform. The volume of both total lipid extracts was reduced under a N_2 stream and separated into neutral, glyco- and polar lipid classes using silica solid phase extraction (SPE) columns (Alltech 500mg, #209200). Prior to loading them with lipids, the SPE columns were prepared by washing with 5 mL methanol followed by 10 mL chloroform. After loading the silica columns with the total lipid extract, neutral lipids were eluted in 10 mL chloroform, glycolipids in 10 mL acetone, and polar lipids in 10 mL methanol. Fatty acid methyl esters (FAMEs) were prepared by mild alkaline methanolysis with 5% KOH:methanol (White and Ringelberg, 1998). All samples and blanks were injected with an internal standard (methyl tridecanoate (13:0), CAS# 1731-88-0) for quantification. The position of the double bond in monounsaturated PLFAs was determined by making their dimethyl disulfide adducts (Dunkelblum et al., 1985). Two ubiquitous FAMEs were commonly seen in blanks (C16:0 and C18:0) and were generally on the order of 2 nmol total.

GC-MS Procedures

FAMEs were analyzed on an Agilent 7890A as chromatograph with a DB-1MS column (60m x 0.25 mm I.D.), and quantified using a flame ionization detector (FID) coupled to an Agilent 5975C Inert XL mass spectrometer for FAME identification (Agilent Technologies, St. Louis, MO). The identity of each FAME was preliminarily assigned based on comparison of retention times with those of FAMEs from a standard mixture (Sigma Aldrich #47785-U). The injector temperature was 280˚C, the FID set to 200˚C, and the ion source temperature set to 250˚C. The oven temperature program began at 50˚C, increased to 150˚C at 20˚C min^{-1}, to 210˚C at 1.5˚C min^{-1}, and to a final temperature of 280˚C at 10˚C min^{-1} where it was held for 8 min. FAME identity was confirmed after ionization with electron impact at 70 eV. PELs were analyzed on the same instrument and column under the following temperature program: initial 70˚C, increased to 130˚C at 25 C˚ min^{-1}, increased to 190˚C at 6 C˚ min^{-1}, increased to 320˚C at 25 C˚ min^{-1} where it was held for a final 20 min.

PLFA Nomenclature

Phospholipid fatty acids are described in this work using the following nomenclature: A:BωC, where A is the number of carbon atoms in the molecule, B is the number of points of unsaturation in the molecule, and C is the number of carbons away from the ω terminal end that the double bond is located. The prefix *i* denotes a methyl branch at the *iso* position of the carbon chain, *ai* corresponds to a methyl group at the *anteiso* position, and 10Me denotes a methyl group at the 10th carbon from the carboxyl end of the lipid. The prefix *cy* denotes a *cyclopropyl* functionality in the carbon chain.

qPCR analysis

Quantitative (real time) polymerase chain reaction (qPCR) analysis was used to enumerate methanogens based on the presence of the mcrA functional gene unique to methanogenic organisms. Bulk deoxyribonucleic acid (DNA) was extracted from samples using the MoBio Powersoil® Kit. Methyl coenzyme reductase, subunit alpha (mcrA) genes were amplified using the primer set mlas/mcrA-rev (mlas 5'-GGTGGTGTM GGDTTCACMCARTA-3'/ mcrA-rev 5'-CGTTCATBGCGTA GTTVGGRTAGT-3') (Steinberg and Regan, 2008). Quantification of copy numbers was performed using a Lightcycler 480 II instrument (Roche). Cycling conditions were as follows: initial denaturation step at 95°C for 3 min, followed by five cycles of denaturation at 95°C for 30 s, annealing at 48°C for 45 s, and extension at 72°C for 30 s, with a ramp rate of 0.1°C/s from the annealing to the extension temperature. These five cycles were followed with 30 cycles of denaturation at 95°C for 30 s, annealing at 55°C for 45 s, and extension at 72°C for 30 s, followed by a final extension step at 72°C for 10 min. Plasmids containing the mcrA gene were generated (TOPO-TA cloning kit, Invitrogen), linearized and used as standards.

3.4 Results

Microcosm Experiments

Figures 3.1 and 3.2 show methane production for experiment A. Total methane production reached 30 µmol $g^{-1}coal^{-1}$ after 10 days in microcosms with 0.2 atm CO_2 while those with higher pCO_2 took almost 20 days to reach methane production values greater than 20 µmol $g^{-1}coal^{-1}$. Figures 3.1 and 3.2 show that urea amendment did not enhance methanogenesis relative to the control experiments at the same pCO_2. The pH remained between 6.3 and 6.5 in these experiments (data not shown). Although each microcosm had similar maximum acetate concentrations (4.11 ± 0.3 mM [average of all microcosms]; Figure 3.3), the rate of acetate consumption in each varied and depended on the CO_2 pressure and the urea concentration. Acetate was completely consumed by day 10 in microcosms with 0.2 atm CO_2, whereas at 1.1 atm CO_2 the acetate concentrations ranged from 1 to 2.5 mM at day 10 (Figure 3.3).

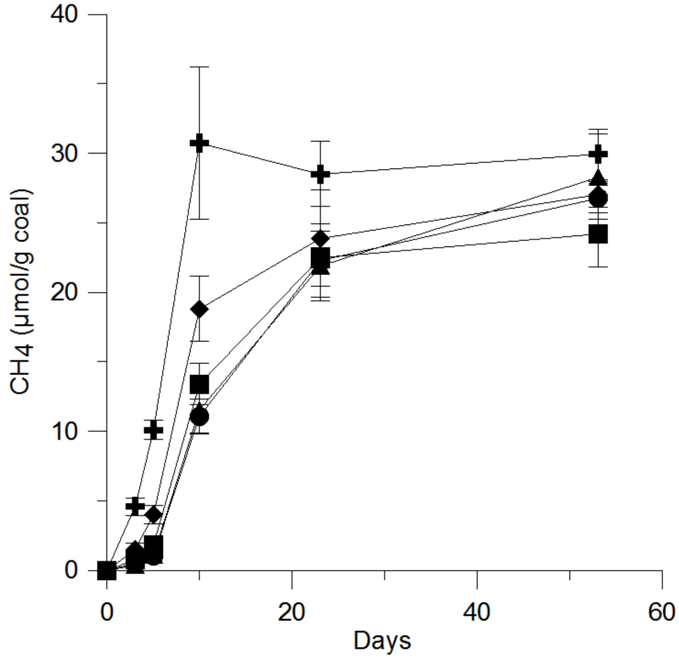

Figure 3.1: Methane production for microcosms with 1.1 atm CO_2 in experiment A. Error bars represent 1 standard deviation of triplicate incubations. ✚ 0.2 atm CO_2; ♦ 1.1 atm CO_2; ■ 1.1 atm CO_2 + 1g/L urea; ● 1.1 atm CO_2 + 2.5 g/L urea; ▲ 1.1 atm CO_2 + 5 g/L urea.

In order to isolate the effect of adding urea to coal microcosms, experiment B was conducted with four different concentrations of urea (0.5, 1, 2.5, and 5 g/L urea) and a single $p\mathrm{CO_2}$ (0.2 atm). Figure 3.4 shows the methane production in experiment B. Microcosms with 0.5 and 1 g/L urea did not produce significantly more methane than microcosms without urea (2.6 ± 0.9 µmol $g^{-1}coal^{-1}$ and 3.5 ± 1.3 µmol $g^{-1}coal^{-1}$ versus 2.5 ± 0.4 µmol $g^{-1}coal^{-1}$, respectively). Methane production was significantly different

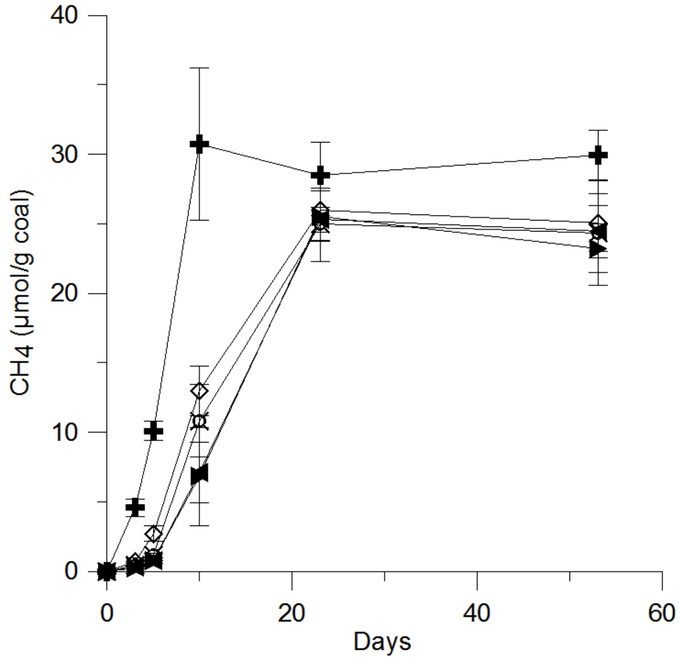

Figure 3.2: Methane production for microcosms with 1.3 atm CO_2 in experiment A. Error bars represent 1 standard deviation of triplicate incubations. ✚ 0.2 atm CO_2; ◊ 1.3 atm CO_2; ¤ 1.1 atm CO_2 + 1g/L urea; ► 1.3 atm CO_2 + 2.5 g/L urea; ◄ 1.3 atm CO_2 + 5 g/L urea.

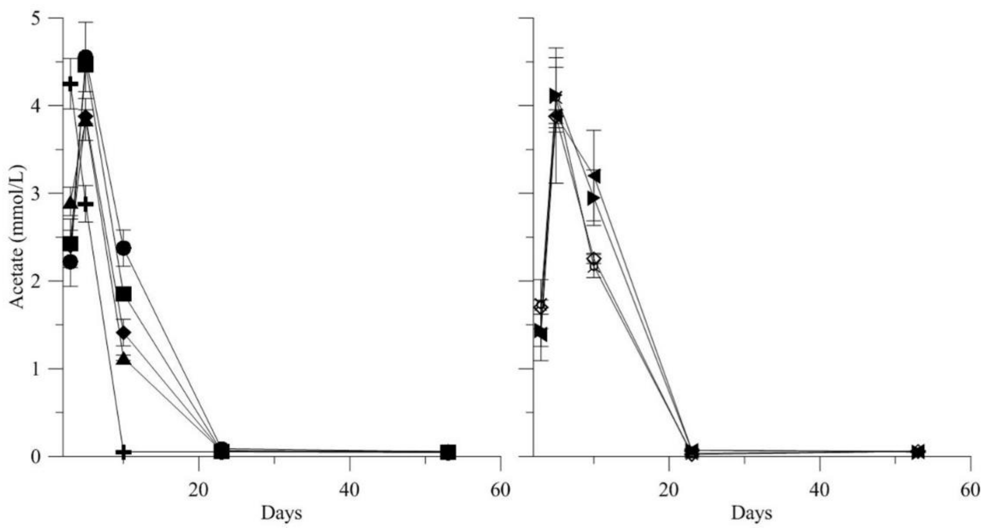

Figure 3.3: Acetate consumption in experiment A. Error bars represent 1 standard deviation of triplicate incubations. ✚ 0.2 atm CO_2; ♦ 1.1 atm CO_2; ■ 1.1 atm CO_2 + 1g/L urea; ● 1.1 atm CO_2 + 2.5 g/L urea; ▲ 1.1 atm CO_2 + 5 g/L urea; ◊ 1.3 atm CO_2; ¤ 1.1 atm CO_2 + 1g/L urea; ► 1.3 atm CO_2 + 2.5 g/L urea; ◄ 1.3 atm CO_2 + 5 g/L urea.

between microcosms with no urea (2.6 ± 0.9 μmol $g^{-1}coal^{-1}$), with 2.5 g/L urea (0.8 ± 0.2 μmol $g^{-1}coal^{-1}$; t= 6.63, p = 0.007, 2 tailed), and with 5 g/L urea (0.8 ± 0.2 μmol $g^{-1}coal^{-1}$; t= 6.85, p = 0.006, 2 tailed). Initial acetate concentrations were similarly ~ 100 μM for each urea concentration, indicating that each experiment had approximately the same methanogenic potential (Figure 3.5). This acetate was not added as part of the experimental setup, but appears to have been produced from the coal. The change in pH (Figure 3.6) suggests that urea hydrolysis commenced in all samples between days 7 and 12. The initial pH was ~ 6.3-6.5 in all samples at the start of the experiment, and rose to 6.90, 7.23, 7.75, and 8.42 in the 0.5, 1, 2.5, and 5 g/L urea amended samples, respectively (Figure 3.6). This increase in pH corresponded with the cessation of acetate consumption and methanogenesis in samples with 2.5 and 5 g/L urea (Figures 3.4 and 3.5). In addition the headspace pCO_2 was reduced in the samples amended with urea from starting values of ~0.18 atm CO_2 to final values of 0.07 ± 0.009 atm and 0.04 ± 0.008 atm in samples with 2.5 and 5 g/L urea, respectively (Figure 3.7). Samples with no urea, 0.5, and 1 g/L urea also showed reduced but similar pCO_2 at the end of the incubation (~0.12 atm CO_2; Figure 3.7).

In order to assess the response of the microbial community to a greater ΔpCO_2, experiment C was initiated with pCO_2 ranging from 0.2 atm to 2.5 atm. A pCO_2 of 2.5 atm was the practical upper limit for these experiments due to difficulties with liquid and gas sampling at higher pressures. Figure 3.8 shows the methane production in experiment C. Over the first 90 days the methane production in every microcosm of this experiment reached a maximum of 0.4 μmol g^{-1} $coal^{-1}$. This is lower by as much as 2 orders of magnitude than in either of the previous two experiments (Figures 3.1 and 3.4).

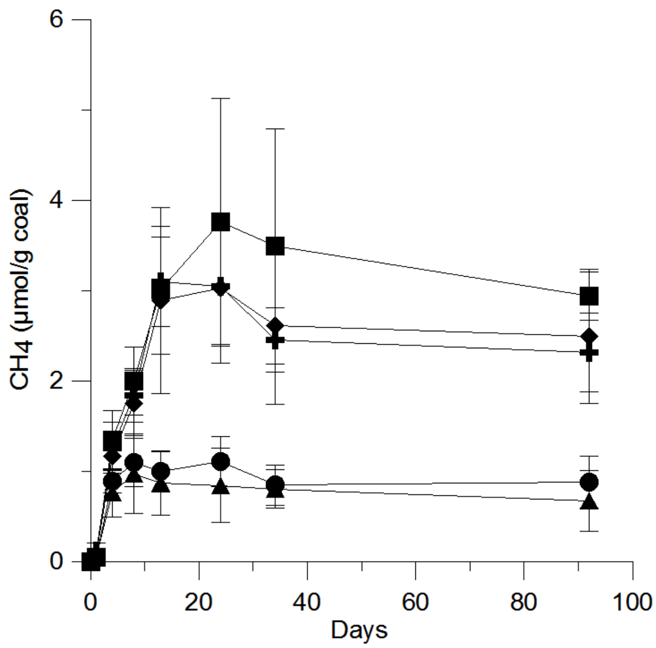

Figure 3.4: Methane production in experiments with variable urea concentrations and constant CO_2 of 0.2 atm. Error bars represent 1 standard deviation of triplicate incubations. ✚ No urea; ♦ 0.5 g/L urea; ■ 1 g/L urea; ● 2.5 g/L urea; ▲ 5 g/L urea.

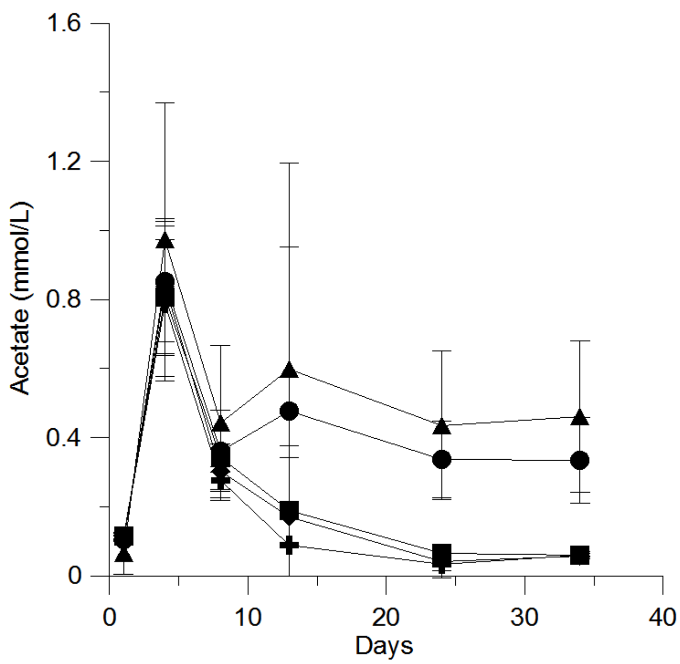

Figure 3.5: Acetate concentrations in experiment B. Error bars represent 1 standard deviation of triplicate incubations. ✚ No urea; ♦ 0.5 g/L urea; ■ 1 g/L urea; ● 2.5 g/L urea; ▲ 5 g/L urea.

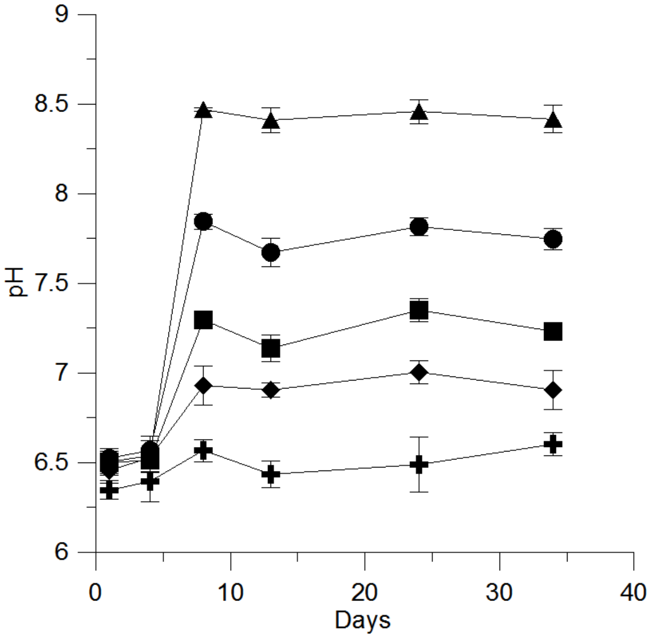

Figure 3.6: pH in experiment B. Error bars represent 1 standard deviation of triplicate incubations. ✚ No urea; ♦ 0.5 g/L urea; ■ 1 g/L urea; ● 2.5 g/L urea; ▲ 5 g/L urea.

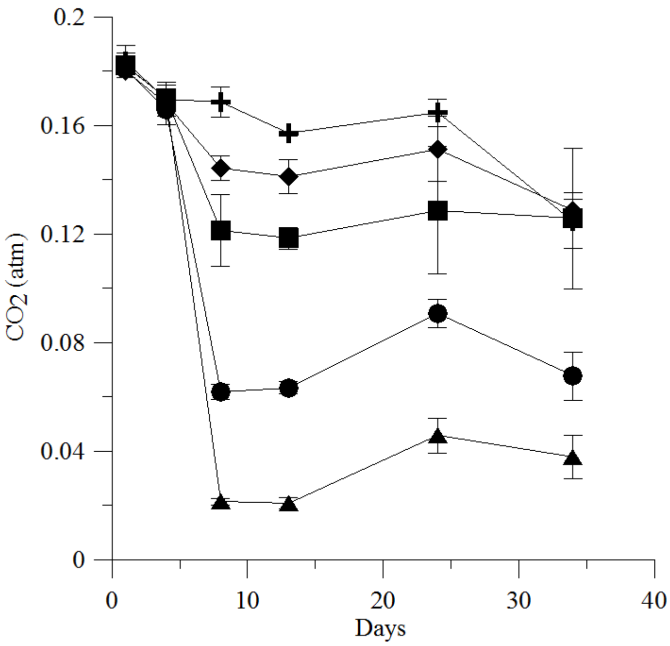

Figure 3.7: Headspace CO_2 in experiment B. Error bars represent 1 standard deviation of triplicate incubations;✚ No urea; ♦ 0.5 g/L urea; ■ 1 g/L urea; ● 2.5 g/L urea; ▲ 5 g/L urea.

The initial acetate concentration measured in experiment C was also lower by at least 10x (data not shown). Neither methane production nor acetate production/consumption showed any correlation with pCO_2 or any relationship with urea amendment. The pCO_2 in each microcosm remained constant over the first 90 days (Figure 3.10). The pH in each microcosm in experiment C remained relatively constant over the first 90 days (data not shown).

In order to test the hypothesis that urea hydrolysis depended on the availability of an organic electron donor, a suite of 8 microcosms from experiment C (2 replicates each of 0.2 atm CO_2, 1.3 atm CO_2, 0.2 atm CO_2 + 1 g/L urea, and 1.3 atm CO_2 + 1 g/L urea) was amended with acetate (1 mM final) following the first 90 days of incubation. The largest increase in methane occurred in microcosms with 0.2 atm CO_2, followed by microcosms with 0.2 atm CO_2 + 1 g/L urea (Figure 3.8). Microcosms with 1.3 atm CO_2 showed increases in headspace methane following acetate amendment, but lagged behind their counterparts with 0.2 atm CO_2. Acetate was consumed most quickly in microcosms with 0.2 atm CO_2, followed by 1.3 atm CO_2 + 1 g/L urea. In both urea-amended experiments the pH rose to higher levels than their respective controls without urea (from pH 6.7 to 7.4 in microcosms with 0.2 atm CO_2 + 1 g/L urea; from pH 6.2 to 6.5 in microcosms with 1.3 atm CO_2 + 1 g/L urea (Figure 3.9). This increase in pH also accompanied a decrease in headspace pCO_2 in the acetate amended microcosms with 0.2 atm CO_2 + 1 g/L urea (Figure 3.10). This is consistent with the drop in headspace CO_2 observed in experiment B (Figure 3.7).

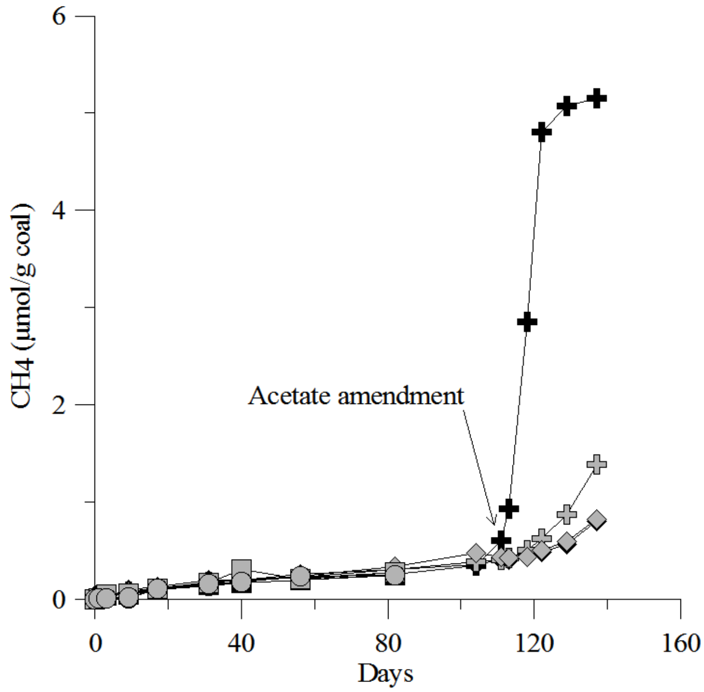

Figure 3.8: Methane production in experiment C. ✚ 0.2 atm CO_2; ♦ 1.1 atm CO_2; ■ 1.5 atm CO_2; ● 2.5 atm CO_2; gray symbols correspond to microcosms amended with 1 g/L urea.

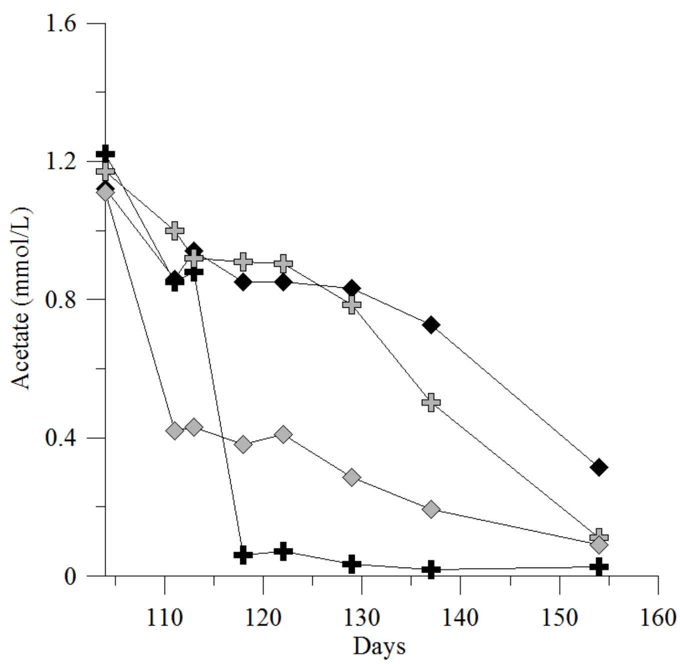

Figure 3.9: Acetate consumption in experiment C following acetate amendment at 105 days, see Fig. 8. Symbols represent average of duplicate microcosms. ✚ 0.2 atm CO_2; ♦ 1.1 atm CO_2; gray symbols correspond to each experiment amended with 1 g/L urea.

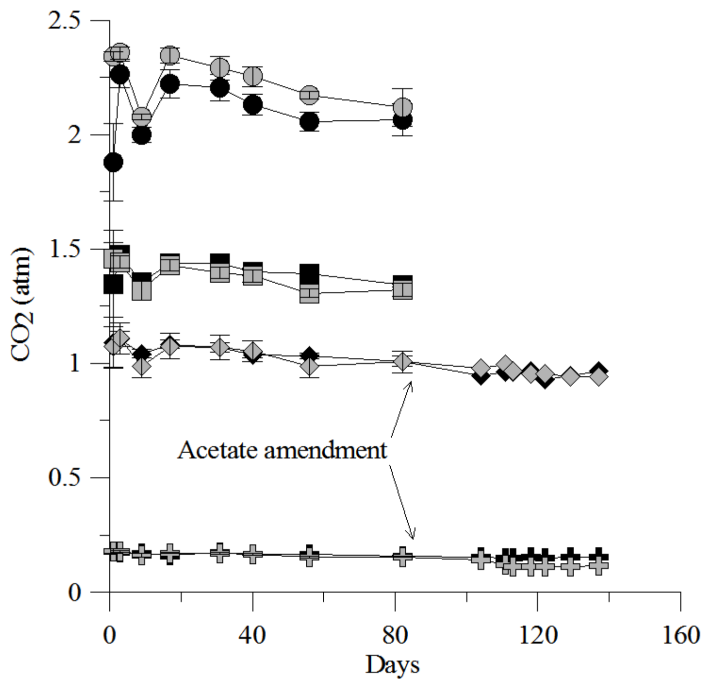

Figure 3.10: Headspace pCO2 in experiment set C. Error bars represent 1 standard deviation of triplicate incubations. ✚ 0.2 atm CO_2; ♦ 1.1 atm CO_2; ■ 1.5 atm CO_2; ● 2.5 atm CO_2; gray symbols correspond to each experiment amended with 1 g/L urea.

Microbial community analysis

PLFA analysis confirmed the presence of a diverse bacterial community in all incubation experiments. The microbial community composition remained consistent across the three sets of experiments in this work. Tables 3.1, 3.2, and 3.3 show the PLFAs extracted from experiments A, B, and C, respectively. The PLFAs observed in these experiments include the unbranched, saturated PLFAs 14:0, 15:0, 16:0, 17:0, and 18:0, as well as branched PLFAs including *i*15:0, *ai*15:0, 10Me16:0, *i*17:0, and *ai*17:0. Monoenoic PLFAs observed included 16:1ω5, 16:1ω7*cis*, 16:1ω7*trans*, 18:1ω9*cis* and 18:1ω9*trans*. The dominant PLFAs observed in all incubations were 16:1ω7 and 16:0, comprising 60% of total PLFAs detected. The total quantity of PLFAs recovered varied between experiments, from 1908 to 4774 nmole, in experiment A, from 1421 ±320 to 1925 ± 378 in experiment B, from 362 to 743 nmoles in unamended microcosms of

Experiment C and from 460 to 1832 nmoles in acetate-amended microcosms of experiment C.

The total mass of PLFA extracted corresponds to the total bacterial biomass extracted from the each microcosm. Using the conversion factor of Balkwill et al. (1988) of 2.4×10^4 cells/pmole $PLFA^{-1}$ an average bacterial density was calculated for each experimental condition (Tables 3.1, 3.2, and 3.3). The total microbial biomass measured by PLFA extraction in experiment A ranged from 9.54×10^8 cells $g^{-1}coal^{-1}$ to 2.39×10^9 cells $g^{-1}coal^{-1}$. Total bacterial biomass in experiment B ranged from $7.11 \pm 1.6 \times 10^8$ cells $g^{-1}coal^{-1}$ to $9.63 \pm 1.9 \times 10^8$ cells $g^{-1}coal^{-1}$. Microcosms with 5 g/L urea supported significantly higher biomass than the non-amended control ($t = 2.29$, $p = 0.04$) in experiment B. Experiment C had the lowest biomass estimates based on PLFAs, with total bacterial biomass ranging from 1.84×10^8 cells $g^{-1}coal^{-1}$ to 3.71×10^8 cells $g^{-1}coal^{-1}$ in the non-amended experiments, and from 2.3×10^8 cells $g^{-1}coal^{-1}$ to 9.16×10^8 cells $g^{-1}coal^{-1}$ in the microcosms amended with acetate (Table 3.3).

In order to test the hypothesis that urea hydrolysis correlated with microbial growth, for experiment B, Pearson's correlation coefficients were calculated for each PLFA observed and the amended urea concentration. The branched PLFA 10Me16:0 and the saturated PLFA 15:0 correlated negatively with the amended urea concentration (Pearson's $r = -0.66$ and -0.541, respectively, $p = 0.05$, 2-tailed). The only PLFA to show a positive correlation with methane production was the monoenoic PLFA 18:1ω9*trans* ($r = 0.639$, $p= 0.05$, 2-tailed).

qPCR of the mcrA gene

Microcosms from experiment C were analyzed using qPCR of the mcrA gene in an effort to quantify the relative changes to the archaeal methanogen population in experiments amended with acetate, and non-amended controls. Initial mcrA copy numbers were similar across all microcosms on day 1 at approximately 10^6 copies mL^{-1} and remained relatively constant across microcosms tested prior to acetate amendment (Figure 3.11). Following acetate amendment microcosms with 0.2 atm CO_2 showed the greatest increase in mcrA gene copy numbers up to 1.8 $x10^7$ copies mL^{-1}. Other microcosms in this series showed relatively constant mcrA copy numbers or decreased slightly following acetate amendment. One microcosm with 1.1 atm CO_2 which was not amended with acetate showed greater mcrA copy numbers (1.2 x 10^7 copies mL^{-1}) relative to the acetate amended microcosms at the same pCO_2 after 150 days (Figure 3.11).

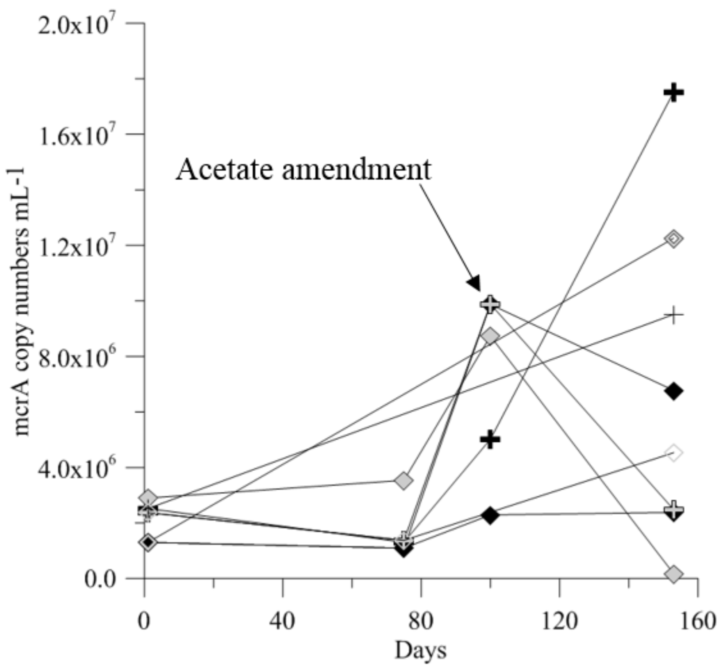

Figure 3.11: mcrA copy numbers in experiment C. ✚ 0.2 atm CO_2; ♦ 1.1 atm CO_2; gray symbols correspond to each experiment amended with 1 g/L urea, open symbols correspond to microcosms not amended with acetate under the conditions previously specified.

3.5 Discussion

Effect of increasing pCO_2 on methanogenesis

A series of microcosm experiments were conducted to understand what effect increasing pCO_2 would have on a complex microbial consortium metabolizing coal to form methane. In all experiments pCO_2 was observed to have no discernable effect on the rate of methanogenesis. This observation is consistent with recent modeling work wherein CO_2 injection was found to have a moderate impact on methanogenesis only if H_2 concentrations are very low (<1μM) (Onstott, 2005). Because H_2 has not been observed to be a significant byproduct of coal fermentation under laboratory conditions (Harris et al., 2008; Jones et al., 2010), it holds that increasing pCO_2 would have little effect on total methanogenesis. Our work has demonstrated that acetate is the dominant byproduct and precursor for methanogenesis from coal under the conditions tested. Onstott (2005) also found that the free energy available for acetoclastic methanogenesis would remain relatively constant at a variety of temperatures and pressures associated with a deep subsurface CO_2 injection reservoir. Therefore, if acetate availability remains constant, methanogenesis could remain unaffected by CO_2 injection in coal seams. Increasing pCO_2 from 0.2 atm to 2.5 atm did decrease the microcosm pH from 6.8 to approximately pH 6 in microcosms with only 1 g/L HCO_3^{-1} present as buffer. However, this change in pH did not significantly affect either methanogenesis or total microbial biomass (Figure 3.8 and Table 3.3).

Effect of urea on methanogenesis

Urea was observed in these experiments to have either a negligible or positive impact on methanogenesis, depending on pCO_2. In experiment B with 0.2 atm CO_2 and variable urea concentrations, the greatest methanogenesis was observed at a urea concentration of 1 g/L, while concentrations at 2.5 and 5 g/L urea showed inhibited methanogenesis and a corresponding increase in the pH by 1.5 and 2 pH units, respectively (Figure 3.6). This increase in pH likely resulted in the inhibition of acetoclastic methanogenesis observed in experiment B (Figure 3.5). This is consistent with the findings of Hunik et al. (1990), though the substrate in their study was poultry manure and the concentrations of acetate and ammonia were much higher than in the present work. A few known species of alkaliniphilic methanogens, including *Methanobacterium thermoalcaliphilum* (Blotevogel et al., 1985) and *Methanohalophilus zhilinae* (Mathrani et al., 1988) have pH optima > 8, but these species tend to be found in hypersaline, alkaline lakes. It is therefore unlikely that alkaliniphilic methanogens were present in these experiments, nor were they observed in microbial enrichments from Powder River Basin coals (Green et al., 2008; Ulrich and Bower, 2008; Gallagher et al., 2013). Ammonia, a byproduct of urea hydrolysis, has also been shown to inhibit methanogenesis in pure cultures at concentrations greater than 400 mM (Sprott and Patel, 1986). However, this concentration is more than double the maximum concentration possible from these experiments, and is therefore not the likely cause for the observed inhibition.

In all other experiments amended with urea at $pCO_2 \geq 1.1$ atm, urea had no effect on total methane production relative to control experiments at the same pCO_2 (Figures 3.1, 3.2, and 3.8). In experiment A, increasing urea concentrations decreased the rate at which acetate was consumed by methanogens (Figure 3.3) but not total methanogenesis (Figures 3.1 and 3.2). It is unclear why urea had this inhibitory effect on methanogenesis, but this effect was also seen in experiment C following the addition of acetate after the first 90 days of incubation. This addition was made to test the hypothesis that acetate was necessary for urea hydrolysis in this system. Some studies examining bacterially induced urea hydrolysis have utilized external carbon sources for heterotrophic growth (Stocks-Fischer et al., 1999; Bang et al., 2001; Bachmeier et al., 2002) while others have utilized "restrictive media" (Dupraz et al., 2009) with only mineral salts and urea to induce ureolysis (Fujita et al., 2004; Mitchell and Ferris, 2005; Mitchell and Ferris, 2006; Dupraz et al., 2009). Because the primary difference between experiments B and C was the initial acetate concentration, this substrate was hypothesized to be critical for urea hydrolysis in this system. In these microcosms the addition of 50 µmoles of acetate could have resulted in a maximum of 50 µmoles of methane (or 5 µmoles $g^{-1}coal^{-1}$; Figure 8) if all of it was converted to CH_4. This occurred in the two microcosms amended with acetate with 0.2 atm CO_2 (Figure 3.8). However, the acetate-amended microcosms with 1.1 atm CO_2**,** and each microcosm containing 1 g/L urea, converted less than 10 µmoles, or roughly 20% of the added acetate, to methane. The remainder of the acetate added appears to have been assimilated for growth, as evidenced by an increase in the total amount of PLFAs in all microcosms amended with acetate relative to the acetate amended microcosms with 0.2 atm CO_2 (Table 3.3). Acetate amended microcosms with 1.1 atm CO_2 plus urea produced less biomass and CH_4 than microcosms at the same pCO_2 but without urea (Table 3.3). The acetate added to these microcosms did not support greater microbial cell numbers presumably because a majority of that acetate was utilized by the ureolytic organisms in these microcosms as an electron donor to hydrolyze urea.

The pH of microcosms in experiment C increased following acetate amendment, supporting the hypothesis that in the presence of coal as the only additional carbon source, 1 mM acetate was the minimum requirement to stimulate urea hydrolysis under the anaerobic conditions of these experiments. For microcosms with pCO_2 greater than 1 atm the pH ranged from 6.0 to 6.3 prior to the amendment. The urease enzyme is commonly found in alkalophilic organisms that cannot grow below pH 6.5 (Okwadha and Li, 2010), and the activity of the enzyme has also been shown to increase with increasing pH (Stocks-Fischer et al., 1999). This may explain the lack of urea hydrolysis observed in experiments A and C with pCO_2 higher than 0.2 atm. Furthermore, it suggests that urea amendment may be impractical at CO_2 injection sites where pH below 6.5 is expected. Previous studies utilizing ureolytic pure cultures to precipitate calcite have often included a complex growth substrate such as Brain Heart Infusion or tryptic soy broth (Ferris et al., 2004; Fujita et al., 2004; Okwadha and Li, 2010; Tobler et al., 2011; Martin et al., 2012), molasses (Fujita et al., 2008), or yeast extract (Mortensen et al., 2011). In addition, these studies have almost exclusively been performed under aerobic conditions that are more optimal for higher growth rates and cell densities.

Inherent complexities and shortcomings of laboratory incubation experiments

Due to inter-experiment variability and the complex nature of the coal substrate, it is difficult to compare result of the various experiments. Each experiment was initiated by adding sterile, anaerobic media to coal that had been stored at 4˚C for months or even years under anoxic conditions in vacuum sealed bags with O_2-scrubbing packets.

Previous studies of sampling procedures from marine sediments have shown that native microbial communities can change as a result of short term oxygen exposure (Rochelle et al., 1994) and/or long term storage (Lin et al., 2010). Other studies have shown an increase in the numbers of viable bacteria and a decrease in diversity of terrestrial subsurface microcosms (Hirsch and Rades-Rohkohl, 1988; Brockman et al., 1992; Haldeman et al., 1994; Fredrickson et al., 1995; Haldeman, 1995). Although the coal remained water-saturated and anoxic during these storage conditions, it also appears to have supported the growth of fermentative organisms that in some cases made significant amounts of acetate, as confirmed by subsequent HPLC analysis. Acetate has been shown to build up via fermentation of high molecular weight organic matter and incomplete mineralization at low temperatures (3 ˚C; Matsui et al., 2013). This pre-formed acetate was added to the experimental media as part of the coal inoculum and often stimulated methane production shortly thereafter. This occurred for experiments shown in Figures 3.1, 3.2, and 3.3, each of which had initial acetate concentrations between 1 and 4 mM that strongly influenced methane production throughout the experiments. In contrast, the experiments shown in Figure 3.8 had initial acetate concentrations of less than 100 µM and consequently produced far less methane throughout the incubation period. In the first two experiments when methane production was greater than 1 µmol/g coal, most of the production occurred within the first 21 days. In experiment C methane production only reached ~0.3 µmole/g coal during the first 90 days of incubation, but was continuous until the final time point (Figure 3.8). This trend suggests ongoing acetate production, albeit at very low rates, supporting very low rates of methanogenesis (average 0.035 µmole CH_4 day^{-1}). This situation is probably more akin to what would be expected in the subsurface, where acetate is maintained at near-zero concentrations by methanogens consuming it as rapidly as it is made.

The free energy yield of acetoclastic methanogenesis under experimental conditions ($\Delta G'$) (Thauer et al., 1977) was calculated in an effort to understand why methanogenesis commenced immediately after acetate amendment in microcosms with 0.2 atm CO_2 but not in other acetate-amended microcosms in experiment C. Conditions were hypothesized to remain unfavorable for methanogenesis despite acetate amendment. The bicarbonate concentration [HCO_3^-] in each microcosm was calculated based on the measured pCO_2 and pH (Stumm and Morgan, 1996), and the concentration of aqueous methane calculated based on the measured headspace gas concentration and the Henry's Law constant (NIST), corrected for temperature. Acetoclastic methanogenesis was favorable under all experimental conditions ($\Delta G' \sim$ -34 to -38 kJ/mol) suggesting that thermodynamic limitation was not a factor in determining methanogenic potential in these microcosms.

Microbial community analysis

The total microbial biomass measured via PLFA extraction varied between 10^8 and 10^9 cells $g^{-1}coal^{-1}$ for all of the microcosms in this study (Tables 3.1, 3.2, and 3.3), supporting the conclusion that the coal supported a limited microbial community. Interestingly, the PLFA profiles were similar for each experiment, suggesting a relatively stable microbial community composition in all of them. This was unexpected given the differences observed in acetate production and subsequent methane production in the various experiments. Of all of the experiments, experiment A exhibited the highest microbial cell numbers (Table 3.1), initial acetate concentrations (Figure 3.3) and methane production (Figures 3.1 and 3.2). The higher acetate in these experiments may have resulted from higher levels of fermentative bacteria. Because the PLFA profiles in all experiments were similar, the higher acetate and methane production in experiment A likely resulted from a more active and abundant microbial community at the start of these experiments than in experiments B or C. However, one cannot exclude the possibility that a unique microbial community composition of experiment A that was undetectable via PLFA analysis, simply produced more acetate and methane. However, the observation that methane production was highest in these experiments when bacterial abundance was highest (while methanogenic archaea were undetectable via phospholipid analysis) is consistent with the importance of fermentative bacteria in methane production from coal.

The interpretation of individual PLFAs as biomarkers can be problematic as many are ubiquitous in microbes and therefore non-diagnostic (Pinkart et al., 2002; Ringelberg et al., 2008). In experiment B two PLFAs correlated negatively with urea concentration (15:0 and 10me16:0, $r = -0.541$ and -0.667, respectively), suggesting that the organisms responsible for making these lipids were negatively affected by urea amendment. 10me16:0 is commonly attributed to *Desulfobacter spp*. (Dowling et al., 1986) when detected in the absence of 10me18:0 (Kroppenstedt et al., 1985). Change in pH is the most likely reason for inhibited growth of *Desulfobacter* spp., which increased with increasing urea concentrations (Figure 3.6). The maximum growth rate of *Desulfobacter postgateii* generally declines with increasing pH above its optimal range of 7 – 7.5 (O'Flaherty et al., 1998). The increase in pH caused by urea hydrolysis may have inhibited the growth of *Desulfobacter*, or related species, in these experiments. However, PLFA analysis is not sufficient to make an absolute determination as this without additional DNA assays.

Quantification of the mcrA gene in microcosms in experiment C showed that each experiment contained approximately the same mcrA copy numbers at the start of the experiment, and similar copy numbers prior to acetate amendment (Figure 3.11), indicating that methanogens were present in similar numbers in each microcosm. The largest mcrA copy numbers at the conclusion of the experiment were observed in acetate amended microcosms with 0.2 atm CO_2, consistent with this experiment exhibiting the largest methane production (Figure 3.9). However, microcosms which were not amended with acetate showed similar, if slightly lower, mcrA copy numbers, suggesting that acetate amendment was not the determining factor in mcrA copy numbers in these microcosms. The predominance of polyploidism in the methanogenic archaea (Hildenbrand et al., 2011) means that no estimate of methanogenic cells numbers can be derived from mcrA copy numbers. However, the lack of any correlation between mcrA copy numbers and methane production in acetate amended and unamended microcosms of experiment C suggests that the abundance of methanogenic archaea alone does not explain the variation in methane production observed in these experiments. This finding also supports the conclusion, stated previously, that the activity of fermenters is the overarching factor in determining the methanogenic potential of coal microcosms.

Implications for CO_2 storage in deeply buried coal seams

The limitations of the experimental setup with respect to headspace CO_2 pressure make it difficult to speculate on the effects of CO_2 injection on the actual scales of a geological reservoir. Reservoir modeling has suggested that supercritical CO_2 injection into the Wyodak coal seam of the Powder River Basin is technically feasible (Ross et al., 2012).The results of this study suggest that CO_2 pressure is not a defining factor in microbial methanogenesis from coal. Other factors including swelling and water displacement (Pashin and McIntyre, 2003; Perera et al., 2011; Ross et al., 2012) may have a larger impact on microbial processes in coal reservoirs following scCO_2 injection. The determining factor in methanogenesis from coal appears to be the microbial community structure, specifically the presence and activity of fermentative organisms making acetate. The lack of correlation between CO_2 pressure and methanogenesis or microbial biomass, as measured by PLFAs, suggests that CO_2 storage could have a negligible effect on the native microbial community in coal seams distal to the scCO_2 injection well, where pCO_2 could remain below 2.5 atm. Any technology designed to enhance methanogenesis from coal would, it seems, be required to liberate fermentable organic molecules from the coal macrostructure. Kolak and Burruss (2006) recently showed that a number of polycyclic aromatic hydrocarbons (PAHs) and high molecular weight *n*-alkanes were mobilized from coal by extraction with supercritical CO_2. These molecules could become a potential feedstock for fermenters if they diffuse into the formation water away from the injection site, potentially increasing the rate of acetate production and enhancing methanogenesis *in situ*. No data yet exist on the effect of supercritical CO_2 on microbes associated with coal, nor is it known what effect physical factors such as coal swelling due to scCO_2 contact (Perera et al., 2011) may have on the process of methanogenesis from coal. Future work should address these questions as well.

Table 3.1: PLFA in experiment A extracted after 53 days (quantities in nanomoles PLFA).

PLFA	1.1 atm CO_2	1.1 atm CO_2 + 1g/L urea	1.1 atm CO_2 + 2.5g/L urea	1.1 atm CO_2 + 5 g/L urea	1.3 atm CO_2	1.3 atm CO_2 + 1 g/L urea	1.3 atm CO_2 + 2.5 g/L urea	1.3 CO_2 + 5 g/L urea
14:0	170	218	158	274	120	174	145	144
*i*15:0	298	137	104	214	166	200	102	126
*ai*15:0	207	133	96.1	215	145	195	113	132
15:0	64.8	82.8	52.3	100	43.0	64.4	58.7	61.2
i16:0	0.0	0.0	0.0	0.0	0.0	0.0	34.9	59.4
16:1ω7*cis*	774	418	329	683	687	984	427	629
16:1ω5	0.0	0.0	0.0	0.0	39.3	66.3	0.0	39.4
16:0	1160	718	597	854	863	1286	530	2355
10Me16:0	119	201	81.2	181	78.6	94.0	72.3	77.4
*i*17:0	74.5	539	302	671	71.8	105	221	67.6
*ai*17:0	46.2	0.0	87.5	62.4	44.4	70.7	0.0	42.2
*cy*17:0	36.2	0.0	67.1	81.9	48.6	96.5	30.7	15.8
17:0	31.5	492	294	647	22.7	0.0	45.4	30.5
18:1ω9	101	377	141	383	95.6	341	112	113
18:0	201	205	168	186	116	195	18.2	882
Total PLFA (nmole)	3284	3521	2476	4551	2540	3871	1908	4774
Total biomass (cells)	$8.92x10^{10}$	$8.80x10^{10}$	$6.19x10^{10}$	$1.14x10^{11}$	$6.90x10^{10}$	$9.68x10^{10}$	$4.77x10^{10}$	$1.19x10^{11}$
Cells/g coal	$1.78x10^{9}$	$1.76x10^{9}$	$1.24x10^{9}$	$2.28x10^{9}$	$1.38x10^{9}$	$1.94x10^{9}$	$9.54x10^{8}$	$2.39x10^{9}$

Table 3.2: PLFAs extracted from experiment B after 92 days (Quantities in nanomoles PLFA, standard deviation of triplicate incubations in parentheses).

PLFA	No Urea	0.5 g/L urea	1g/L urea	2.5 g/L urea	5 g/L urea
14:0	70.8 (8)	66.2 (18)	107 (67)	88.1 (22)	72.8 (3)
*i*15:0	80.4 (20)	68.1 (19)	68.9 (19)	55.2 (28)	53.6 (3)
*ai*15:0	46.1 (5)	41.8 (11)	47.8 (16)	35.6 (13)	34.7 (4)
15:0	23.6 (6)	22.8 (5)	25.0 (8)	16.5 (2)	16.0 (5)
16:1ω7*cis*	382 (107)	370 (103)	580 (74)	647 (659)	703 (183)
16:1ω5	28.8 (4)	24.5 (10)	31.2 (12)	127 (139)	17.3 (2)
16:1ω7*trans*	27.0 (1)	26.7 (9)	34.2 (15)	28.0 (15)	23.4 (3)
16:0	495 (98)	455 (92)	632 (107)	585 (489)	598 (87)
10Me16:0	35.8 (2)	28.8 (6)	34.2 (7)	23.6 (11)	22.9 (5)
*i*17:0	20.6 (4)	22.3 (9)	24.1 (10)	16.7 (4)	15.5 (2)
*ai*17:0	21.4 (4)	22.0 (8)	24.3 (8)	17.5 (5)	17.5 (4)
*cy*17:0	31.8 (3)	50.4 (16)	88.5 (26)	85.4 (70)	61.4 (11)
17:0	16.4 (4)	17.0 (5)	15.3 (4)	10.8 (4)	11.9 (2)
18:1ω9*cis*	28.3 (25)	46.3 (10)	53.8 (16)	39.1 (16)	45.8 (9)
18:1ω9*trans*	52.5 (11)	56.9 (11)	53.8 (16)	0	0
18:0	99.9 (45)	102 (14)	105 (36)	65.9 (20)	73.7 (14)
Total PLFA (nmole)	1461 (220)	1421 (320)	1925 (378)	1710 (1125)	1812 (258)
Total biomass (cells)	$3.65x10^{10}$ ($5.5x10^{9}$)	$3.55x10^{10}$ ($8x10^{9}$)	$4.81x10^{10}$ ($9.5x10^{9}$)	$4.41x10^{10}$ ($3.7x10^{10}$)	$4.53x10^{10}$ ($6.4x10^{9}$)
Cells/g coal	$7.30x10^{8}$ ($1.1x10^{8}$)	$7.11x10^{8}$ ($1.6x10^{8}$)	$9.63x10^{8}$ ($1.9x10^{8}$)	$8.32x10^{8}$($7.3x10^{8}$)	$9.06x10^{8}$ ($1.3x10^{8}$)

Table 3.3: PLFA quantities in experiment C after 153 days (quantities in nanomoles) Non-shaded columns correspond to microcosms amended with 1 mM acetate following 90 days incubation.

	0.2 atm CO_2	0.2 atm CO_2	0.2 atm CO_2	0.2 atm CO_2 + urea	0.2 atm CO_2 + urea	0.2 atm CO_2 + urea	1.1 atm CO_2	1.1 atm CO_2	1.1 atm CO_2	1.1 atm CO_2 + urea	1.1 atm CO_2 + urea	1.1 atm CO_2 + urea
PLFA												
14:0	37.6	29.0	21.9	41.2	47.1	33.3	63.5	94.6	29.8	44.2	24.8	22.6
*i*15:0	33.5	13.7	23.4	47.5	55.0	22.0	56.3	99.9	20.6	47.8	28.6	16.7
*ai*15:0	32.1	13.1	28.3	33.5	38.2	24.1	35.6	60.9	42.3	36.3	10.9	21.5
15:0	8.8	5.2	9.9	13.2	12.7	12.2	17.4	28.1	21.0	14.9	8.8	12.0
16:1ω7	120.1	50.1	68.2	124.6	144.4	70.5	241.4	425.8	80.4	189.0	106.7	55.5
16:1ω5	12.6	8.0	5.8	11.8	14.1	7.6	18.1	29.9	6.3	14.2	6.4	5.2
16:0	201.1	161.4	134.3	256.6	304.3	155.0	427.6	606.9	253.4	326.7	231.6	169.6
$_i$17:0	9.2	12.9	7.6	12.5	13.4	12.8	14.8	22.7	14.6	13.3	5.3	10.7
17:1ω7	0.0	0.0	29.1	37.5	46.2	41.1	21.6	51.7	16.2	26.4	12.5	20.8
17:0	5.3	6.0	5.1	8.0	7.2	5.5	13.3	19.0	11.4	10.1	8.7	10.4
18:1ω9*cis*	49.2	36.8	39.2	58.5	58.6	42.1	66.6	91.8	74.1	58.7	33.6	58.0
18:1ω9*trans*	77.2	48.5	59.6	69.2	66.9	68.6	119.4	185.0	114.8	120.8	50.4	86.3
18:0	48.3	75.1	39.8	77.0	76.4	44.3	105.1	115.8	57.5	72.8	119.5	46.3
Total PLFA (nmole)	635	460	472	791	885	539	1201	1832	743	975	648	536
Total biomass (cells)	1.59×10^{10}	1.15×10^{10}	1.18×10^{10}	1.98×10^{10}	2.21×10^{10}	1.35×10^{10}	3.00×10^{10}	4.58×10^{10}	1.86×10^{10}	2.44×10^{10}	1.62×10^{10}	1.34×10^{10}
Cells/g coal	3.17×10^{8}	2.30×10^{8}	2.36×10^{8}	3.96×10^{8}	4.42×10^{8}	2.70×10^{8}	6.0×10^{8}	9.16×10^{8}	3.71×10^{8}	4.88×10^{8}	3.24×10^{8}	2.68×10^{8}

Table 3.3: PLFA quantities in experiment C after 153 days (quantities in nanomoles) Non-shaded columns correspond to microcosms amended with 1 mM acetate following 90 days incubation (cont'd).

	1.5 atm CO_2	1.5 atm CO_2 + urea	2.5atm CO_2
PLFA			
14:0	27.9	17.9	14.0
*i*15:0	18.3	14.4	14.9
*ai*15:0	21.6	10.6	17.0
15:0	18.0	9.8	13.7
16:1ω7	61.3	35.0	34.3
16:1ω5	4.9	6.2	8.1
16:0	185.4	183.7	108.3
$_i$17:0	8.8	0.0	0.0
17:1ω7	13.1	15.6	18.0
17:0	12.7	5.8	7.9
18:1ω9*cis*	55.9	33.8	33.2
18:1ω9*trans*	62.2	68.4	60.5
18:0	58.9	71.9	31.9
Total PLFA (nmole)	549	473	362
Total biomass (cells)	$1.39x10^{10}$	$1.18x10^{10}$	$9.18x10^{9}$
Cells/g coal	$2.79x10^{8}$	$2.36x10^{8}$	$1.84x10^{8}$

3.6 References

Bachmeier K. L., Williams A. E., Warmington J. R. and Bang S. S. (2002) Urease activity in microbiologically-induced calcite precipitation. *J. Biotechnol.* **93**, 171–181.

Balkwill D. L., Leach F. R., Wilson J. T., NcNabb J. F. and White D. C. (1988) Equivalence of microbial biomass measures based on membrane lipid and cell wall components, adenosine triphosphate, and direct counts in subsurface aquifer sediments. *Microbial Ecol.* **54**, 273–291.

Bang S. S., Galinat J. K. and Ramakrishnan V. (2001) Calcite precipitation induced by polyurethane-immobilized Bacillus pasteurii. *Enzyme. Microb. Technol.* **28**, 404–409.

Banik A., Sen M. and Sen S. P. (1996) Effects of inorganic fertilizers and micronutrients on methane production from wetland rice (Oryza sativa L.). *Biol. Fert. Soils.* **21**, 319–322.

Beckmann S., Lueders T., Krüger M., Von Netzer F., Engelen B. and Cypionka H. (2011) Acetogens and acetoclastic methanosarcinales govern methane formation in abandoned coal mines. *Appl. Environ. Microbiol.* **77**, 3749–56.

Bidle K. (1999) A phylogenetic analysis of microbial communities associated with methane hydrate containing marine fluids and sediments in the Cascadia margin (ODP site 892B). *FEMS. Microbiol. Lett.* **177**, 101–108.

Blotevogel K.-H., Fischer U., Mocha M. and Jannsen S. (1985) Methanobacterium thermoalcaliphilum spec. nov., a new moderately alkaliphilic and thermophilic autotrophic methanogen. *Arch. Microbiol.* **142**, 211–217.

Bodelier P. L. E., Hahn A. P., Arth I. R. and Frenzel P. (2000) Effects of ammonium-based fertilisation on microbial processes involved in methane emission from soil planted with rice. *Biogeochem.* **51**, 225–257.

Boone D. R., Whitman W. B., Rouveire P. and Ferry J. G. (1993) Diversity and taxonomy of methanogens. In *Methanogenesis: Ecology, Physiology, Biochemistry and Genetics* Chapman and Hall, New York. pp. 35–80.

Bräuer S. L., Yavitt J. B. and Zinder S. H. (2004) Methanogenesis in McLean Bog, an acidic peat bog in upstate New York: stimulation by H_2/CO_2 in the presence of rifampicin, or by low concentrations of acetate. *Geomicrobiol. J.* **21**, 433–443.

Brockman F. J., Kieft T. L., Fredrickson J. K., Bjornstad B. N., Li S. W., Spangenburg W. and Long P. E. (1992) Microbiology of vadose zone paleosols in south-central Washington State. *Microbial Ecol.* **23**, 279–301.

Bronson K. F., Neue H. U., Singh U. and Abao E. B. (1997) Automated chamber measurements of methane and nitrous oxide flux in a flooded rice soil .1. Residue, nitrogen, and water management. *Soil. Sci. Soc. Am. J.* **61**, 981–987.

Chanton J. P., Bauer J. E., Glaser P. A., Siegel D. I., Kelley S. C., Tyler S. C., Romanowicz E. H. and Lazrus A. (1995) Radiocarbon evidence for the substrates supporting methane formation within northern Minnesota peatlands. *Geochim. Cosmochim. Acta* **59**, 3663–3668.

Chin K.-J., Lueders T., Friedrich M. W., Klose M. and Conrad R. (2004) Archaeal community structure and pathway of methane formation on rice roots. *Microbial Ecol.* **47**, 59–67.

Cicerone R. J. and Shetter J. D. (1981) Sources of atmospheric methane: Measurements in rice paddies and a discussion. *J. Geophys. Res*. **86**, 7203.

Dan J., Krüger M., Frenzel P. and Conrad R. (2001) Effect of a late season urea fertilization on methane emission from a rice field in Italy. *Agricult. Ecosys. Env*. **83**, 191–199.

DOE (2010) *DOE/NETL Carbon Dioxide Capture and Storage R&D Roadmap*.

Dowling N. J. E., Widdle F. and White D. C. (1986) Phospholipid ester-linked fatty acid biomarkers of acetate-oxidizing sulfate-reducers and other sulfide-forming bacteria. *J. Gen. Microbiol.* **132**, 1815–1825.

Dunkelblum E., Tan S. H. and Silk P. J. (1985) Double-bond location in monounsaturated fatty acids by dimethyl disulfide derivatization and mass spectrometry. *J. Chem. Ecol.* **11**, 265–277.

Dupraz S., Parmentier M., Ménez B. and Guyot F. (2009) Experimental and numerical modeling of bacterially induced pH increase and calcite precipitation in saline aquifers. *Chem. Geol.* **265**, 44–53.

Edwards C., Hales B. ., Hall G. ., Mcdonald I. ., Murrell J. ., Pickup R., Ritchie D. ., Saunders J. ., Simon B. . and Upton M. (1998) Microbiological processes in the terrestrial carbon cycle: methane cycling in peat. *Atmos. Environ.* **32**, 3247–3255.

Ermler U., Grabarse W., Shima S., Goubeaud M. and Thauer R. K. (1997) Crystal structure of methyl-coenzyme M reductase: the key enzyme of biological methane formation. *Science.* **278**, 1457–1462.

Ferris F. G., Phoenix V., Fujita Y. and Smith R. W. (2004) Kinetics of calcite precipitation induced by ureolytic bacteria at 10 to 20°C in artificial groundwater. *Geochim. Cosmochim. Acta* **68**, 1701–1710.

Ferris F. G. and Stehmeier L. G. (1992) Bacteriogenic mineral plugging. U.S. Patent No. 5,143,155

Ferris F. G., Stehmeier L. G., Kantzas A. and Mourits F. M. (1996) Bacteriogenic mineral plugging. *Can. J. Petrol. Tech.* **35**, 56–61.

Flores R. M., Rice C. A., Stricker G. D., Warden A. and Ellis M. S. (2008) Methanogenic pathways of coal-bed gas in the Powder River Basin, United States: The geologic factor. *Int. J. Coal. Geol.* **76**, 52–75.

Fredrickson J. K., Li S. W., Brockman F. J., Haldeman D. L., Amy P. S. and Balkwill D. L. (1995) Time-dependent changes in viable numbers and activities of aerobic heterotrophic bacteria in subsurface samples. *J. Microbiol. Meth.* **21**, 253–265.

Fujioka M., Yamaguchi S. and Nako M. (2010) CO_2-ECBM field tests in the Ishikari Coal Basin of Japan. *Int. J. Coal. Geol.* **82**, 287–298.

Fujita Y., Ferris F. G., Lawson D. L., Colwell F. S. and Smith R. W. (2000) Calcium carbonate precipitation by ureolytic subsurface bacteria. *Geomicrobiol. J.* **17**, 305–318.

Fujita Y., Redden G. D., Ingram J. C., Cortez M. M., Ferris F. G. and Smith R. W. (2004) Strontium incorporation into calcite generated by bacterial ureolysis. *Geochim. Cosmochim. Acta* **68**, 3261–3270.

Fujita Y., Taylor J. L., Gresham T. L. T., Delwiche M. E., Colwell F. S., McLing T. L., Petzke L. M. and Smith R. W. (2008) Stimulation of microbial urea hydrolysis in groundwater to enhance calcite precipitation. *Environ. Sci. Technol.* **42**, 3025–3032.

Fukuzaki S., Nishio N. and Nagai S. (1990) Kinetics of the methanogenic fermentation of acetate. *Appl. Environ. Microbiol.* **56**, 3158–3163.

Galand P. (2002) Depth related diversity of methanogen Archaea in Finnish oligotrophic fen. *FEMS. Microbiol. Ecol.* **42**, 441–449.

Gallagher L. K., Glossner A. W., Landkamer L. L., Figueroa L. W., Mandernack K. W. and Munakata-Marr J. (2013) The effect of coal oxidation on methane production and microbial community structure in Powder River Basin coal. *Int. J. Coal. Geol.* **In press**.

Green M. S., Flanegan K. C. and Gilcrease P. C. (2008) Characterization of a methanogenic consortium enriched from a coalbed methane well in the Powder River Basin, U.S.A. *Int. J. Coal. Geol.* **76**, 34–45.

Haldeman D. (1995) Microbial growth and resuscitation alter community structure after perturbation. *FEMS. Microbiol. Ecol.* **17**, 27–37.

Haldeman D. L., Amy P. S., White D. C. and Ringelberg D. B. (1994) Changes in bacteria recoverable from subsurface volcanic rock samples during storage at 4 ˚C. *Appl. Environ. Microbiol.* **60**, 2697–2703.

Harder Nielsen T. (1998) Significance of microbial urea turnover in N cycling of three Danish agricultural soils. *FEMS. Microbiol. Ecol.* **25**, 147–157.

Harris S. H., Smith R. L. and Barker C. E. (2008) Microbial and chemical factors influencing methane production in laboratory incubations of low-rank subsurface coals. *Int. J. Coal. Geol.* **76**, 46–51.

Harvey H. R., Fallon R. D. and Patton J. S. (1986) The effect of organic matter and oxygen on the degradation of bacterial membrane lipids in marine sediments. *Geochim. Cosmochim. Acta* **50**, 795–804.

Hildenbrand C., Stock T., Lange C., Rother M. and Soppa J. (2011) Genome copy numbers and gene conversion in methanogenic archaea. *J. Bacteriol.* **193**, 734–743.

Hirsch P. and Rades-Rohkohl E. (1988) Some special problems in the determination of viable counts of groundwater microorganisms. *Microbial Ecol.* **16**, 99–113.

Huguet C., Martens-Habbena W., Urakawa H., Stahl D. A. and Ingalls A. E. (2010) Comparison of extraction methods for quantitative analysis of core and intact polar glycerol dialkyl glycerol tetraethers (GDGTs) in environmental samples. *Limnol. Oceanogr. Meth.* **8**, 127–145.

Hunik J. H., Hamelers H. V. M. and Koster I. W. (1990) Growth-rate inhibition of acetoclastic methanogens by ammonia and pH in poultry manure digestion. *Biol. Waste.* **32**, 285–297.

Inagaki F., Tsunogai U., Suzuki M., Kosaka A., Machiyama H., Takai K., Nunoura T., Nealson K. H. and Horikoshi K. (2004) Characterization of C1-metabolizing prokaryotic communities in methane seep habitats at the Kuroshima Knoll, southern Ryukyu Arc, by analyzing pmoA, mmoX, mxaF, mcrA, and 16S rRNA genes. *Appl. Environ. Microbiol.* **70**, 7445–7455.

IPCC (2005) *Carbon Dioxide Capture and Storage*. eds. B. Metz, O. Davidson, H. de Coninck, M. Loos, and L. Meyer, Cambridge University Press, Cambridge, U.K.

Jabri E., Carr M. B., Hausinger R. P. and Karplus P. A. (1995) The crystal structure of urease from Klebsiella aerogenes. *Science.* **268**, 998–1004.

Janssen P. H. and Kirs M. (2008) Structure of the archaeal community of the rumen. *Appl. Environ. Microbiol.* **74**, 3619–3625.

Jones E. J. P., Voytek M. A., Corum M. D. and Orem W. H. (2010) Stimulation of methane generation from nonproductive coal by addition of nutrients or a microbial consortium. *Appl. Environ. Microbiol.* **76**, 7013–7022.

Jones E. J. P., Voytek M. A., Warwick P. D., Corum M. D., Cohn A., Bunnell J. E., Clark A. C. and Orem W. H. (2008) Bioassay for estimating the biogenic methane-generating potential of coal samples. *Int. J. Coal. Geol.* **76**, 138–150.

Kolak J. J. and Burruss R. C. (2006) Geochemical investigation of the potential for mobilizing non-methane hydrocarbons during carbon dioxide storage in deep coal beds. *Energy Fuels.* **20**, 566–574.

Kotsyurbenko O. R., Chin K.-J., Glagolev M. V, Stubner S., Simankove M. V, Nozhevnikova A. N. and Conrad R. (2004) Acetoclastic and hydrogenotrophic methane production and methanogenic populations in an acidic West-Siberian peat bog. *Env. Microbiol.* **6**, 1159–1173.

Kroppenstedt R. M., Goodfellow M. and Minnikin D. D. (1985) Fatty acid and menaquinone analysis of actinomycetes and related organisms. In *Chemical Methods in Bacterial Systematics* Academic Press, Orlando, FL. p. 410.

Lin Y.-S., Biddle J. F., Lipp J. S., Orcutt B. N., Holler T., Teske A. and Hinrichs K.-U. (2010) Effect of storage conditions on archaeal and bacterial communities in subsurface marine sediments. *Geomicrobiol. J.* **27**, 261–272.

Lindau C. W. (1994) Methane emissions from Louisiana rice fields amended with nitrogen fertilizers. *Soil. Biol. Biochem.* **26**, 353–359.

Lloyd D. (1998) Micro-ecology of peat: minimally invasive analysis using confocal laser scanning microscopy, membrane inlet mass spectrometry and PCR amplification of methanogen-specific gene sequences. *FEMS. Microbiol. Ecol.* **25**, 179–188.

Lovley D. R. and Goodwin S. (1988) Hydrogen concentrations as an indicator of the predominant terminal electron-accepting reactions in aquatic sediments. *Geochim. Cosmochim. Acta* **52**, 2993–3003.

Lueders T., Chin K.-J., Conrad R. and Friedrich M. (2001) Molecular analysis of methyl coenzyme M reductase alpha subunit (mcrA) genes in rice field soil and enrichment cultures reveal the methanogenic phenotype of a novel archaeal lineage. *Microbial Ecol.* **3**, 194–204.

Luton P. E., Wayne J. M., Sharp R. J. and Riley P. W. (2002) The mcrA gene as an alternative to 16S rRNA in the phylogenetic analysis of methanogen populations in landfill. *Microbiology* **148**, 3521–3530.

Martin D., Dodds K., Ngwenya B. T., Butler I. B. and Elphick S. C. (2012) Inhibition of Sporosarcina pasteurii under anoxic conditions: implications for subsurface carbonate precipitation and remediation via ureolysis. *Environ. Sci. Technol.* **46**, 8351–5.

Mathrani I. M., Boone D. R., Mah R. A., Fox G. E. and Lau P. P. (1988) Methanohalophilus zhilinae sp. nov. , an alkaliphilic, halophilic, methylotrophic methanogen. *Int. J. Syst. Bacteriol.* **38**, 139–142.

Matsui T., Kojima H. and Fukui M. (2013) Effects of temperature on anaerobic decomposition of high-molecular weight organic matter under sulfate-reducing conditions. *Estuar. Coast. Shelf Sci.* **119**, 139–144.

Mitchell A. C., Dideriksen K., Spangler L. H., Cunningham A. B. and Gerlach R. (2010) Microbially enhanced carbon capture and storage by mineral-trapping and solubility-trapping. *Environ. Sci. Technol.* **44**, 5270–5276.

Mitchell A. C. and Ferris F. G. (2005) The coprecipitation of Sr into calcite precipitates induced by bacterial ureolysis in artificial groundwater: Temperature and kinetic dependence. *Geochim. Cosmochim. Acta* **69**, 4199–4210.

Mitchell A. C. and Ferris F. G. (2006) The influence of bacillus pasteurii on the nucleation and growth of calcium carbonate. *Geomicrobiol. J.* **23**, 213–226.

Mortensen B. M., Haber M. J., DeJong J. T., Caslake L. F. and Nelson D. C. (2011) Effects of environmental factors on microbial induced calcium carbonate precipitation. *J. Appl. Microbiol.* **111**, 338–349.

NIST Standard Chemistry Reference Database 69: NIST Chemistry Webbook.

Nunoura T., Oida H., Toki T., Ashi J., Takai K. and Horikoshi K. (2006) Quantification of mcrA by quantitative fluorescent PCR in sediments from methane seep of the Nankai Trough. *FEMS. Microbiol. Ecol.* **57**, 149–157.

O'Flaherty V., Mahony T., O'Kennedy R. and Colleran E. (1998) Effect of pH on growth kinetics and sulphide toxicity thresholds of a range of methanogenic, syntrophic and sulphate-reducing bacteria. *Process Biochem.* **33**, 555–569.

Okwadha G. D. O. and Li J. (2010) Optimum conditions for microbial carbonate precipitation. *Chemosphere.* **81**, 1143–1148.

Onstott T. C. (2005) Impact of CO_2 injections on deep subsurface microbial ecosystems and potential ramifications for the subsurface biosphere. In *Carbon Dioxide Capture and Storage in Deep Geologic Formations- Results from the CO_2 Capture Project* (ed. S. M. Benson). Elsevier Ltd., New York.

Pashin J. C. (2007) Variable gas saturation in coalbed methane reservoirs of the Black Warrior Basin: Implications for exploration and production. *Int. J. Coal. Geol.* **82**, 135–146.

Pashin J. C. and McIntyre M. R. (2003) Temperature-pressure conditions in coalbed methane reservoirs of the Black Warrior basin: implications for carbon sequestration and enhanced coalbed methane recovery. *Int. J. Coal. Geol.* **54**, 167–183.

Perera M. S. A., Ranjith P. G., Choi S. K. and Airey D. (2011) The effects of sub-critical and super-critical carbon dioxide adsorption-induced coal matrix swelling on the permeability of naturally fractured black coal. *Energy* **36**, 6442–6450.

Pinkart H. C., Ringelberg D. B., Piceno Y. M., McNaughton S. J. and White D. C. (2002) Biochemical approaches to biomass measurements and community structure analysis. In *Manual of Environmental Microbiology (Second Edition)* (eds. C. J. Hurst, R. Crawford, G. Knudsen, M. J. McInerney, and L. D. Stezenbach). American Society for Microbiology Press, Washington D.C. pp. 101–113.

Rice D. D. and Flores R. M. (1991) Controls of bacterial gas accumulations in thick Tertiary coal beds and adjacent channel sandstones, Powder River basin, Wyoming and Montana. *AAPG Bull.* **75**, 661.

Ringelberg D., Richmond M., Foley K. and Reynolds C. (2008) Utility of lipid biomarkers in support of bioremediation efforts at army sites. *J. Microbiol. Meth.* **74**, 17–25.

Rochelle P. A., Cragg B. A., Fry J. C., Parkes R. J. and Weightman A. J. (1994) Effect of sample handling on estimation of bacterial diversity in marine sediments by 16S rRNA gene sequence analysis. *FEMS. Microbiol. Ecol.* **15**, 215–225.

Ross H. E., Hagin P. and Zoback M. D. (2012) CO_2 storage and enhanced coalbed methane recovery: Reservoir characterization and fluid flow simulations of the Big George coal, Powder River Basin, Wyoming, USA. *Int. J. Greenhouse Gas Control* **9**, 103–112.

Scott A. R., Kaiser W. R. and Ayers Jr. W. B. (1994) Thermogenic and secondary biogenic gases, San Juan Basin, Colorado and New Mexico- Implications for coalbed gas producibility. *AAPG Bull.* **78**, 1186–1209.

Shigematsu T., Tang Y., Kobayashi T., Kawaguchi H., Morimura S. and Kida K. (2004) Effect of dilution rate on metabolic pathway shift between aceticlastic and nonaceticlastic methanogenesis in chemostat cultivation. *Appl. Environ. Microbiol.* **70**, 4048–4052.

Shumkov S., Terekhova S. and Laurinavichius K. (1999) Effect of enclosing rocks and aeration on methanogenesis from coals. *Appl. Microbiol. Biotechnol.* **52**, 99–103.

Singh S. (1999) Methane flux from irrigated rice fields in relation to crop growth and N-fertilization. *Soil. Biol. Biochem.* **31**, 1219–1228.

Slyter L. L., Bryant M. P. and Wolin M. J. (1966) Effect of pH on population and fermentation in a continuously cultured rumen ecosystem. *Appl. Microbiol.* **14**, 573–578.

Sprott G. D. and Patel G. B. (1986) Ammonia toxicity in pure cultures of methanogenic bacteria. *Syst. Appl. Microbiol.* **7**, 358–363.

Steinberg L. M. and Regan J. M. (2009) mcrA-targeted real-time quantitative PCR method to examine methanogen communities. *Appl. Environ. Microbiol.* **75**, 4435–4442.

Steinberg L. M. and Regan J. M. (2008) Phylogenetic comparison of the methanogenic communities from an acidic, oligotrophic fen and an anaerobic digester treating municipal wastewater sludge. *Appl. Environ. Microbiol.* **74**, 6663–6671.

Stocks-Fischer S., Galinat J. K. and Bang S. S. (1999) Microbiological precipitation of $CaCO_3$. *Soil. Biol. Biochem.* **31**, 1563–1571.

Strąpoć D., Mastalerz M., Dawson K., Macalady J. L., Callaghan A. V, Wawrik B., Turich C. and Ashby M. (2011) Biogeochemistry of microbial coal-bed methane. *Annu. Rev. Earth. Planet. Sci.* **39**, 617–656.

Stumm W. and Morgan J. J. (1996) *Aquatic Chemistry*. 3rd Edition., John Wiley and Sons, Inc., New York City.

Swensen B. and Bakken L. R. (1998) Nitrification potential and urease activity in a mineral subsoil. *Soil. Biol. Biochem.* **30**, 1333–1341.

Tanner R. S. (2006) Cultivation of bacteria and fungi. In *Manual of Environmental Microbiology* (ed. J. L. Garland). ASM Press, Washington D.C. pp. 52–60.

Thauer R. K., Jungermann K. and Decker K. (1977) Energy conservation in chemotrophic anaerobic bacteria. *Bacteriol. Rev.* **41**, 100–180.

Tobler D. J., Cuthbert M. O., Greswell R. B., Riley M. S., Renshaw J. C., Handley-Sidhu S. and Phoenix V. R. (2011) Comparison of rates of ureolysis between Sporosarcina pasteurii and an indigenous groundwater community under conditions required to precipitate large volumes of calcite. *Geochim. Cosmochim. Acta* **75**, 3290–3301.

Ulrich G. and Bower S. (2008) Active methanogenesis and acetate utilization in Powder River Basin coals, United States. *Int. J. Coal. Geol.* **76**, 25–33.

White D. C., Davis W. M., Nickels J. S., King J. D. and Bobbie R. J. (1979) Determination of sedimentary microbial biomass by extracting lipid phosphate. *Oecologia.* **40**, 51–62.

White D. C. and Ringelberg D. B. (1998) Signature lipid biomarker analysis. In *Techniques in Microbial Ecology* (eds. R. S. Burlage, R. Atlas, D. Stahl, G. Geesey, and G. Sayler). Oxford University Press, New York.

Williams R. T. and Crawford R. L. (1985) Methanogenic bacteria, including an acid-tolerant strain, from peatlands. *Appl. Environ. Microbiol.* **50**, 1542–1544.

Wilms R., Sass H., Köpke B., Cypionka H. and Engelen B. (2007) Methane and sulfate profiles within the subsurface of a tidal flat are reflected by the distribution of sulfate-reducing bacteria and methanogenic archaea. *FEMS. Microbiol. Ecol.* **59**, 611–621.

CHAPTER 4

Effects of supercritical CO_2 on a mixed anaerobic microbial consortium

Andrew W. Glossner, Daisuke Katsuki, Christopher T. Mills, Marte Gutierrez, Kevin Mandernack

The experiments described in this chapter were designed and conducted by Andrew Glossner, with Daisuke Katsuki controlling the high pressure injection apparatus during the injection procedures. All writing in this chapter was done by Andrew Glossner. This chapter will be submitted to the International Journal of Greenhouse Gas Control.

4.1 Abstract

Geologic sequestration of CO_2 is one way to mitigate the effects of climate change. One of the challenges to be addressed before CO_2 sequestration can be deployed on a significant scale is the permanence of the trapping of injected CO_2 in a suitable reservoir. The temperature and pressure conditions required for injection of supercritical CO_2 are also amenable to a wide variety of microorganisms which could potentially impact CO_2 injection, migration, and storage permanence. Supercritical CO_2 has been shown to be harmful to pelagic microbes, and less so to biofilm-attached organisms. However, little is known about the effects of supercritical CO_2 on mixed assemblages of anaerobic microbes which would be more representative of those found in storage reservoirs. Experiments were conducted using a high pressure (10 MPa), moderate temperature injection system with Berea sandstone cores and an enrichment of anaerobic bacteria and methanogenic archaea growing with acetate to determine if specific microbes were more susceptible to the harmful effects of supercritical CO_2. Three cores were injected with a microbial enrichment containing cells, followed by supercritical CO_2 for one core. Four other cores were incubated with this microbial enrichment for 30 days and then injected with either supercritical CO_2 followed by sterile media or just sterile media. The permeability of each core

tested was reduced by as much as 83% by injection of the microbial enrichment. The differential pressure across all cores rose significantly over the course of injection of both microbial enrichment fluid as well as sterile fluid. Injection of supercritical CO_2 did not significantly impact permeability in both incubated and non-incubated cores. The microbial community structure was monitored using phospholipid fatty acid and phosphoether lipid techniques following injection, which showed that total bacterial biomass was not impacted by supercritical CO_2.

4.2 Introduction

Geologic sequestration of supercritical carbon dioxide ($scCO_2$) is considered one component of reducing atmospheric CO_2 in order to mitigate the effects of climate change (IPCC, 2005). Sedimentary basins, including depleted oil and gas reservoirs, and deep, hypersaline aquifers are considered potential storage sites in which sandstone may be the host rock (IPCC, 2005; Litynski et al., 2009). The permanence of geologic CO_2 storage can depend not only on the trapping mechanisms (solubility, mineral, and physical), but also on the interaction between the CO_2 and any microbes living in the injection formation.

When CO_2 is compressed above its critical point, temperature and pressure of 31.1 ˚C and 7.4 MPa, it is characterized by unique density and viscosity properties (10.6 mol/L and 3.7 $x10^{-5}$ Pa·S, respectively (Lemmon et al.)). The unique properties imparted by compressing CO_2 have led to its wide use in a variety of fields, including the food and beverage, pharmaceutical, and biomedical industries (Chen and Ling, 2000; Rozzi and Singh, 2002; Zhang et al., 2006). Supercritical CO_2 is often used as a sterilizing agent because it is nontoxic, not flammable, and does not degrade polymers or heat-sensitive materials (Zhang et al., 2006). Bacteria are generally more sensitive to changes in temperature than pressure, with hydrostatic pressures between 100 and 1000 MPa required to kill bacteria in the absence of $scCO_2$ (Cheftel, 1995). The primary mechanism for cell deactivation with $scCO_2$ is believed to be the diffusion of $scCO_2$ through the cell membrane with subsequent extraction of cellular materials, though rapid depressurization (< 5 minutes) is known to enhance the efficiency of $scCO_2$ sterilization (Zhang et al., 2006). This rapid depressurization is known to result in cells which appear to have burst when examined by scanning electron microscopy. Because both CO_2 diffusion and cellular eruption are impacted by the nature of the cell membrane, both pressure and $scCO_2$ affect different organisms in different ways. Generally gram positive organisms have been found to be more resistant to both $scCO_2$ and to sterilization by pressure than gram negative organisms (Cheftel, 1995; Zhang et al., 2006). In the geologic subsurface we might therefore expect $scCO_2$ to cause a relative change in a microbial community that is comprised of gram negative bacteria, gram positive bacteria, and archaea.

Several recent studies have looked at the effect of supercritical CO_2 on microbes in geologic media, either Berea sandstone or unconsolidated sand (Mitchell et al., 2008; Mitchell et al., 2009). Mitchell et al. (2008) utilized a pure culture of *Shewanella frigidimarina*, a halotolerant biofilm-forming organism isolated from an oil field, for experiments designed to test the response of biofilm organisms to $scCO_2$ exposure. The authors report an increase in permeability of the Berea core of 1.5 mD and a negligible effect of $scCO_2$ on their biofilm forming organism, as measured by colony forming units (cfu mL^{-1}) before and after CO_2 exposure (Mitchell et al., 2009). This study demonstrated that $scCO_2$ does not completely sterilize geologic media when the organisms are attached to the rock surface. A previous study by these same authors also demonstrated a 3 log_{10} reduction in the number of cells of planktonic *Bacillus mojavensis* while biofilm-attached *B. mojavensis* showed only a 1 log_{10} reduction in cells, further supporting the hypothesis that microbes growing in contact with rock surfaces are better able to survive exposure to $scCO_2$ (Mitchell et al., 2008). In both studies the authors utilized a high pressure system (at least 8 MPa) at moderate temperatures (32-35 ˚C) with aerobic pure cultures used as inocula (Mitchell et al., 2008; Mitchell et al., 2009). No one to date has attempted similar experiments with a mixed consortium of anaerobic microorganisms including archaea.

The extraction and quantification of archaeal membrane lipids is a commonly utilized technique for describing the living microbial community in a variety of settings, including lake (Martz et al., 1983; Mancuso et al., 1990; Schouten et al., 2001) and marine sediments (Hopmans et al., 2000; Bouloubassi et al., 2006; Oba et al., 2006; Roberts et al., 2008). Archaeal membrane lipids differ structurally from bacterial and eukaryotic membrane lipids in that the core components are branched isoprenoids linked via ether bonds to a glycerol backbone at the *sn* 2 and 3 positions (Koga et al., 1993; Koga and Morii, 2007). Since the polar phosphate or inisotol head groups ester-bound to the glycerol backbone are believed to be removed via hydrolysis upon cell death in natural environments (White et al., 1979; White and Ringelberg, 1998), their quantification is thought to be a reliable measure of viable microbial biomass (Sturt et al., 2004; Biddle et al., 2006). There is a growing body of evidence, however, suggesting that Archaeal membrane lipids are less susceptible to degradation under anaerobic conditions in the environment than bacterial membrane lipids (Harvey et al., 1986; Logemann et al., 2011). This prospect is probably less important for non-sedimentary samples.

This paper describes two types of experiments which were undertaken to test the effect of $scCO_2$ on a mixed anaerobic microbial consortium. The first set involved injection of a dense microbial enrichment into a sterile Berea sandstone core followed by $scCO_2$ injection into the core. This first set was designed to be a control set with which to compare the second set of incubated samples. The second set of samples consisted of cores that were pre-incubated with a microbial enrichment and then injected with either sterile media or sterile media following $scCO_2$. The viability of methanogens was measured following either $scCO_2$ or media injections using the most probable number method.

4.3 Methods

Sandstone core preparation

Core samples were cut from a Berea sandstone block and the ends of the cores milled with a lathe such that they were made parallel (Figure 4.1). The cores were then rinsed with deionized water following milling to reduce potential pore blockage caused by displaced particles. The average length of the cores was 6.08 cm (min 5.55 cm, max 6.60cm) and the average radius was 5.98 ± 0.004 mm. All cores were treated with 70% ethanol on their surfaces and allowed to dry under UV light in a laminar flow hood for 30 minutes prior to beginning the 30 day incubation period in order to remove surface contaminant microbes. The non-incubated cores were then stored at 20 ˚C in sterile Whirl-Pak bags.

Four cores were incubated in microbial enrichment media (see below) for 30 days to allow for complete saturation of the core and attachment of microbial cells to the core surface and pores, while 3 other cores remained sterile and were placed in sterile media 2 days prior to the start of the injection experiments in order to saturate the pore spaces of the cores.

Permeability calculations

The permeability of each core was measured using a triaxial core holder and compressed air (600 kPa confining pressure) with a mass flow meter to measure discharge prior to starting any microbial incubations. An average permeability of 34.5 mD was calculated based on the Darcy equation (Equation 4.1), where Q = discharge (m^3s^{-1}), k = permeability (m^2), A = cross sectional area (m^2), μ = viscosity (Pa·s), and P_b and P_a are the pressure at each end of the core in the direction of flow (Pa). The gas permeability (k_g) was corrected for the Klinkenberg effect (Klinkenberg, 1941; Bloomfield and Williams, 1995) to obtain an estimate of the liquid permeability using Equation 4.2, where k_l = liquid permeability, P_{pore} = pore pressure (atm), and b = Klinkenberg slip factor. The slip factor was determined experimentally for the cores in this study by assuming a liquid permeability of 23 mD, based on previous measurements with Berea sandstone cores in this lab (Daisuke Katsuki, personal communication), then using this calculated slip factor to calculate k_l for all other cores.

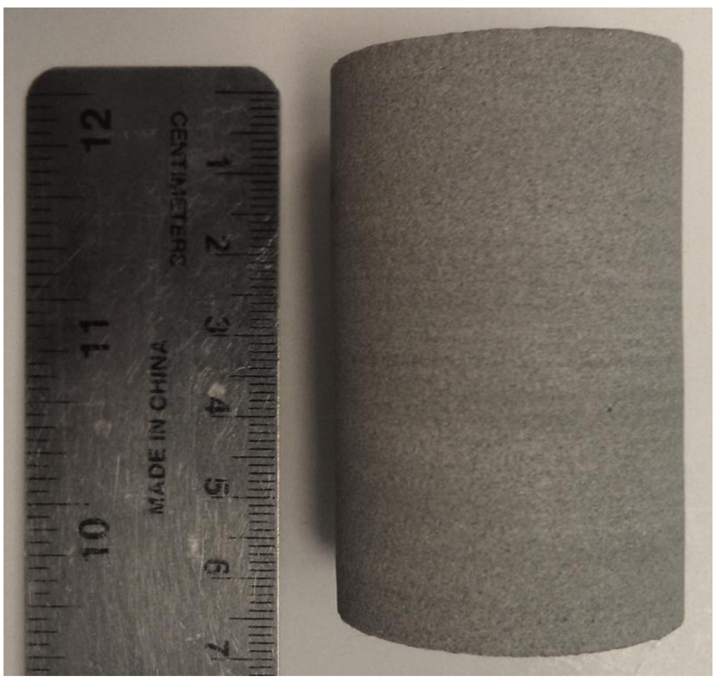

Figure 4.1: Representative photo of Berea sandstone core used in this study

The permeability of each core was also calculated during the injection experiments using data from the differential pressure transducer. The average differential pressure was taken from the first 5s of aqueous fluid injection after the pressure had stabilized, and calculated again for the final 5s of injection. The flow rate (Q) was specified during the injection at 5 mL min^{-1}, and the viscosity (μ) of water at 40 ˚C and 10 MPa of 6.539 x10^{-4} Pa·s was assumed to be a reasonable approximation for the purpose of comparing each core.

$$Q = \frac{-kA}{\mu} \cdot \frac{(P_b - P_a)}{L} \tag{4.1}$$

$$\frac{k_g}{k_l} = 1 + \frac{b}{P_{pore}} \tag{4.2}$$

Microbial enrichment

An anaerobic microbial consortium consisting primarily of heterotrophic and fermentative bacteria as well as methanogenic archaea was enriched from coal degradation experiments using a 50 mM acetate medium. The medium was prepared according to Tanner (2006), and the trace mineral solution was modified to reduce the amount of sulfate from the media by replacing $MgSO_4$ with $MgCl_2$. The medium included (g/L) $NaCH_3COOH{\cdot}3H_2O$ (6.8), NaCl (0.8), NH_4Cl (1.0), KH_2PO_4 (0.1), KCl (0.1), $MgCl_2{\cdot}6H_2O$ (0.17), $CaCl_2{\cdot}2H_2O$ (0.04), $NaHCO_3$ (1.0), nitrilotriacetic acid (0.02), $MnSO_4{\cdot}H_2O$ (0.01), $Fe(NH_4)2SO_4{\cdot}6H_2O$ (0.008), $CoCl_2{\cdot}6H_2O$ (0.002), $ZnSO_4{\cdot}7H_2O$ (0.002), $CuCl_2{\cdot}2H_2O$ (0.0002), $NiCl_2{\cdot}6H_2O$ (0.0002), $Na_2MoO_4{\cdot}2H_2O$ (0.0002), Na_2SeO_4 (0.0002), Na_2WO_4 (0.0002). Medium was prepared by autoclaving deionized water for 10 minutes to reduce oxygen saturation, then sparged with 80% N_2: 20% CO_2 for 15 minutes before adding 10 mL trace metal solution, 50 mL trace mineral solution, and 1 g/L $NaHCO_3$ just before sealing under N_2:CO_2 and autoclaving for 45 minutes (Tanner, 2006). 10 mL per liter of filter-sterilized trace vitamin solution (Tanner, 2006) was added to the nutrient medium after cooling the medium in an anaerobic chamber with 5% H_2 and 95% N_2. The “pre-incubated” cores were added to 4.5 L of anaerobic medium in a sterile 6 L anaerobic jar and inoculated with 500 mL of the methanogenic microbial enrichment. The anaerobic jars containing the cores were then incubated inside the anaerobic chamber with 5% H_2, 5% CO_2, 90% N_2 atmosphere for 30 days. A second anaerobic jar containing 4.5 L of sterile

50 mM acetate nutrient media was inoculated with 500 mL of the same microbial enrichment and incubated alongside the jar containing the incubating cores. The contents of both anaerobic jars were mixed prior to the initiation of the high pressure injection experiments.

Triaxial core holder description

Figure 4.2 shows the configuration of the high pressure injection apparatus, which is described in more detail elsewhere (Katsuki et al., In press). Briefly, this system consisted of a triaxial core holder with a maximum working confining pressure of 70 MPa, two high pressure syringe pumps which control the back pressure and the injection pressure, a dome-loaded back pressure regulator, a syringe pump for regulating the cell pressure, and a differential pressure transducer. Each core was prepared by wrapping it in a layer of packing tape and then surrounding it with a Viton sleeve. Two metal discs with holes in the center were placed on the ends of each core to homogenize flow. The metal discs and Viton sleeve were sterilized with 70% ethanol prior to installing the core. One syringe pump was used as a back pressure regulator and filled with sterilized 50 mM acetate media (same as above). The second syringe pump was used for injection of the microbial enrichment and $scCO_2$. The syringe pump used as the back pressure regulator had a flow rate range of 1 x10^{-5} to 50 mL min^{-1} at pressures 0.7 to 70 MPa. The syringe pump used for microbial enrichment and $scCO_2$ injection had a flow rate and pressure range of 1 x10^{-3} to 107 mL min^{-1} at pressures up to 50 MPa. The temperature of the core holder and syringe pumps was controlled by rubber electric blankets and the temperature of the core holder was monitored by a T-type sheath thermocouple. The syringe pumps were controlled by a computer interface which also served collected the data. The differential pressure in the core holder was measured using a variable reluctance diaphragm with a maximum range of 860 KPa and a temperature range of 255 to 344 K.

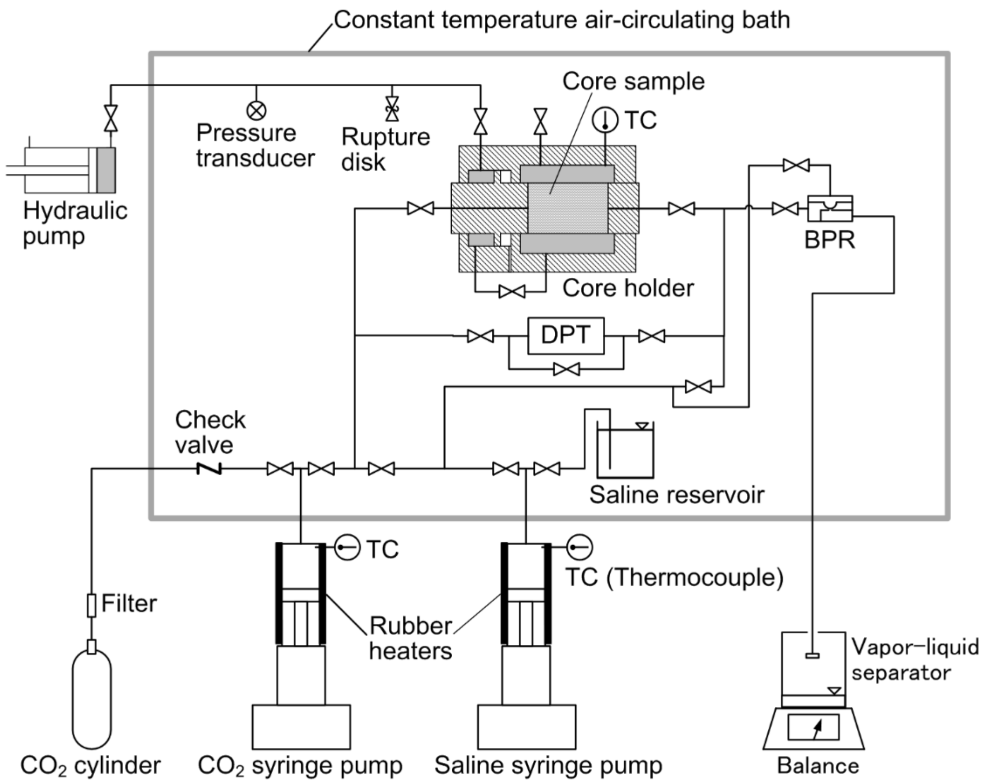

Figure 4.2: Schematic of the triaxial core holder and syringe pump injection system used for sandstone core experiments (Courtesy D. Katsuki).

Triaxial core holder system preparation

Prior to beginning the microbial enrichment experiments, the triaxial core holder and all tubing associated with it was cleaned with dish detergent to remove any residual paraffin oil from previous experiments. The syringe pumps and core holder were disassembled and washed with detergent, then rinsed with deionized water and reassembled prior to sterilizing the injection system. The system was sterilized based on the procedure of Mitchell et al. (2008b) by flushing with a 10% bleach solution containing 6 g/L TWEEN 80 followed by a 70% ethanol solution (Barkley and Richardson, 1994), then rinsed with a further 3 L of the sterile 50 mM acetate media until ethanol could no longer be detected in the effluent of the syringe pumps or tubing.

Injection procedures

After the core was loaded into the holder, the remaining volume of the chamber was filled with either the microbial enrichment media or sterile medium and the overburden pressure applied by syringe pump which functioned as a back pressure regulator. The core was pressurized slowly at a rate of 2000 kPa min^{-1} up to 10 MPa using sterile media from the syringe pump. The second syringe pump was then filled with 263 mL (max volume) of either sterile or microbial enrichment medium and placed under vacuum for 2-3 hours in order to reduce any air saturation in the core or the injection fluid which could cause perturbations in the pressure or flow rate. For samples that received $scCO_2$ injection the syringe pump was filled with gaseous CO_2 (General Air, Denver, CO grade 99.997%) and then compressed in the syringe pump to 10 MPa until the volume and pressure of the $scCO_2$ stabilized (approximately 2h). At the start of the experiment microbial enrichment medium was injected into the cores at a constant flow rate of 5 mL min^{-1}, but the flow rate was reduced once a decrease in permeability caused the differential pressure to rise above acceptable limits. Supercritical CO_2 was injected at 1 mL min^{-1}, and the total volume of $scCO_2$ used was 50 mL, or approximately 5 pore volumes. Liquid medium was collected in sterile 50 mL centrifuge tubes and placed on ice until filtration for further analysis of the microbial cells.

Most Probable Number Determinations

Methanogens were quantified using a 3 tube most probable number (MPN) technique, using 25 mL serum bottles, each containing 9 mL of the anaerobic 50 mM acetate medium. Bottles were sealed with rubber septa in an anaerobic chamber containing 5% H_2 and 95% N_2, allowing for growth of hydrogenotrophic as well as acetoclastic methanogens. A 1.0 mL sample of the microbial enrichment medium in which the cores were incubated was injected into each serum bottle using a sterile syringe for each core sampled prior to the injection experiment. This sample was then used to aseptically inoculate the first dilution of a 3 bottle MPN dilution series, which was then diluted 5 more times (total = 18 bottles per sample). After the core was injected with microbial medium, the second MPN sample for each core was taken from the effluent after passing through the high pressure apparatus. For core samples that were pre-incubated in the microbial enrichment medium and injected with $scCO_2$ (cores 4 & 5), the second MPN sample was taken after 50 mL of sterile medium had pulsed through the core following $scCO_2$ injection. MPN bottles were then incubated for 5 weeks at 37 ˚C following inoculation without shaking. Methane was separated using a HayesepQ packed column (2m; Supelco), then measured with a flame ionization detector (200 ˚C) on a Shimadzu GC-17A gas chromatograph (Shimadzu, Kyoto, Japan). A methane peak area value of at least 3 times the background methane peak area in control bottles was arbitrarily chosen to be considered positive for methanogen growth.

Phospholipid Extraction and Analysis

All liquid media injected into the cores was collected in sterile 50 mL centrifuge tubes and stored on ice until it was vacuum filtered using sterile polycarbonate filters (0.22 µm X 40 mm). Each filter was frozen at -80 ˚C prior to lipid extraction. Samples were then transferred to glass centrifuge tubes with Teflon lined caps and extracted using a modified Bligh-Dyer extraction (White and Ringelberg 1998) by shaking on a rotary shaker table at 150 rpm for two hours, followed by centrifugation at 1000 rpm for 30 minutes. The supernatant was decanted into separatory funnels and the solvent ratios adjusted to 1:1:0.8 (chloroform: methanol: buffer) by adding chloroform and 50 mM phosphate buffer and then allowed to separate overnight. The chloroform phase was then removed from the separatory funnels and the aqueous phase re-extracted for archaeal phosphoether lipids by shaking the separatory funnels with an additional 20 mL of 10% trichloroacetic acid (wt:vol), 25 mL chloroform, and 25 mL methanol. The supernatant from the phosphoether lipid extraction was phase separated overnight by adding 20 mL water and 25 mL chloroform. The chloroform from the TCA extraction was then washed with HPLC grade water, allowed to phase separate, and combined with the chloroform phase of the first extraction. The combined chloroform phases provided a total lipid extract, which was reduced under N_2 stream and separated into neutral, glyco- and polar lipid classes using silica solid phase extraction (SPE) columns (Alltech 500mg, #209200). Prior to loading the silica columns with lipids, the SPE columns were prepared by eluting first with 5 mL methanol followed by 10 mL chloroform. After loading the silica columns with the total lipid extract, neutral lipids were eluted in 10 mL chloroform, glycolipids in 10 mL acetone, and polar lipids in 10 mL methanol. Fatty acid methyl esters (FAMEs) were prepared by mild alkaline methanolysis (White and Ringelberg, 1998). All samples and blanks were injected with an internal standard (methyl tridecanoate (13:0), CAS# 1731-88-0) for quantification.

Following high pressure fluid injection and subsequent depressurization, the sandstone cores were removed from the triaxial core holder and placed in sterile Whirlpak bags and then frozen at -80 ˚C. Cores were then lyophilized and extracted by adding solvent in the same sequence as above to pre-baked glass beakers containing the cores. Each core was sonicated for 15 minutes. The volumes of each solvent were adjusted to account for the size of the cores, and included 30 mL buffer (pH 7.4 phosphate buffer or 10% TCA), 37.5 mL chloroform, and 75 mL methanol. Total lipid extracts were then added to separatory funnels containing 30 mL buffer and 37.5 mL chloroform and allowed to phase separate overnight. The procedures from this point proceeded in the same manner as above.

GC-MS Procedures

FAMEs were analyzed on an Agilent 7890A gas chromatograph with a DB-1MS column (60m x 0.25 mm i.d. x 0.25 µm), and quantified using a flame ionization detector (FID) coupled to an Agilent 5975C Inert XL mass spectrometer for FAME identification. The identity of each FAME was preliminarily assigned based on comparison of retention times of FAMEs from a standard mixture (Sigma Aldrich #47785-U). The injector temperature was 280°C, the FID set to 200 °C, and the ion source temperature set to 250°C. The oven temperature program began at 50 °C, to 150°C at 20 C° min^{-1}, to 210°C at 1.5 C° min^{-1}, to 280°C at 10 C° min^{-1} and held for a final 8 min at 280°C. FAME identity was confirmed after ionization with electron impact at 70 eV. Silylated PELs were analyzed on a Restek Rxi-5sil MS column (30 m x 0.25 mm i.d. x 0.25 µm; Restek, Bellefonte, PA) with a flow rate of 1.5 mL min-1. The oven temperature program began at 70°C, increasing to 130°C at 25 C° min^{-1}, to 190°C at 6 C° min^{-1}, to 320°C at 25 C° min^{-1} where it was held for a final 20 min at 320°C.

4.4 Results

Differential Pressure and Permeability

Figure 4.3 shows the differential pressure (ΔP) across cores 5 (incubated + $scCO_2$), 6, and 7 (incubated + no $scCO_2$). Core 5, which was injected with $scCO_2$, showed a marked difference in ΔP response from those injected with only sterile media. The ΔP for core 5 increased to a maximum of 486 kPa upon contact of $scCO_2$ with the core, then decreased to approximately 260 kPa, before increasing again at a rate of 11.9 kPa min^{-1} during the first 250 mL injection of sterile media (Figure 4.3). The rate of increase in ΔP for cores 6 and 7, shown in Figure 4.3, was 8.4 and 12.2 kPa min^{-1}, respectively. The sharp decrease in ΔP seen in each sample was caused by the refilling of the 260 mL syringe pump used to inject the fluid. Figure 4.4 shows the ΔP for a Berea sandstone core injected with sterile saline solution at varying flow rates for comparison with the data shown in Figure 4.3.

The permeability of each core was calculated during the initial fluid injection, and then at the end of the 500 mL fluid injection (Table 4.1). These permeability values can be compared to those determined for each core prior to experimentation, which were estimated using the

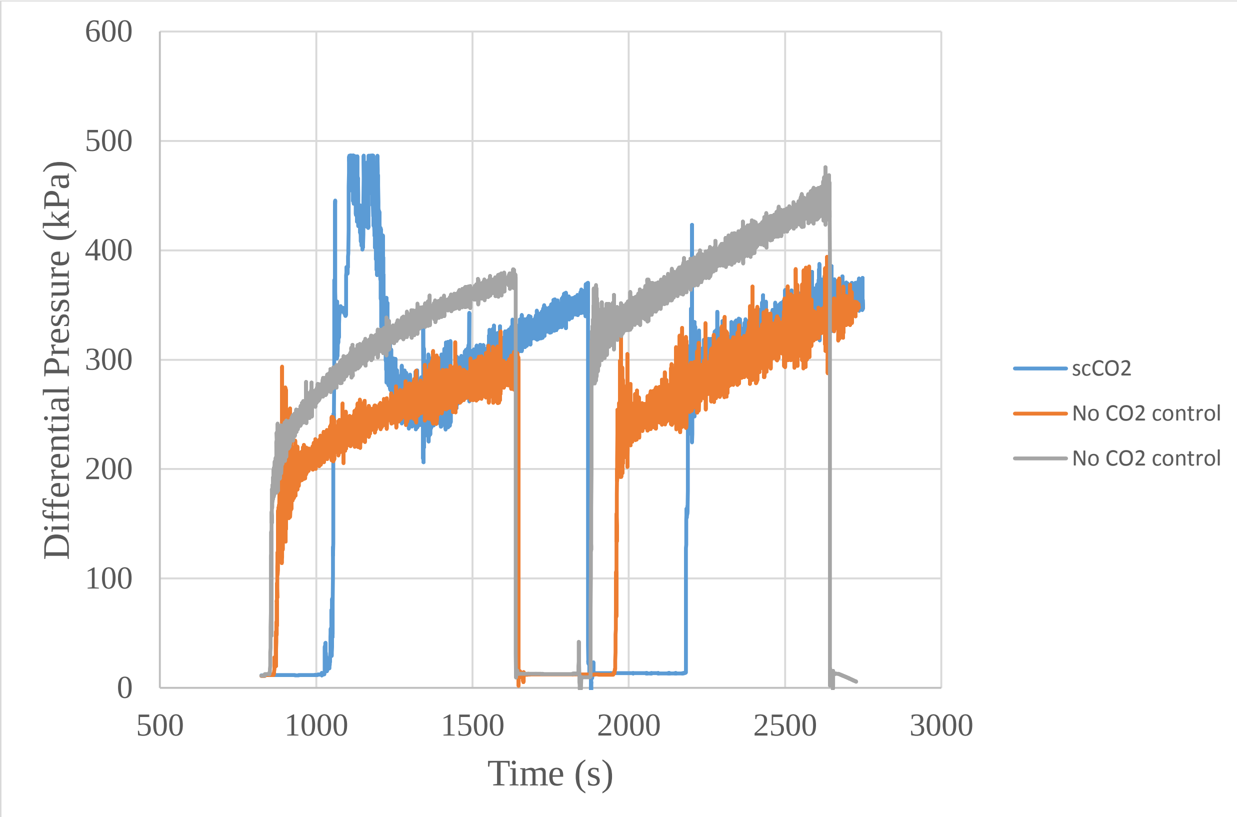

Figure 4.3: Differential pressure behavior of pre-incubated Berea sandstone cores. Blue: core 5 ($scCO_2$-injected); Gray: core 6 (incubated, no $scCO_2$) Orange: core 7 (incubated, no $scCO_2$).

Klinkenberg slip factor to account for the difference in gas and liquid permeability (see Methods). The permeability at the start of injection for cores 4 and 5, (pre-incubated + $scCO_2$) could not be estimated from the ΔP data as both core discharge and fluid viscosity fluctuated rapidly during the period of $scCO_2$ injection (Figure 4.3). Therefore, the permeability at the start of fluid injection was instead calculated based on the ΔP and injection rate of the first 250 mL of sterile media following $scCO_2$ injection. The calculated permeability compared well with values estimated for cores 6 and 7 which were not injected with $scCO_2$ (Table 4.1). Pre-incubation of the cores 4 and 5 in microbial enrichment media had a significant effect on the

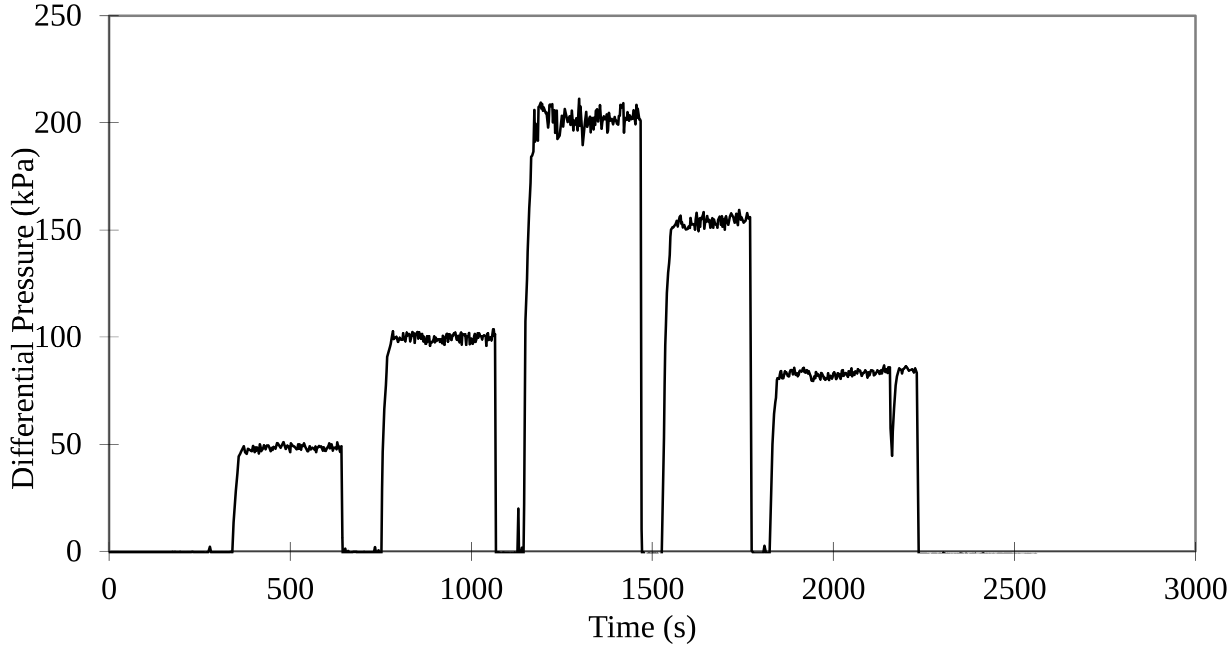

Figure 4.4: ΔP of Berea sandstone core injected with saline fluid without microbial enrichment. Stepwise increase in ΔP due to increase in flow rate (left to right: 1.6 mL min^{-1}, 3.3 mL min^{-1}, 6.6 mL min^{-1}, 5.0 mL min^{-1}, 2.6 mL min^{-1}) (D. Katsuki, unpublished data)

permeability of the cores at the start of the fluid injection. Cores 1, 2, and 3 were not pre-incubated and their permeability did not change significantly from their pre-determined values of ~31-34 mD (Table 4.1). In contrast, cores 4 through 7 exhibited between a 33 and 63% reduction in permeability relative to their pre-determined values. All cores showed similar permeability values following fluid injection of approximately 6 to 8 mD, which corresponded to a total reduction of between 77% and 83% of the pre-determined values.

Phospholipid fatty acid profiles and biomass estimates

Table 4.2 shows the relative mole percent of PLFAs extracted from Berea sandstone cores following the high pressure injections with media or $scCO_2$. The PLFAs observed in the consortium included the straight chain 14:0, 15:0, 16:0, 17:0, and 18:0; branched PLFAs such as *i*15:0, *ai*15:0, *i*16:0, *i*17:0, and *ai*17:0; and the monounsaturated PLFAs 16:1ω7, 16:1ω5, 17:1ω7, cy17:0, 18:1ω7*cis*, 18:1ω7*trans*, and 18:1ω9. The relative abundance of PLFAs recovered from the sandstone cores remained consistent across all treatments (Table 4.2). Total biomass estimates were also consistent across treatments and ranged from 1.3 x10^9 to 6.2x10^9 cells per core (Table 4.2). The initial cellular enrichment (T_0) contained 7.7 x10^7 cells/mL. The same PLFAs were recovered from filters collected after high pressure fluid injection but total biomass estimates were two orders of magnitude lower in the post-injection filtrate as compared to the extracted cores.

Phosphoether lipids

Intact archaeal phosphoether lipids (PELs) were recovered from the Berea sandstone cores following high pressure fluid injection, but none were recovered from the filtrate. The only PEL recovered was archaeol, and its recovery from each experiment can be seen in Table 4.2, expressed as µmole archaeol from each core. No archaeol was observed from core 3, while core 6 was lost during processing. Approximately 2.4 µmole archaeol was recovered from each remaining core. Based on the concentration of archaeol in the T_0 filtrate sample, 36.8 µmole L^{-1} archaeol, this corresponds to a 13% recovery for cores 1 and 2, which were injected with 500 mL of the microbial enrichment.

Most probable number (MPN) determinations for methanogens

The number of methanogens in the enrichment fluid was determined via the MPN method, with the results shown in Table 4.3. The microbial enrichment was sampled prior to initiation of the high pressure injection experiments and contained 4.6 x10^4 methanogen cells mL^{-1}. The microbial enrichment injected along with each core was also tested at the start of the experiment and is given as T_0 methanogen cell numbers in Table 3. For cores 1-3, which were not pre-incubated, T_{Final} samples were taken during the second 250 mL injection of microbial enrichment fluid, and ranged from 0 to 0.36 x10^3 cells mL^{-1}. T_0 samples for cores 4-7 ranged from 0 to 9.3 x 10^3 methanogen cells mL^{-1}. The T_{Final} samples for cores 4-7 were taken from the first 50 mL of sterile media pumped through the core either after $scCO_2$ injection (cores 4 and 5) or without $scCO_2$ injection (cores 6 and 7). For cores 4-7 (pre-incubated cores), all T_{Final} samples showed no growth after 5 weeks.

4.5 Discussion

The experiments described here were designed to assess the effects of $scCO_2$ on a mixed anaerobic consortium of microorganisms which included acetoclastic methanogens. This consortium mimics more closely the microbial community in a subsurface CO_2 sequestration reservoir. The combination of phospholipid (PLFA and PEL) analysis and MPN counts of methanogens was used to assess the viability of microorganisms subjected to $scCO_2$ injection. It was hypothesized that $scCO_2$ would impact the different groups of bacteria in the consortium differently (i.e. gram positive vs. gram negative bacteria) and that methanogenic archaea would be able to withstand $scCO_2$ exposure better than bacteria due to their cellular membrane structures. The lack of any significant differences in MPN counts, both bacterial PLFAs and archaeal PELs, from cores injected with or without $scCO_2$ suggests that $scCO_2$ did not have a significant impact on the microbial community in these experiments.

Microbial community structure

No significant differences were observed between PLFA profiles from cores which were injected with $scCO_2$ versus those which were not. However, bacterial community structure appears to have been affected by pre-incubation of the cores. Monounsaturated PLFAs such as 16:1ω7, 16:1ω5, 18:1ω7, and 18:1ω9 collectively accounted for 86% of total PLFAs in the T_0 filter samples, 63-72% in cores 1 through 3, and 53-61% in cores 4-7 (Table 4.2). The decrease in the percentages of these monounsaturated PLFAs, which are commonly attributed to gram negative organisms (Lechevalier and Lechevalier, 1988; Pinkart et al., 2002), suggests that gram positive bacteria represented a greater percentage of the microbial community in the incubated vs. unincubated cores. The total PLFA recovered from cores 1-3 varied from 2.87 $x10^6$ to 1.23 $x10^7$ cells mL^{-1} of injected fluid, which corresponds to a 4-16% recovery. This compares with the T_0 cell density of 7.67 $x10^7$ cells mL^{-1}. These low recoveries suggest that the majority of bacterial cells injected into cores 1-3 may have remained in the cores, and were perhaps inaccessible via solvent extraction using sonication. It is not possible to compare the recovery of cells from cores 1-3 to cores 4-7, as the triaxial core holder displaced the volume of media surrounding the core as the cover was secured. However, cores 4-7 retained approximately the same quantity of cells based on estimates from PLFA extractions (Table 4.2), suggesting that $scCO_2$ had no effect on the microbial community. Interestingly, all cores examined in this study yielded similar biomass estimates based on PLFA extractions. These similarities resulted despite cores 1-3 having been injected with 500 mL of microbial enrichment, while cores 4-7, which were pre-incubated, would only have contained microbes in their pore spaces or surface. These similar biomass estimates may be an artifact of the lipid extraction procedure. If the solvent did not sufficiently penetrate the core, the extraction may have been incomplete and underestimated total cells associated with each core. The biomass recoveries from cores 1-3 suggest that this method may have underestimated cells in the cores by as much as 25X, assuming a negligible number of cells passed through the cores. However, even if the extraction procedure was only effective at removing cells on the surface of each core, it is unlikely that each core would have had equivalent biomass on its surface given the variation in their treatment.

The results of the MPN analysis for methanogens are inconclusive with respect to the effects of $scCO_2$ injection on methanogen viability. With the exception of core 4, every core had between 2 $x10^3$ and 9 $x10^3$ methanogenic cells mL^{-1} prior to the injections (Table 4.3). However, the results of the MPN analysis suggest that no methanogen cells were able to pass through the cores regardless of treatment with $scCO_2$. While other studies have shown that bacteria can pass through Berea sandstone cores (Mitchell et al., 2009), it appears that the methanogens in this study were unable to do so. This may be due in part to the relatively low number of methanogens in the mixed microbial enrichment (4.6×10^4 cells mL^{-1}), but also to cell aggregation and clogging of pores, as evidenced by the increase in ΔP for each core (Figure 4.3). Results of the PEL analysis are consistent with the results of the MPN analysis in that each core had approximately the same amount of archaeol extracted from it, regardless of $scCO_2$ treatment. Using the conversion factor of Mancuso et al. (1990) of 4.24×10^{-19} mole diether lipid $cell^{-1}$, the T_0 microbial enrichment was estimated to contain 8.7×10^{10} cells mL^{-1}, which is approximately 6 orders of magnitude higher than the MPN results suggest the original microbial enrichment contained. This discrepancy may be attributed to multiple factors. First, methanogens may not have comprised the majority of archaeal cells in the microbial enrichment, as other groups of archaea also produce archaeol as a part of their cellular membranes (Koga and Morii, 2005). Heterotrophic archaea have been shown to dominate subsurface marine sediments offshore Peru (Biddle et al., 2006). However, other studies have shown methanogens to be the dominant type of archaea found in produced waters of the Powder River Basin (Green et al., 2008), the source of organisms used in this study. It is also possible that detectable PELs from dead or non-viable cells were trapped on the filters and cores, which would not have been detected by MPN analysis. Intact PELs have been shown to be relatively long-lived in anaerobic marine sediments (Schouten et al., 2010). Therefore, the detection of intact PELs from cores in this experiment may not truly represent living archaeal biomass.

Evaluation of experimental setup

Only two other studies have examined the survivability of microorganisms following exposure to $scCO_2$ in porous geologic media, each with different $scCO_2$ exposure regimes. Mitchell et al. (2008) inoculated sterile sand with *Bacillus mojavensis*, an aerobic biofilm-forming organism (Roberts et al., 1994), and pulsed $scCO_2$ through cartridges containing the sand and cells for 19 min at 1 mL min^{-1} at 35 ˚C and 13.8 MPa. These conditions corresponded to a total $scCO_2$ exposure time of 20 minutes (1 min. hold plus 19 min. flow), with nearly identical total cell numbers but a 3 log_{10} reduction in viable cells following $scCO_2$ exposure of the suspended cells (Mitchell et al., 2008). In a separate study, Mitchell et al. (2009) inoculated 2 Berea sandstone cores with *Shewanella fridgidimarina* and alternately starved the microbial assemblage of nutrient medium and stressed them with $scCO_2$ for 16 and 119 hours, respectively (flow rate unspecified). Following inoculation with *S. fridgidimarina*, core permeability decreased by >95% over the first several days as a biofilm was formed. This study also found that $scCO_2$ increased core permeability slightly (< 5% of original permeability) but that exposure time did not significantly impact this change.

The exposure time for cells in sandstone cores of this study was 50 minutes of flow plus 4 minutes of hold time at 10 MPa while the syringe pump was refilled with sterile nutrient medium. This exposure time is almost three times as long as the 19 min that Mitchell et al. (2008) showed to be effective at reducing viable numbers of pelagic cells in sand, and is longer than exposure times commonly employed for microbial sterilization (Zhang et al., 2006). It was therefore reasonable to expect a reduction in viable organisms following $scCO_2$ exposure of pelagic cells for 50 min. The injection scheme for cores 1-3 would not have permitted biofilm formation, meaning that cells present in the core were essentially pelagic, while cores 4-7 were pre-incubated to allow for microbial attachment or biofilm formation. The equivalence of biomass extracted from cores 1-3 suggests that $scCO_2$ did not affect pelagic cells present in the cores. Cores 4 and 5 were incubated in the microbial enrichment prior to injection of $scCO_2$. The equivalence of biomass extracted from cores 4-7 also suggests that $scCO_2$ did not affect total cell numbers when cells were allowed to penetrate and attach to the cores prior to the start of the injections.

A possible explanation for the equivalent microbial biomass extracted from the cores across all treatments is that the flow regime tested in this study (5 mL min^{-1} at 10 MPa) caused pelagic cells to be embedded in the surface pore sites of each core, essentially forming an artificial biofilm. This artificial aggregation would have two effects; 1) retarding fluid flow through the core, thereby reducing permeability, and 2) allowing cells on the outside of the aggregate to protect cells on the inner side from potential damage. The decrease in permeability from ~30 mD to 6-8 mD seen across all experimental conditions is consistent with this explanation, as is the deviance in ΔP behavior observed in these experiments from that observed when straight saline fluid is injected through the Berea sandstone under identical conditions (Figures 3 and 4). Mitchell et al. (2008) showed that cells within a biofilm were less susceptible to the effects of $scCO_2$ than pelagic cells, which is also consistent with this explanation. Wu et al. (2010) showed that *Shewanella oneidensis* could better withstand CO_2 pressures up to 150 psi if cells were aggregated on filters prior to CO_2 exposure, confirming that aggregation enhances cell survival. It is therefore possible that aggregation of cells on or near the surface of the cores enhanced their survivability under the conditions utilized in this study.

An assumption implicit in any experiment designed to test the effects of $scCO_2$ on microbes in porous geologic media is that the $scCO_2$ will come into contact with the majority of cells. However, it is possible that $scCO_2$ could bypass cells, or cellular aggregates, due to physical phenomena associated with 2-phase fluid migration. Viscous fingering is a well-known phenomenon in which a lower viscosity fluid is injected into a higher viscosity fluid, resulting in dendritic migration of the lower viscosity fluid through the higher viscosity fluid. Viscous fingering is known to affect other processes involving fluid migration, including heavy oil recovery (Doorwar and Mohanty, 2011), and gastric HCl penetration of mucous membranes in mammals (Bhaskar et al., 1992). The speed at which $scCO_2$ will move away from a point of injection in aqueous fluid is governed by the mobility ratio, $M = \lambda_c/\lambda_w$, where λ_c and λ_w are the viscosities of $scCO_2$ and water, respectively (Nordbotten et al., 2005). If the mobility ratio is ≥ 1, $scCO_2$ will flow faster than the aqueous pore fluid it is displacing, decreasing the areal sweep efficiency of the $scCO_2$ to 40-60% (Van der Meer, 1992). The process of viscous fingering has also been shown to enhance the dissolution of $scCO_2$ into aqueous pore fluids (Pau et al., 2010; Gasda et al., 2011). Chang et al. (2013) investigated $scCO_2$ displacement of aqueous fluid from low permeability sandstone cores and found that $scCO_2$ dissolution remained a non-equilibrium process, which they attribute to non-uniform displacement of the aqueous pore fluids. The difference in pathways of $scCO_2$ migration through the core can be caused by variation in pore sizes (Chang et al., 2013), which could also influence the distribution of microbes throughout the core. Other studies with $scCO_2$ injection into Berea sandstone have also found that $scCO_2$ does not displace aqueous pore fluid in a uniform manner, which can be attributed to heterogeneity within the core sample at the pore-scale (Suekane et al., 2008; Krevor et al., 2012; Berg et al., 2013). The viscous fingering effect may make diffusion of dissolved CO_2 the only mechanism whereby a significant portion of the core is impacted by $scCO_2$, especially on short time scales. The injection regime utilized in this study was such that $scCO_2$ was present in the core for approximately 1 h before it was displaced by aqueous media. This time frame may not have been sufficient for diffusion of the dissolved CO_2 away from higher permeability zones toward lower permeability zones, where it could impact a greater number of microbes. The decrease in permeability seen in all cores in this study is also consistent with microbes clogging pore spaces, reducing permeability, causing $scCO_2$ to migrate through the core preferentially through non-microbe impacted pore spaces. The viscous fingering of $scCO_2$ through relatively permeable portions of the cores, away from the microbes, may explain why little difference was seen between the biomass of cores injected with $scCO_2$ versus those which were not.

4.6 Conclusion

To the best of my knowledge, the work described here represents the first study of the effects of $scCO_2$ on a mixed anaerobic consortium, which is likely more representative of the subsurface biosphere than pure cultures of aerobic organisms. The injection of this mixed consortium into Berea sandstone cores caused a reduction in permeability by as much as 83%, relative to pre-experiment conditions. Incubating sandstone cores for 30 days in this microbial enrichment also reduced the permeability from 33% to 63% at the start of aqueous fluid injection, with further reductions in permeability of 76.8% to 81.9% by the end of the experiment. The injection of $scCO_2$ in three of the cores tested here did not have an impact on permeability, nor did it impact total cell numbers recovered from each core. Heterogeneous flow paths and/or microbial cell aggregation may have enhanced cell survival in cores injected with $scCO_2$.

Future work in this area should investigate the effects of $scCO_2$ on an anaerobic assemblage of organisms allowed to grow for an extended period at high pressure prior to injection of $scCO_2$. The possibility that $scCO_2$ only impacts a small percentage of cells due to heterogeneous flow makes the exposure time for cells in geologic media an important consideration to investigate as well. It would also be beneficial to determine the spatial heterogeneity of microbial cells and $scCO_2$ flow paths within the same core under varying injection regimes.

Table 4.1: Berea sandstone cores and conditions utilized in high-pressure injection experiments with scCO2. "Microbial enrichment" refers to homogenized media + cells in which cores 4-7 were incubated. "Sterile media" refers to anaerobic media prepared with same contents as microbial enrichment but sterile.

Sample	*Experiment condition*	*Volume $scCO_2$ (mL)*	*Pre-experiment permeability (mD)*	*Injection start permeability (mD)*	*Injection end Permeability (mD)*	*% permeability change*
Core 1	500 mL microbe media	0	34	ND	5.92	82.6
Core 2	500 mL microbe media	0	33.4	35.6	7.4	77.8
Core 3	500 mL microbe media + $scCO_2$	50	31.3	31.4	6.4	79.6
Core 4	500 mL sterile media + $scCO_2$	50	33.5	22.3	6.45	80.7
Core 5	500 mL sterile media + $scCO_2$	50	35.9	18.6	7.76	78.4
Core 6	500 mL sterile media	0	35.9	13.4	8.32	76.8
Core 7	500 mL sterile media	0	39.5	26.6	7.15	81.9

Table 4.2: PLFAs extracted from cores following high pressure injection experiments (mole %). (a. nmole/L; b. cells/mL; c. µmole/L; N.D. Not determined; d. lost during work-up

PLFA	T_0 filters	Core 1 Pre-sterile No $scCO_2$	Core 2 Pre-sterile No $scCO_2$	Core 3 Pre-sterile + $scCO_2$	Core 4 Incubated + $scCO_2$	Core 5 Incubated + $scCO_2$	Core 6 Incubated + $scCO_2$	Core 7 Incubated + $scCO_2$
14:0	2.12	1.65	3.10	1.45	1.98	1.37	2.17	1.98
***i*15:0**	1.97	2.10	3.09	2.15	8.41	8.22	9.15	8.01
***ai*15:0**	2.91	2.31	3.89	2.02	5.00	4.81	5.44	5.34
15:0		0.41	0.32	0.33	0.45	0.32	0.57	0.28
***i*16:0**			0.39	0.21	0.51	0.49	0.54	0.62
16:1ω7cis	46.95	24.29	28.61	17.07	24.60	24.30	22.20	23.14
16:1ω5cis	13.94	15.57	14.48	16.10	10.13	10.48	8.81	8.64
16:0	30.27	19.60	25.05	25.18	23.03	21.39	22.77	26.30
***i*17:0**	0.16				0.83	0.77		0.80
***ai*17:0**	0.15				0.47			0.38
17:1ω7*cis*					0.52	0.41	0.60	
***cy*17:0**	0.45	0.35	0.30	1.13	0.97	0.41	1.24	0.78
17:0	0.04	0.29			0.78	0.22	0.83	0.87
18:1ω9*cis*	0.14	0.52	0.36	0.43	0.76	0.60	0.89	0.74
18:1ω7*cis*	25.24	30.13	19.04	30.01	19.00	23.85	21.75	19.79
18:1ω7*trans*		1.84	0.68	2.46	1.06	1.05	1.24	0.94
18:0	0.82	0.94	0.70	1.46	1.50	1.32	1.80	1.41
Total PLFA (nmole)	276[a]	246	57.3	66.9	132	67.0	52.6	60.6
Bacterial biomass (cells)	$7.67x10^{7b}$	$6.15x10^9$	$1.45x10^9$	$1.67x10^9$	$3.30x10^9$	$1.67x10^9$	$1.31x10^9$	$1.52x10^9$
Archaeol (µmole)	36.8[c]	2.38	2.37	N.D.	2.42	2.44	d	2.42
PEL recovery (%)	-	13%	13%	N.D.	-	-	-	-

Table 4.3: Most probable number (MPN) determinations of methanogen cell numbers, with upper and lower 95% confidence intervals based on 3 tube MPN dilution series.

Sample	Methanogenic cells (x 10^3/mL)	95% C.L. lower	95 % C.L. upper
Methanogenic enrichment (T_0)	46	9	200
Core 1 (T_0)	0.92	0.14	3.8
Core 1 (T_{final})	0	-	0.95
Core 2 (T_0)	2.3	0.46	9.4
Core 2 (T_{final})	0.36	0.017	1.8
Core 3 (T_0)	2.3	0.46	9.4
Core 3 (T_{final})	0	-	0.95
Core 4 (T_0)	0.3	0.015	1.1
Core 4 (T_{final})	0	-	0.95
Core 5 (T_0)	4.3	0.9	18
Core 5 (T_{final})	0	-	0.95
Core 6 (T_0)	2.3	0.46	9.4
Core 6 (T_{final})	0	-	0.95
Core 7 (T_0)	9.3	1.8	42
Core 7 (T_{final})	0	-	0.95

4.8 References

Barkley W. and Richardson J. (1994) Laboratory Safety. In *Manual of Methods for General Bacteriology.* American Society of Microbiology, Washington D.C. pp. 715–734.

Berg S., Oedai S. and Ott H. (2013) Displacement and mass transfer between saturated and unsaturated CO_2–brine systems in sandstone. *Int. J. Greenhouse Gas Control*. **12**, 478–492.

Bhaskar K. R., Garik P., Turner B. S., Bradley J. D., Bansil R., Stanley H. E. and LaMont J. T. (1992) Viscous fingering of HCl through gastric mucin. *Nature.* **360**, 458–61.

Biddle J. F., Lipp J. S., Lever M. A., Lloyd K. G., Sorensen K. B., Anderson R., Fredricks H. F., Elvert M., Kelly T. J., Schrag D. P., Sogin M. L., Brenchley J. E., Teske A., House C. H. and Hinrichs K.-U. (2006) Heterotrophic archaea dominate sedimentary subsurface ecosystems off Peru. *Proc. Nat. Acad. Sci.* **103**, 3846–3851.

Bloomfield J. P. and Williams A. T. (1995) An empirical liquid permeability--gas permeability correlation for use in aquifer properties studies. *Quart. J. Eng. Geol. Hydrogeol.* **28**, S143–S150.

Bouloubassi I., Aloisi G., Pancost R. D., Hopmans E. C., Pierre C. and Sinninghe Damsté J. S. (2006) Archaeal and bacterial lipids in authigenic carbonate crusts from eastern Mediterranean mud volcanoes. *Org. Geochem.* **37**, 484–500.

Chang C., Zhou Q., Xia L., Li X. and Yu Q. (2013) Dynamic displacement and non-equilibrium dissolution of supercritical CO_2 in low-permeability sandstone: An experimental study. *Int. J. Greenhouse Gas Control*. **14**, 1–14.

Cheftel J. C. (1995) Review : High-pressure, microbial inactivation and food preservation / Revision: Alta-presion, inactivacion microbiologica y conservacion de alimentos. *Food Sci. Technol. Int.* **1**, 75–90.

Chen Y. T. and Ling Y. C. (2000) An overview of supercritical fluid extraction in Chinese herbal medicine: From preparation to analysis. *J. Food Drug Anal*. **8**, 235–247.

Doorwar S. and Mohanty K. K. (2011) Viscous fingering during non-thermal heavy oil recovery. In *SPE Annual Technical Conference and Exhibition, Denver*

Gasda S. E., Nordbotten J. M. and Celia M. a. (2011) Vertically averaged approaches for CO_2 migration with solubility trapping. *Water Resour. Res.* **47**, W05528.

Green M. S., Flanegan K. C. and Gilcrease P. C. (2008) Characterization of a methanogenic consortium enriched from a coalbed methane well in the Powder River Basin, U.S.A. *Int. J. Coal. Geol.* **76**, 34–45.

Harvey H. R., Fallon R. D. and Patton J. S. (1986) The effect of organic matter and oxygen on the degradation of bacterial membrane lipids in marine sediments. *Geochim. Cosmochim. Acta* **50**, 795–804.

Hopmans E. C., Schouten S., Pancost R. D., Van der Meer M. T. J. and Sinninghe Damsté J. S. (2000) Analysis of intact tetraether lipids in archaeal cell material and sediments by high performance liquid chromatography/atmospheric pressure chemical ionization mass spectrometry. *Rapid. Comm. Mass. Spectrom.* **14**, 585–589.

IPCC (2005) *Carbon Dioxide Capture and Storage*. eds. B. Metz, O. Davidson, H. de Coninck, M. Loos, and L. Meyer, Cambridge University Press, Cambridge, U.K.

Katsuki D., Gutierrez M. and Almrabat A. Development of a testing system for characterization of CO_2 injection in deep saline aquifers. *Int. J. Greenhouse Gas Control*, **In press**.

Klinkenberg L. J. (1941) The permeability of porous media to liquids and gases. In *Drilling and Production Practice* American Petroleum Institute. pp. 200–213.

Koga Y. and Morii H. (2007) Biosynthesis of ether-type polar lipids in Archaea and evolutionary considerations. *Microbiol. Mol. Biol. Rev*. **71**, 97–120.

Koga Y. and Morii H. (2005) Recent advances in structural research on ether lipids from Archaea including comparative and physiological aspects. *Biosci. Biotechnol. Biochem.* **69**, 2019–2034.

Koga Y., Nishihara M., Morii H. and Masayo A. M. (1993) Ether polar lipids of methanogenic bacteria: structures, comparative aspects, and biosyntheses. *Microbiol. Rev.* **57**, 164–182.

Krevor S. C. M., Pini R., Zuo L. and Benson S. M. (2012) Relative permeability and trapping of CO_2 and water in sandstone rocks at reservoir conditions. *Water Resour. Res.***48**, W02532.

Lechevalier H. and Lechevalier M. P. (1988) Chemotaxonomic use of lipids- an overview. In *Microbial Lipids vol. 1* (eds. C. . Ratledge and S. G. Wilkinson). Academic Press, San Diego. pp. 869–902.

Lemmon E. W., McLinden M. O. and Friend D. G. Thermophysical Properties of Fluid Systems. In *NIST Chemistry WebBook, NIST Standard Reference Database Number 69* (eds. P. J. Linstrom and W. G. Mallard). National Institute of Standards and Technology, Gaithersburg, MD.

Litynski J., Plasynski S., Spangler L., Finley R., Steadman E., Ball D., Nemeth K. J., McPherson B. and Myer L. (2009) U.S. Department of Energy’s Regional Carbon Sequestration Partnership Program: Overview. *Energy Proced.* **1**, 3959–3967.

Logemann J., Graue J., Köster J., Engelen B., Rullkötter J. and Cypionka H. (2011) A laboratory experiment of intact polar lipid degradation in sandy sediments. *Biogeosci.* **8**, 2547–2560.

Mancuso C. A., Franzmann P. D., Burton H. R. and Nichols P. D. (1990) Microbial community structure and biomass estimates of a methanogenic Antarctic lake ecosystem as determined by phospholipid analyses. *Microbial Ecol*. **19**, 73–95.

Martz R. F., Sebacher D. I. and White D. C. (1983) Biomass measurement of methane forming bacteria in environmental samples. *J. Microbiol. Methods.* **1**, 53–61.

Van der Meer L. G. H. (1992) Investigations regarding the storage of carbon dioxide in aquifers in the Netherlands. *Energy Convers. Manage.* **33**, 611–618.

Mitchell A. C., Phillips A. J., Hamilton M. A., Gerlach R., Hollis W. K., Kaszuba J. P. and Cunningham A. B. (2008) Resilience of planktonic and biofilm cultures to supercritical CO_2. *J. Supercrit. Fluid.* **47**, 318–325.

Mitchell A. C., Phillips A. J., Hiebert R., Gerlach R., Spangler L. H. and Cunningham A. B. (2009) Biofilm enhanced geologic sequestration of supercritical CO_2. *Int. J. Greenhouse Gas Cont.* **3**, 90–99.

Nordbotten J. M., Celia M. a. and Bachu S. (2005) Injection and storage of CO_2 in deep saline aquifers: analytical solution for CO_2 plume evolution during injection. *Transp. Porous Media.* **58**, 339–360.

Oba M., Sakata S. and Tsunogai U. (2006) Polar and neutral isopranyl glycerol ether lipids as biomarkers of archaea in near-surface sediments from the Nankai Trough. *Org. Geochem.* **37**, 1643–1654.

Pau G. S. H., Bell J. B., Pruess K., Almgren A. S., Lijewski M. J. and Zhang K. (2010) High-resolution simulation and characterization of density-driven flow in CO_2 storage in saline aquifers. *Adv. Water Resour.* **33**, 443–455.

Pinkart H. C., Ringelberg D. B., Piceno Y. M., McNaughton S. J. and White D. C. (2002) Biochemical approaches to biomass measurements and community structure analysis. In *Manual of Environmental Microbiology (Second Edition)* (eds. C. J. Hurst, R. Crawford, G. Knudsen, M. J. McInerney, and L. D. Stezenbach). American Society for Microbiology Press, Washington D.C. pp. 101–113.

Roberts M. S., Nakamura L. K. and Cohan F. M. (1994) Bacillus mojavensis sp. nov., distinguishable from bacillus subtilis by sexual isolation, divergence in DNA sequence, and differences in fatty acid composition. *Int. J. Syst. Bact.* **44**, 256–264.

Roberts Z. E., Meldrum F. C. and Pancost R. D. (2008) The archaeal lipid composition of partially lithified cold seep mats. *Org. Geochem.* **39**, 1000–1006.

Rozzi N. L. and Singh R. K. (2002) Supercritical fluids and the food industry. *Comp. Rev. Food Sci. Food Safety*. **1**, 33–44.

Schouten S., Middelburg J. J., Hopmans E. C. and Sinninghe Damsté J. S. (2010) Fossilization and degradation of intact polar lipids in deep subsurface sediments: A theoretical approach. *Geochim. Cosmochim. Acta* **74**, 3806–3814.

Schouten S., Rijpstra W. I. C., Kok M., Hopmans E. C., Summons R. E., Volkman J. K. and Sinninghe Damsté J. S. (2001) Molecular organic tracers of biogeochemical processes in a saline meromectic lake (Ace Lake). *Geochim. Cosmochim. Acta* **65**, 1629–1640.

Sturt H. F., Summons R. E., Smith K., Elvert M. and Hinrichs K. U. (2004) Intact polar membrane lipids in prokaryotes and sediments deciphered by high-performance liquid chromatography/electrospray ionization multistage mass spectrometry - new biomarkers for biogeochemistry and microbial ecology. *Rapid. Commun. Mass. Spectrom.* **18**, 617–628.

Suekane T., Nobuso T., Hirai S. and Kiyota M. (2008) Geological storage of carbon dioxide by residual gas and solubility trapping. *Int. J. Greenhouse Gas Cont.* **2**, 58–64.

Tanner R. S. (2006) Cultivation of bacteria and fungi. In *Manual of Environmental Microbiology* (ed. J. L. Garland). ASM Press, Washington D.C. pp. 52–60.

White D. C., Davis W. M., Nickels J. S., King J. D. and Bobbie R. J. (1979) Determination of sedimentary microbial biomass by extracting lipid phosphate. *Oecologia.* **40**, 51–62.

White D. C. and Ringelberg D. B. (1998) Signature lipid biomarker analysis. In *Techniques in Microbial Ecology* (eds. R. S. Burlage, R. Atlas, D. Stahl, G. Geesey, and G. Sayler). Oxford University Press, New York.

Wu B., Shao H., Wang Z., Hu Y., Tang Y. J. and Jun Y.-S. (2010) Viability and metal reduction of Shewanella oneidensis MR-1 under CO_2 stress: implications for ecological effects of CO_2 leakage from geologic CO_2 sequestration. *Environ. Sci. Technol.* **44**, 9213–9218.

Zhang J., Davis T. A., Matthews M. A., Drews M. J., LaBerge M. and An Y. H. (2006) Sterilization using high-pressure carbon dioxide. *J. Supercrit. Fluid.* **38**, 354–372.

CHAPTER 5

Conclusion

The studies described in this dissertation utilized an anaerobic consortium of bacteria and archaea to examine the fundamental microbial dynamics of methanogenesis from coal, and the potential microbiological impacts of geologic CO_2 sequestration. The motivation for this work was the need to understand how complex microbial communities may interact with CO_2 in the subsurface. A second motivation was the stimulation of methanogenesis from coal in situ, in order to meet humanity's ever-increasing energy demand. Deeply buried coal beds and sandstone reservoirs could serve as sequestration sites for CO_2 (Bachu, 2000), reducing the atmospheric CO_2 concentration and mitigating the harmful effects of climate change. This dissertation addresses both previously stated research areas by advancing our understanding of the microbial metabolic pathways within coal beds, as well as the effects of supercritical CO_2 on anaerobic microbes in sandstone. This chapter will summarize the general conclusions from the presented work, while addressing some limitations and areas for future research.

5.1 Sulfate reduction and methanogenesis in coal beds

Sulfate reduction and methanogenesis are commonly thought to be mutually exclusive processes in anaerobic environments. Results from the work presented in this dissertation demonstrate, however, that they may co-occur in coal beds, regardless of the sulfate concentration. In experiments where acetate was added to stimulate both processes, methanogenesis was enhanced by the addition of molybdate as an inhibitor of microbial sulfate reduction (Figure 2.3). Without additional acetate both processes were shown to occur, and sulfate concentration did not impact overall methanogenic potential (Figures 2.1 and 2.2). Contrary to the model of Lovley and Klug (1986), the relative importance of methanogenesis to acetate consumption decreased with increasing acetate concentration as more acetate was consumed for bacterial cell growth (Figure 2.8 and Tables 2.2 and 2.3). Bacterial PLFAs suggestive of sulfate reducers correlated with acetate concentration in the absence of molybdate, showing that sulfate reducers were stimulated by acetate amendment. DsrA, the functional gene for sulfate reduction, was also found to increase in number in the absence of molybdate, confirming the growth of sulfate reducers in these experiments (Figures 2.6 and 2.7).

5.2 Acetate limitation of metabolic activity in coal beds

Acetate was shown to be a key intermediate in the breakdown of coal in Chapters 2 and 3. As such, it proved to be a limiting factor for all metabolic activity in microcosm experiments in these chapters. The methanogenic potential of microcosms described in Chapter 3 depended not on pCO_2, as hypothesized, but rather on the metabolic activity of fermenters breaking down coal prior to the initiation of any experiments (Figures 3.1, 3.2, and 3.8). Acetate was also shown to be required for biotic urea hydrolysis, which was stimulated during long-term incubations after acetate was amended (Figures 3.8 and 3.10). As discussed in Chapter 2, acetate-amended experiments showed greater bacterial biomass, as estimated by PLFA analysis, than those without acetate (Table 2.3 and 2.4). The importance of acetate was further shown in Chapter 3: experiments with higher initial acetate concentrations (> 1mM) from coal fermentation also produced more methane and supported greater bacterial biomass than experiments with lower initial acetate concentrations (< 100 µM) (Figures 3.1, 3.2, and 3.8).

Based on the results of Chapter 2, a mechanism was proposed whereby sulfate reduction and methanogenesis may coexist in coal bed methane reservoirs, regardless of sulfate concentration, when both processes are limited by acetate. This model is used to explain the geochemical evidence in the Illinois Basin that suggests sulfate reduction preceded methanogenesis in most of the basin (Schlegel et al., 2011). My data suggest, however, that both processes may be ongoing and ultimately be limited by the slow rate of recalcitrant organic matter breakdown.

One limitation of the work described in Chapters 2 and 3 was the lack of sufficient methanogen biomass to quantify their contribution to the overall microbial community via lipid analysis. The sensitivity of archaeal lipid analysis was hindered by the need to perform multiple hydrolysis and derivatization steps in order to analyze PELs using a GC/MS. This lack of data makes it difficult to compare the results here from coal microcosms to other methanogenic environments where archaeal biomass was measured.

5.3 Effects of CO_2 sequestration in the subsurface

Chapters 3 and 4 examined the effects of a range of CO_2 pressures, from 0.2 atm to 2.5 atm, and supercritical CO_2, on a mixed anaerobic microbial consortium. The absolute CO_2 pressures described in Chapter 3 were lower than might be expected in a sequestration reservoir, but were chosen to understand the general relationship between increasing pCO_2 and methanogenesis from coal. Microbial methanogenesis from coal was not found to be sensitive to increasing pCO_2 up to 2.5 atm (Figures 3.1, 3.2, and 3.8), suggesting that methanogenesis may not be negatively impacted in areas distal to actual injection sites. Experiments with variable pCO_2 were amended with urea in order to test the hypothesis that urea hydrolysis could buffer the decrease in pH caused by increasing pCO_2, and thus enhance methanogenesis as pCO_2 rises. Biotic urea hydrolysis was shown to increase the pH of microcosms with 0.2 atm CO_2 (Figure 3.6), thereby increasing the solubility of CO_2 (Figure 3.7). This strategy could potentially enhance solubility trapping of CO_2 in coal seams, as has been proposed for other subsurface sites (Mitchell et al., 2010). Experiments with more than 2.5 g/L urea showed inhibition of methanogenesis, likely due to the increase in pH (Figure 3.4). However, urea hydrolysis was also found to vary with pCO_2, as pressures greater than 1 atm CO_2 inhibited its hydrolysis.

The injection of supercritical CO_2 ($scCO_2$) into sandstone containing an anaerobic microbial consortium was hypothesized to have a significant impact on cell viability of an anaerobic consortium due to its disruptive effect on bacterial cells (Zhang et al., 2006). However, the anaerobic consortium, enriched from the coal degradation studies, did not show a measureable decrease in bacterial and archeal biomass (via PLFA and ether lipid analysis, respectively) after injection of $scCO_2$ into Berea sandstone cores at 10 MPa . These results suggest that $scCO_2$ had a negligible effect on these organisms (Table 4.2). To explain this, a mechanism was proposed in Chapter 4 in which the viscous fingering of $scCO_2$ through heterogeneous flow paths in the sandstone may result in a large number of cells not being in contact with $scCO_2$. Viscous fingering of $scCO_2$ can cause large fluctuations in differential pressure across cores (Chang et al., 2013), as was observed in these experiments. Incubating sandstone cores in the microbial enrichment fluid for 30 days prior to the experiments in Chapter 4 caused a 30-60% reduction in permeability (Table 4.1). An injection of the microbial enrichment in cores not incubated with the enrichment also caused a significant reduction in core permeability, consistent with the aggregation of cells in pore spaces and on the core surface. The reduction in permeability was not significantly affected by $scCO_2$ injection, which is consistent with PLFA and PEL data that suggest that microbes were able to withstand $scCO_2$ injection.

5.4 Future work

While the research presented in this dissertation has enhanced our knowledge of the microbial dynamics associated with methanogenesis from coal, key questions remain unanswered and warrant future study. An important area of future research would be the identification of common fermentative organisms associated with coal breakdown, their substrates and enzymes involved with the fermentation of complex geopolymers, and the mechanisms of solubilization which allow organisms to access these macromolecules. Additionally, several studies have shown that the carbon and hydrogen isotopes of methane in coal bed reservoirs such as the Powder River Basin are consistent with hydrogenotrophic methanogenesis being the dominant metabolic pathway for methane formation (Flores et al., 2008; Rice et al., 2008). However, laboratory studies have not shown hydrogen generation from coal to be a significant contributing factor toward methane generation. It remains to be seen which organisms or physicochemical factors are necessary for hydrogen generation via fermentation of coal in the laboratory, and why this discrepancy exists between laboratory and field studies.

Because deeply buried coal seams are considered attractive target formations for CO_2 sequestration (Bachu, 2000), the potential microbiological effects of $scCO_2$ injection in coal should be investigated further. Of particular interest is the potential for $scCO_2$ to mobilize non-methane hydrocarbons, such as long chain alkanes and polycyclic aromatic hydrocarbons (Kolak and Burruss, 2006), which could be a feedstock for fermenters and potentially enhance methanogenesis. CO_2 sequestration in coal beds could thus offer the dual benefit of enhanced methane production in conjunction with mitigation of increasing atmospheric CO_2 concentration.

The work described in Chapter 4 showed that microbial biomass is not negatively impacted by relatively short exposure (~1h) to $scCO_2$, but future studies should examine the relationship between exposure time and microbial viability in different rock types (sandstone, shale, and coal). Results from Chapter 4 also suggest that the location of cells (i.e. surface versus inner pores) relative to flow paths of $scCO_2$ may be crucial in determining post-injection microbial cell viability. Other studies have shown that $scCO_2$ does not migrate evenly through sandstone (Chang et al., 2013; Kneafsey et al., 2013), and it remains to be seen if microbial cells themselves may influence $scCO_2$ flow. One way to address this would be micro computed tomography (micro-CT) scanning of cores with and without microbial cells during real-time experiments to determine if $scCO_2$ flow paths are influenced by cells, in the manner of Kneafsey et al. (2013).

5.5 References

Bachu S. (2000) Sequestration of CO_2 in geological media: criteria and approach for site selection in response to climate change. *Energy Convers. Manage.* **41**, 953–970.

Chang C., Zhou Q., Xia L., Li X. and Yu Q. (2013) Dynamic displacement and non-equilibrium dissolution of supercritical CO2 in low-permeability sandstone: An experimental study. *Int. J. Greenhouse Gas Control*. **14**, 1–14.

Flores R. M., Rice C. A., Stricker G. D., Warden A. and Ellis M. S. (2008) Methanogenic pathways of coal-bed gas in the Powder River Basin, United States: The geologic factor. *Int. J. Coal. Geol.* **76**, 52–75.

Kneafsey T. J., Silin D. and Ajo-Franklin J. B. (2013) Supercritical CO_2 flow through a layered silica sand/calcite sand system: Experiment and modified maximal inscribed spheres analysis. *Int. J. Greenhouse Gas Control.* **14**, 141–150.

Kolak J. J. and Burruss R. C. (2006) Geochemical investigation of the potential for mobilizing non-methane hydrocarbons during carbon dioxide storage in deep coal beds. *Energy & Fuels*. **20**, 566–574.

Lovley D. R. and Klug M. J. (1986) Model for the distribution of sulfate reduction and methanogenesis in freshwater sediments. *Geochim. Cosmochim. Acta* **50**, 11–18.

Mitchell A. C., Dideriksen K., Spangler L. H., Cunningham A. B. and Gerlach R. (2010) Microbially enhanced carbon capture and storage by mineral-trapping and solubility-trapping. *Environ. Sci. Technol.* **44**, 5270–5276.

Rice C. A., Flores R. M., Stricker G. D. and Ellis M. S. (2008) Chemical and stable isotopic evidence for water/rock interaction and biogenic origin of coalbed methane, Fort Union Formation, Powder River Basin, Wyoming and Montana U.S.A. *Int. J. Coal. Geol.* **76**, 76–85.

Schlegel M. E., Zhou Z., McIntosh J. C., Ballentine C. J. and Person M. A. (2011) Constraining the timing of microbial methane generation in an organic-rich shale using noble gases, Illinois Basin, USA. *Chem. Geol.* **287**, 27–40.

Zhang J., Davis T. A., Matthews M. A., Drews M. J., LaBerge M. and An Y. H. (2006) Sterilization using high-pressure carbon dioxide. *J. Supercrit. Fluids*. **38**, 354–372.

APPENDIX

A.1 Aromatic compound experiments

As part of an ongoing project investigating the potential of enhancing microbial methanogenesis from coal, a series of microcosm experiments were also performed as part of this dissertation. The results of these experiments were not presented in the previous chapters as they did not directly address the hypotheses posed in those chapters, but were instructive in developing the hypotheses and experimental methodology employed therein. One such set of microcosms included mono-substituted aromatic compounds, introduced without coal, and otherwise prepared with the same medium and in the same manner as previously stated in Chapters 2 and 3.

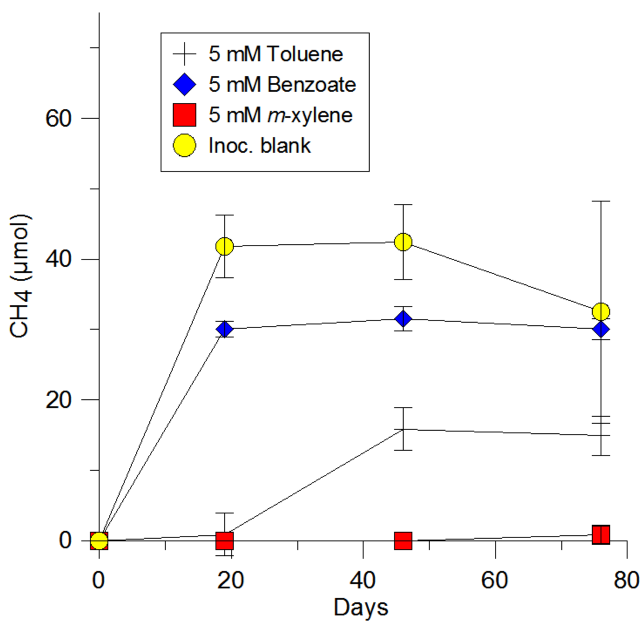

Figure A.1: Relative to a non-amended blank control experiment, methane production was inhibited in microcosm experiments to which substituted aromatic compounds (5 mM) were added in the absence of coal.

A.2 Hexadecane experiments

Experiments were conducted in 2009 and 2010 to test the hypothesis that coal degradation followed a similar mechanistic path to anaerobic alkane oxidation, as reported for crude oil reservoirs (Rueter et al., 1994; Caldwell et al., 1998; Zengler et al., 1999; Aitken et al., 2004). Early results suggested alkane oxidation may be a mechanism for coal degradation, as experiments with coal and hexadecane amended to the slurry showed enhanced methanogenesis relative to unamended coal slurry microcosms (Figure A.2), but this result could not be replicated during a repeat experiment. A series of microcosms were also conducted to test if the microbial consortium utilized in coal degradation experiments could metabolize n-hexadecane in the absence of coal. Figure A.3 shows that n-hexadecane was not observed to stimulate methanogenesis in the absence of coal.

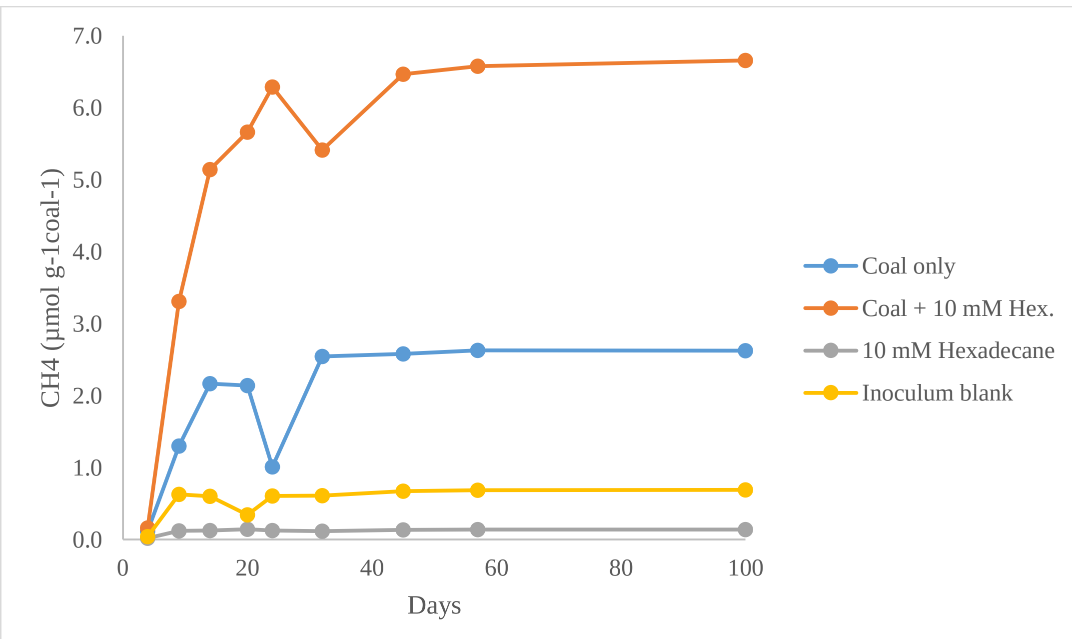

Figure A.2: Experiments with coal + n-hexadecane showed enhanced methanogenesis over unamended coal slurry experiments.

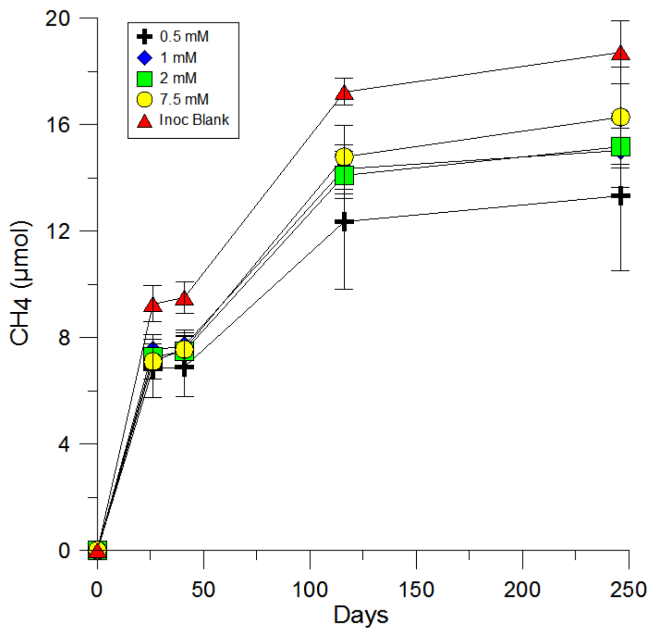

Figure A.3: CH_4 production in microcosm experiments with variable concentrations of n-hexadecane without coal.

A.3 Anaerobic chamber experiments

Experiments were conducted in order to understand how experimental design affects methane production. Coal for the microcosms was prepared in the same manner as previous ones, but one set of triplicate microcosms was removed from the anaerobic chamber after 2h and the headspace of each bottle flushed with 4:1 N_2:CO_2. A second set of microcosms was left in the anaerobic chamber with 5% H_2, 5% CO_2, and 90% N_2 atmosphere for 24 h.

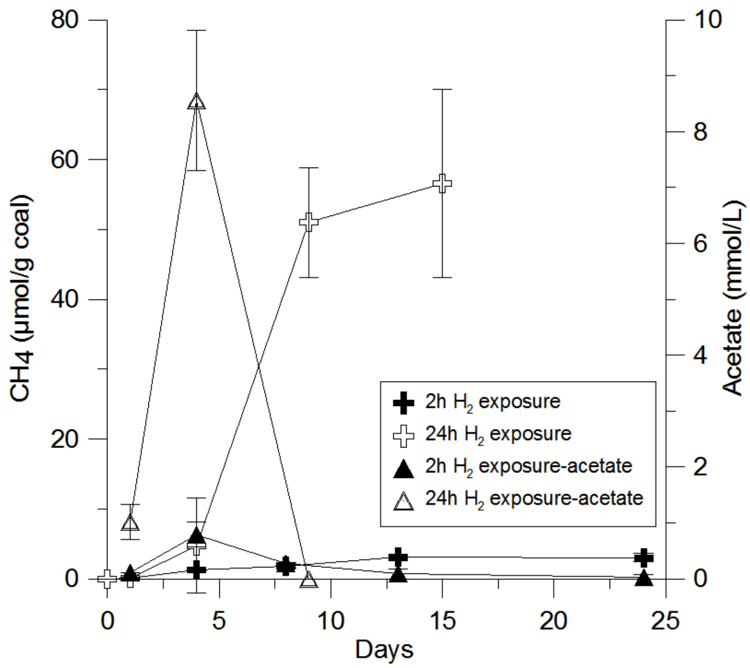

Figure A.4: CH_4 and acetate production of microcosms after 2h and 24h exposure to anaerobic chamber gas. Samples exposed to anaerobic chamber H_2 made significantly more acetate and significantly more methane as a result.

A.4 Effects of ethanol use during experiment set up

All experimental data presented in this thesis was obtained after it was determined that the use of 70% ethanol in the anaerobic chamber enhanced methane production in microcosms with coal. The ethanol was used to sterilize equipment and working surfaces that could not be autoclaved. This finding was made after it was discovered that microcosms prepared in this manner showed higher production of methane and acetate than similar experiments conducted without ethanol sterilization. Figure A.5 shows clearly that ethanol utilized in the anaerobic chamber caused significantly more methane to accumulate than in experiments without ethanol. The ethanol was most likely oxidized to acetate, resulting in higher acetate concentrations in these microcosms as well (Figure A.6).

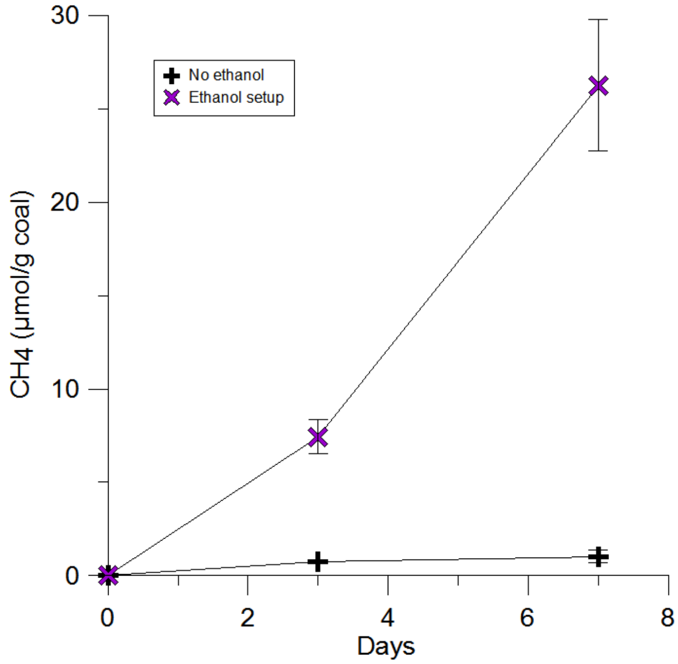

Figure A.5: CH_4 production in microcosms set up with ethanol sterilization used in the anaerobic chamber and without any ethanol present.

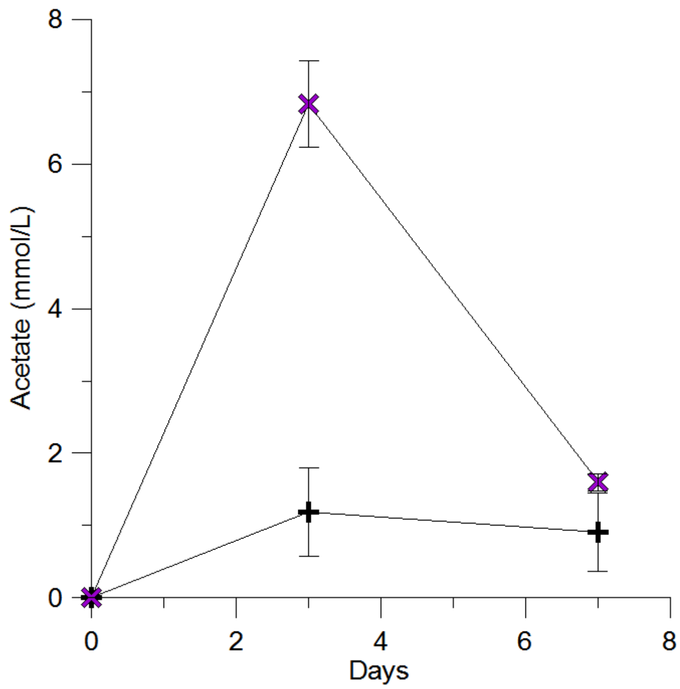

Figure A.6: Acetate concentration in microcosms set up with and without 70% ethanol used in the anaerobic chamber.

Table A.1: MPN Data for Chapter 4 (GC-FID peak areas; shaded boxes were considered positive samples for methanogen growth; result considered positive if peak area equals 2 x average of blanks, A = 3500)

Dilution	*T_0*	*Core1 (T_1)*	*Core 1 (T_2)*	*Core 2 (T_1)*	*Core 2 (T_2)*	*Core 3 (T_1)*	*Core 4 (T_1)*	*Core 4 (T_2)*	*Core 5 (T_1)*	*Core 5 (T_2)*	*Core 6 (T_1)*	*Core 6 (T_2)*	*Core 7 (T_1)*	*Core 7 (T_2)*
10^{-1}A	158134	3614	2340	5008	4548	12956	2777	2680	1465422	2370	1632551	2267	8607	2241
10^{-1}B	92237	2777	2877	4784	1950	26487	2547	1586	13470	1821	791730	1982	1289745	1682
10^{-1}C	401348	3778	2160	4287	1622	9291	2675	1465	26058	1868	543234	1931	1415781	2235
10^{-2}A	829219	968	1381	1191	3370	3172	2667	2542	3557	2562	1905	1976	2175	1438
10^{-2}B	326098	779	1492	891	1671	1384	3571	3066	2930	1434	2449	1333	1381701	1601
10^{-2}C	71682	1012	1475	1428	1450	1318	2206	2009	2226	2375	2093	1853	425743	1420
10^{-3}A	756	1423	983	349	1686	881	2145	3276	2548	1664	1919	1674	1769	
10^{-3}B	931	1431	831	194	2068	1424	2014	1443	2257	1417	1372	1418	1254	
10^{-3}C	626721	3129	1522	299	1467	943	2310	2236	1045	2575	367	1582	1947	
10^{-4}A	770													
10^{-4}B	1224													
10^{-4}C	693													
10^{-5}A														
10^{-5}B														
10^{-5}C														
10^{-6}A														
10^{-6}B														
10^{-6}C														

A.5 PLFA and phosphoether lipid analysis of Powder River Basin groundwater

Samples were collected as part of a preliminary study of the microbial community of coal seam groundwater in the Powder River Basin, Wyoming. Samples were collected from de-watering wells in the Powder River Basin near Gillette, Wyoming in 2007 by filtering produced water using a stainless steel Millipore filtration manifold (142 mm x 0.22 µm filters). Bacterial PLFAs were extracted from the filters using a modified Bligh-Dyer extraction (White and Ringelberg, 1998) in the same manner as in the previous chapters. Archaeal PELs were separated from FAMEs by silica gel chromatography (White and Ringelberg, 1998) and analyzed via cleavage of the ether bond using 56% HI (Nishihara et al., 1989) followed by reduction of the resulting alkyl iodide with $LiAlH_4$ (Kates et al., 1986). The core lipid components liberated by this method were phytane and biphytane (from tetraether lipids), which were analyzed by GC/MS. Wells are named by American Petroleum Institute (API) numbers, which can reference other information using the Wyoming Oil and Gas Conservation Commission's website (http://www.wyogcc.state.wy.us). This data replicated some of the findings of Raleigh Schmidt (R. Schmidt, 2007, M.S. thesis, CSM) that characterized the relative abundance of bacteria and archaea in coal seam ground waters of the Powder River Basin.

The archaeal PELs analyzed in 2007 and 2008 as part of this preliminary work were analyzed via the HI/$LiAlH_4$ method of preparation as it was the best method for analysis with GC/MS known to us at the time. In 2009 Dr. Alex Bradley suggested a new method for core lipid preparation based on liberation of the core glycero-lipid backbone and subsequent silylation of that backbone. I subsequently adopted this method for PEL analysis. The advantages of the HI/$LiAlH_4$ method are the relatively low temperatures involved, unambiguous identification of phytane on a chromatogram through analysis of an authentic standard, quantification of that phytane via standard curve, and analysis of $\delta^{13}C_{lipid}$ without correcting for additional carbon atoms. The primary disadvantages are the need for "ultra dry" THF from a still in the $LiAlH_4$ step, and the safety issues related to working with $LiAlH_4$. Any water present in the THF or glassware will dramatically decrease the efficiency of the reduction and reduce overall yield, potentially causing an underestimation of PEL abundance as well as archaeal biomass. According to Dr. Richard Pancost, the HI/$LiAlH_4$ method also cannot be used with samples containing chlorophyll, as phytane may be liberated from the chlorophyll which would be indistinguishable from phytane from archaeal lipids. The advantages of the silylation method, described in detail in Chapter 4, include the specificity toward archaeal PELs, the ability to measure the $\delta^{13}C$ of the glycerol backbone included with the isoprenoid chain, and the ability to identify lipids containing straight chain hydrocarbons as opposed to isoprenoid chains; information which would be lost using the HI/$LiAlH_4$ method. Disadvantages of the silylation method include the need for multiple hydrolysis steps to remove glycosidic and phospho- polar head groups, the high temperatures and specialized glassware required for these steps, and the need to analyze silylated core lipids immediately following silylation. If isotopic information is desired, the $\delta^{13}C_{lipid}$ must be corrected for the $\delta^{13}C$ of the trimethylsilane (Bradley et al., 2009). Each hydrolysis step leading up to the silylation can reduce yield, requiring more archaeal biomass for the initial sample. This requirement meant that little PEL data could be presented in this dissertation, due to consistently low archaeal biomass in microcosm experiments. For a more detailed discussion of various PEL analysis methods, see Chapter 1.

Table A.2: PLFAs identified in Powder River Basin produced waters (mole %)

well API #	49-005-58438	49-005-55745	49-019-23827 #1	49-019-23827#2	49-019-23827#3	49-019-23836	49-005-55785	49-005-55210	49-005-55211	49-019-23866	49-005-55203	49-005-55749	49-005-51248	49-019-27155	49-005-52882
depth (m)	479	379	611	611	611	551	385	463	392	604	369	408	134	508	451
12:0									0.52						
br13:0	0.59					19.31			2.4		27.22	1.88		4.33	
i14:0									0		7.81	6.88		1.15	
14:0	4.67					28.84		3.56	7.4	29.31		8.26		8.34	6.43
br15:0									0.72					0.6	
br15:0														0.86	
i15:0	8.17							6.03	2.77		2.77	6.73		9.88	3.68
ai15	14.24	28.11	20.6	15.11				19.19	5.92		9.69	18.32		12.44	15.7
15:0	1.37							0.74	1.88			2.53		4.05	1.26
i16:0	4.66							7.65	0.81		4.1	6.79		4.57	11
ai16:0									2						
br16:0									1.17		12.94				
br16:0									1.03						
16:1ω9	4.17						7.78	27	1.68		7.46	3.27		6.98	1.78
16:1ω7c			40.18	42.3	45.16		63.48		0		6.08	7.94		1.08	4.33
16:0	13.06	45.85	46.46	42.59	54.84	29.56	28.75	19.52	16.8	45.91	14.35	20.86		16.52	16.6
10ME16:0									0					3.76	
i17:0								1.7	0					1.16	1.35
ai17:0								3.53	0					2.6	
cy17:0	8.71							4.3	1.16					1.15	1.11
17:1ω5									0					1.93	4.68
17:0	0.85								0.43					1.12	0.95
18:2									20.3						
18:1ω9	2.83							3.53	12.8			2.43		0.85	3.43
18:1w7	7.29							2.19	10.1			3.53		4.58	4.51
18:0	2.08	26.04				22.29		4.6	2.02	24.78	7.58	10.57		3.54	11.3
cy19:0									0.62					1.14	
19:1ω9									1.16					1.15	
20:1									1.72						
20:0									1.16						1.58

Table A.3: PELs and biomass estimates from PRB coal bed methane wells sampled in 2007.

API Well #	Depth (m)	Total PLFA mass (ng)	Mole phytane	Mole biphytane	Total mole PEL	Water volume sampled (L)	Phytane (pmol/L)	Biphytane (pmol/L)	Archaeal (cells/L)	Bacterial (cells/L)	Arch. %
49-005-55745	379	797	$3.5x10^{-9}$		$3.5x10^{-9}$	195	17.9		$4.22x10^{7}$	$1.58x10^{5}$	99.6
49-019-23827#2	611	522	$2.3x10^{-9}$		$2.3x10^{-9}$	345	6.63		$1.56x10^{7}$	$2.29x10^{5}$	98.6
49-019-23836	551	477	$2.1x10^{-9}$		$2.1x10^{-9}$	430	4.86		$1.15x10^{7}$	$8.23x10^{5}$	93.3
49-019-23827 #1	611	1903	$8.3x10^{-9}$		$8.3x10^{-9}$	279	30.0		$7.07x10^{7}$	$1.86x10^{5}$	99.7
49-005-55785	385					39.9				$2.10x10^{6}$	
49-005-55210	463	274	$1.2x10^{-9}$		$1.4x10^{-9}$	287	4.19		$1.17x10^{7}$	$1.05x10^{6}$	91.8
	463	127		$2.3x10^{-10}$				0.79			
49-005-55211	392	553	$2.4x10^{-9}$		$3.5x10^{-9}$	263	9.23		$3.17x10^{7}$	$6.32x10^{6}$	83.4
	392	625		$1.1x10^{-9}$				4.22			
49-019-23827#3	611					375					
49-005-55204	455					294				$1.82x10^{5}$	
49-019-23866	604	918	$4.0x10^{-9}$		$4.0x10^{-9}$	165	24.4		$5.75x10^{7}$	$2.88x10^{5}$	99.5
49-005-55203	369	681	$3.0x10^{-9}$		$3.0x10^{-9}$						
49-005-55749	408	1053	$4.6x10^{-9}$		$4.6x10^{-9}$	210	22.0		$5.20x10^{7}$	$8.02x10^{5}$	98.5
49-005-55211#1	392	524	$2.3x10^{-9}$		$2.3x10^{-9}$	62.1	37.0		$8.74x10^{7}$	$6.32x10^{6}$	93.3
49-005-51248	134	668	$2.9x10^{-9}$		$3.9x10^{-9}$						
	134	568		$1.0x10^{-9}$							
49-019-27155	508					101				$5.92x10^{6}$	
49-005-52882	451	6930	$3.0x10^{-8}$		$3.1x10^{-8}$	876	34.7		$8.39x10^{7}$	$5.77x10^{5}$	99.3
	451	423		$7.5x10^{-10}$				0.86			

Table A.4: Raw methane and acetate data for Figures A.1-A.5 shown in Appendix

Figure A.1 Aromatic compound experiments (CH_4)

Days	5 mM Toluene	Toluene blank	5 mM Benzoate	Benzoate blank	5 mM m-xylene	xylene blank	Inoc blank	toluene std dev	benzoate std dev	xylene std dev	inoc std dev
0	0.00	0.00	0.00	0.00	0.00	0.00	0.00	0.00	0.00	0.00	0.00
19	0.89	0.03	30.04	0.10	0.02	0.02	41.79	1.11	3.08	0.01	4.43
46	15.87	0.00	31.55	0.08	0.00	0.00	42.47	1.78	3.02	0.00	5.33
76	14.90	0.03	30.05	0.10	0.83	0.03	32.47	1.49	2.79	1.38	15.80

Figure A.2 Coal and hexadecane experiments (CH_4)

Days	Coal + Inoc.	Coal + hex	Coal only	10 mM Hex.	Inoc. No Hex.	Lignite + Inoc.	Lignite + BESA
4	0.12	0.16	0.01	0.02	0.04	0.02	0.03
9	1.30	3.31	0.01	0.12	0.63	2.28	1.73
14	2.17	5.14	0.01	0.13	0.60	2.26	1.53
20	2.14	5.66	0.06	0.14	0.34	2.74	2.19
24	1.01	6.29	0.04	0.13	0.61	2.71	2.00
32	2.54	5.41	0.02	0.12	0.61	2.72	1.96
45	2.58	6.46	0.01	0.13	0.67	2.85	2.11
57	2.63	6.57	0.02	0.14	0.69	3.01	2.15
100	2.63	6.66	0.02	0.14	0.69	3.00	1.94

Figure A.3 Hexadecane experiments (CH_4)

Days	0.5 mM	1 mM	2 mM	7.5 mM	Inoc blank	0.5 mM stdev	1 mM stdev	2 mM stdev	7.5 mMstdev	inoc only stdev
0	0.00	0.00	0.00	0.00	0.00	0.00	0.00	0.00	0.00	0.00
26	6.83	7.51	7.28	7.11	9.27	1.09	0.62	0.49	0.67	0.69
41	6.91	7.71	7.49	7.56	9.51	1.13	0.57	0.58	0.62	0.60
116	12.37	14.33	14.11	14.78	17.24	2.54	0.92	0.89	1.21	0.51
246	13.34	15.04	15.19	16.27	18.73	2.80	1.41	0.68	1.90	1.19

Figure A.4 Anaerobic chamber experiments (CH_4)

Days	10 mM phosphate	40 mM phosphate	1 g/L bicarb	N2 flush	anaerobic chamber	7-9stdev	10-12stdev	13-15stdev	16-18stdev	19-21stdev
0	0.00	0.00	0.00	0.00	0.00	0.00	0.00	0.00	0.00	0.00
2	0.79	0.71	1.13	0.03	0.05	0.22	0.23	0.21	0.01	0.02
6	17.74	13.00	16.49	9.10	10.11	2.93	3.25	1.81	1.47	1.87
16	29.19	26.63	26.41	28.95	27.53	3.15	1.12	1.79	1.20	1.68
23	26.35	27.23	23.54	25.89	28.36	3.00	1.12	1.70	2.57	1.37
58	32.58	30.90	31.35	30.68	31.55	3.13	3.10	2.02	1.09	3.01

Acetate (mM)

Days	10 mM phosphate	40 mM phosphate	1 g/L bicarb	N2 flush	anaerobic chamber	7-9stdev	10-12stdev	13-15stdev	16-18stdev	19-21stdev
2	1.67	1.17	2.22	0.50	0.45	0.18	0.06	0.21	0.05	0.01
6	2.54	2.61	2.19	3.44	3.49	0.24	0.58	0.16	0.16	0.11
16	0.05	0.06	0.09	0.08	0.07	0.01	0.00	0.03	0.02	0.01
23	0.05	0.07	0.09	0.07	0.06	0.03	0.01	0.01	0.01	0.00
58	0.11	0.10	0.09	0.09	0.19	0.04	0.02	0.03	0.00	0.04

Figure A.5 Ethanol experiments (CH_4)

Days	No Propionate	5 mM Prop	10 mM Prop	10 mM Prop	15 mM Prop-no coal	Ethanol set up	yoda1-3 stdev	yoda 4-6 stdev	yoda7-9 stdev	yoda 10-12 stdev	yoda 14-16 stdev	yoda 17-19 stdev
0	0.00	0.00	0.00	0.00	0.00	0.00	0.00	0.00	0.00	0.00	0.00	0.00
3	0.76	0.39	0.27	0.26	0.47	7.44	0.07	0.12	0.00	0.06	0.14	0.92
7	1.02	0.80	0.76	0.96	0.92	26.24	0.34	0.23	0.08	0.26	0.50	3.52

Acetate (mM)

Days	No Propionate	5 mM Prop	10 mM Prop	10 mM Prop	15 mM Prop-no coal	Ethanol set up	yoda1-3 stdev	yoda 4-6 stdev	yoda7-9 stdev	yoda 10-12 stdev	yoda 14-16 stdev	yoda 17-19 stdev
0	0.00	0.00	0.00	0.00	0.00	0.00	0.00	0.00	0.00	0.00	0.00	0.00
3	1.19	0.62	0.67	0.68	0.42	6.82	0.61	0.13	0.08	0.11	0.18	0.60
7	0.91	0.85	0.46	0.42	0.23	1.60	0.55	0.09	0.02	0.06	0.14	0.11

References

Aitken C. M., Jones D. M. and Larter S. R. (2004) Anaerobic hydrocarbon biodegradation in deep subsurface oil reservoirs. *Nature.* **431**, 291–294.

Bradley A. S., Hayes J. M. and Summons R. E. (2009) Extraordinary 13C enrichment of diether lipids at the Lost City Hydrothermal Field indicates a carbon-limited ecosystem. *Geochim. Cosmochim. Acta* **73**, 102–118.

Caldwell M. E., Garrett R. M. and Prince R. C. (1998) Anaerobic biodegradation of long-chain n-alkanes under sulfate-reducing conditions. *Environ. Sci. Technol.* **32**, 2191–2195.

Kates M., Burdon R. H. and Knippenberg P. H. (1986) *Techniques in Lipidology: Isolation, Analysis, and Identification of Lipids*., Elsevier, New York.

Nishihara M., Morii H. and Koga Y. (1989) Heptads of polar ether lipids of an Archaebacterium, Methanobacterium theroautotrophicum: Structure and biosynthetic relationship. *Biochemistry* **28**, 95–102.

Rueter P., Rabus R., Wilkes H., Aeckersberg F., Rainey F. A., Jannasch H. W. and Widdel F. (1994) Anaerobic oxidation of hydrocarbons in crude oil by new types of sulphate-reducing bacteria. *Nature.* **372**, 455–458.

Schmidt R. (2007) Characterization of the Bacterial and Archaeal Communitites in Coalbed Methane Aquifers in the Wyodak-Anderson Coal Zone of the Powder River Basin, WY Using Polar Lipid Analysis Techniques. Thesis, Colorado School of Mines, Environmental Science and Engineering.

White D. C. and Ringelberg D. B. (1998) Signature lipid biomarker analysis. In *Techniques in Microbial Ecology* (eds. R. S. Burlage, R. Atlas, D. Stahl, G. Geesey, and G. Sayler). Oxford University Press, New York.

Zengler K., Richnow H. H., Rossello-Mora R., Michaelis W. and Widdel F. (1999) Methane formation from long-chain alkanes by anaerobic microorganisms. *Nature.* **401**, 266–269.